Prediction of Heating and Ignition Properties of Biomass Dusts Using Near Infrared Spectroscopy

by

Jaskaran Dhiman

A thesis submitted to the Graduate Faculty of
Auburn University
in partial fulfillment of the
requirements for the Degree of
Master of Science

Auburn, Alabama
August 02, 2014

Keywords: biomass, bioenergy, combustible dusts, dust ignition, NIR spectroscopy, thermogravimetric analysis, differential scanning calorimetry

Approved by

Oladiran O. Fasina, Chair, Professor of Biosystems Engineering
Brian K. Via, Associate Professor of Forest Products Development Center
Sushil Adhikari, Associate Professor of Biosystems Engineering
Timothy P. McDonald, Associate Professor of Biosystems Engineering

Abstract

Dusts (i.e. particles of size less than 500 μm) are generated during handling and processing of biomass feedstock. Similar to damages that have been reported from ignition of dusts obtained from industries, ignited biomass dust may potentially cause fire and explosion in biorefinery plants that can result in human fatalities, serious injuries and substantial monetary loss. Control measures to prevent the heating and ignition of biomass dusts will play a critical role in development of safety guidelines and standards for bio-based industries. The research aims at quantifying and predicting (using NIR spectroscopy) the heating and ignition properties of dust from ten biomass feedstocks. Three different types of coals were also used for comparison purposes. The range of values obtained for these properties were 240°C-335°C (minimum hot surface ignition temperature, MIT), 266°C-448°C (temperature of onset of rapid volatilization, TORV), 304°C-485°C (temperature of maximum rate of mass loss, TMML), 242°C-423°C (oxidation temperature, TOXY), 206°C-249°C (temperature of onset of rapid exothermic reaction, TRE) and 354°C-429°C (maximum temperature reached during exothermic reaction, TME). Coefficient of determination (R^2) values for internal validation of prediction models developed using PCA on raw NIR spectral data for MIT, TORV, TMML, TOXY, TRE and TME were 0.994, 0.984, 0.963, 0.737, 0.931 and 0.901 respectively, whereas, first derivative NIR spectral data yielded R^2 (calibration) for these properties as 0.976, 0.964, 0.943, 0.798, 0.923 and 0.895 respectively.

Four different biomass dusts (eucalyptus, pine, sweetgum and switchgrass) were used to validate the prediction models externally. Coefficient of determination (R^2) values

for all the models was obtained less than 0.28. Poor performance of models under external validation was attributed to small sample sizes of the feedstocks that were used during building of prediction models.

Acknowledgments

I would like to thank my parents, Dr. J.S. Dhiman and Mrs. Manjeet Kaur Dhiman for their unconditional support and care throughout my life. They were a great source of inspiration to me to study further. I will always be indebted to them. I would also like to thank my brother Mankaran Dhiman for encouraging me. I wish to thank my friend Aman for supporting me and being patient during my course of study.

I would like to express my sincere gratitude to my advisor Dr. Oladiran Fasina for his patience, motivation, guidance and continuous support of my Masters research. I am highly indebted by his guidance in writing of this thesis. I would like to thank my research committee members: Dr. Brian Via, Dr. Sushil Adhikari and Dr. Timothy McDonald for their encouragement, support and insightful comments. I would also like to thank Christian Brodbeck, Jonathan Griffith and James for their support in procurement of raw material for my research. I also wish to thank my lab mates: Oluwatosin, Gbenga, Gurdeep and Anshu for stimulating discussions and hours of working together. I am very thankful to my friends Jatinder, Raman, Gurjot, Jass, Deep, Manbir, Gurjeet and Roger for their encouragement.

I would like to thank Alabama Agricultural Experiment Station, United States Department of Agriculture (USDA) funded Southeast Integrated Biomass Supply System (IBSS) and Department of Energy (DOE) for providing infrastructure and funding for my research.

Table of Contents

List of Tables

List of Figures

Chapter 1 Introduction

The United States and other countries rely heavily on fossil fuels. Since fossil fuels are fast depleting, shortage in the fuel supply could seriously jeopardize a nation's economic and social well-being and national security. In 2013, more than 80% of U.S.'s total energy consumption were obtained from fossil fuels such as petroleum, natural gas and coal (EIA, 2013). In addition, United States also depends on petroleum imports from other countries in order to meet its energy requirements. In 2011, USA produced about 78 quadrillion Btu (quads) of energy but consumed about 96 quads of total energy. The energy deficit was met by importing petroleum fossil fuels (EIA, 2013). Due to environmental impacts, long term availability issues of fossil fuels and its effect on economic and national security, it is very important to derive energy from renewable sources such as biomass energy, solar energy, wind energy and geothermal energy.

Out of the 8.8 quadrillion Btu of energy produced from renewable sources in the year 2012, energy produced from biomass accounts for about 50% (4.4 quadrillion Btu) (EIA, 2013). The advantage that biomass has over other forms of renewable energy is that it is the only renewable resource that can be used to produce liquid fuels, chemicals and other products. However, biomass feedstocks have to be processed and handled before it can be converted into biofuels. Equipment such as mills, grinders, silos, hoppers and conveyors that are needed

to prepare, process and handle biomass also generate dust from the biomass. The National Fire Protection Association (NFPA, 2013) defines combustible dusts as “particles passing through a 500 µm sieve which presents a dust fire or dust explosion hazard”. According to Vijayraghavan (2004), more than 70% of dusts generated in process industries are combustible. Combustible dust, if ignited and when they are suspended in air can cause explosion (Eckhoff, 1996). Dust explosions cause damage to processing plants, injuries to personnel and in extreme cases, fatalities (Eckhoff, 2009). According to U.S. Chemical Safety and Hazard Investigation Board’s report (CSB, 2006), between 1980 and 2005 there were at least 281 dust fire and explosion incidents that resulted in 119 fatalities and at least 718 injuries in the United States. In 2011, there were seven fatalities due to dust explosions in the United States (BLS, 2013). In late June, 2011, the world’s largest biomass pellet factory in the state of Georgia, USA had dust explosion incident that led to shutting down of the plant for 1.5 months (Renewables International Magazine, 2011). In addition to structural damage dust explosions can result in loss of income by a plant due to down time and time required to repair the damaged portion of the plant (Sapko et al., 2000).

The probability of dust causing explosion depends on the ignition of combustible dust. A dust with low minimum ignition temperature value will be more prone to ignition risks. Presence of hot surfaces such as surfaces of dryers, grinders or worn out bearings increase the chances of dust on these surfaces to ignite, thereby rendering the workplace hazardous and prone to dust explosion. Sparks, short circuit faults and electric arcs from electrical equipment as well as

electrical discharges may ignite suspended dust particles and cause explosions. Therefore, it is very important to study the factors that will lead to heating and ignition of biomass dusts in order to incorporate appropriate safety protocols during the preprocessing of biomass (Bilbao et al., 2002).

The parameters that have been used to quantify the heating and ignition risks of dusts include minimum hot surface temperature for dust layer ignition, minimum temperature required for volatilization, temperature of rapid exothermic reaction, temperature of maximum rate of mass loss and temperature of oxidation (Ramirez et al., 2010; Hehar, 2013). The methods used to quantify these properties are time consuming and require the use of expensive pieces of equipment such as thermogravimetric analyzer (TGA) and differential scanning calorimeter (DSC). Near Infrared (NIR) spectroscopy has been used as a quick method of indirectly quantifying the properties of biological samples such as grain moisture content (Norris, 1964), dry matter content and fruit firmness (Nicolai et al., 2008), post-harvest quality of fruits (Bobelyn et al., 2010), moisture content, water activity and salt content of meat (Collell et al., 2011), quality control of potato chips (Shiroma and Rodriguez-Saona, 2009), taste characterization of fruits (Jamshidi et al., 2012) and proximate analysis and heating values of torrefied biomass (Via et al., 2013). Some of the advantages of NIR spectroscopy includes non-destructive measurement, ease of sample preparation, ability to be used by low skilled operator and high data/spectrum acquisition rates (Vergnoux et al., 2009).

This research specifically aims at quantifying the heating and ignition risks of dust generated from biomass feedstocks and to develop NIR spectroscopy methodology to predict heating and ignition risks of biomass dust samples. NIR spectroscopy and principal component analysis (PCA) on the NIR spectral data will be employed for the prediction of heating and ignition parameters. To achieve this goal, the following specific objectives will be carried out on dust samples obtained from ten biomass feedstocks (Bermuda grass, corn cobs, corn stover, eucalyptus, loblolly pine, pecan shell, poultry litter, sugarcane bagasse, sweetgum and switchgrass) and three coal samples (bituminous coal, lignite coal, powder river basin (PRB) coal).

1. Quantify the heating and ignition properties, and the physical and chemical properties of the biomass and coal dust samples.
2. Predict the heating and ignition characteristics of biomass dusts using Near Infrared (NIR) spectroscopy.

Chapter 2 Review of Literature

2.1 Energy Overview

Energy plays a pivotal role in the development of human civilization and will continue to do so in the future. Also, growing population of the world would demand more energy in the future. The current world population is 7.2 billion and is projected to increase to 9.6 billion by the year 2050 (United Nations, 2014). The projection is that there will be a 56% increase in world energy consumption from year 2010 to 2040 (EIA, 2013) as depicted in figure 2.1.

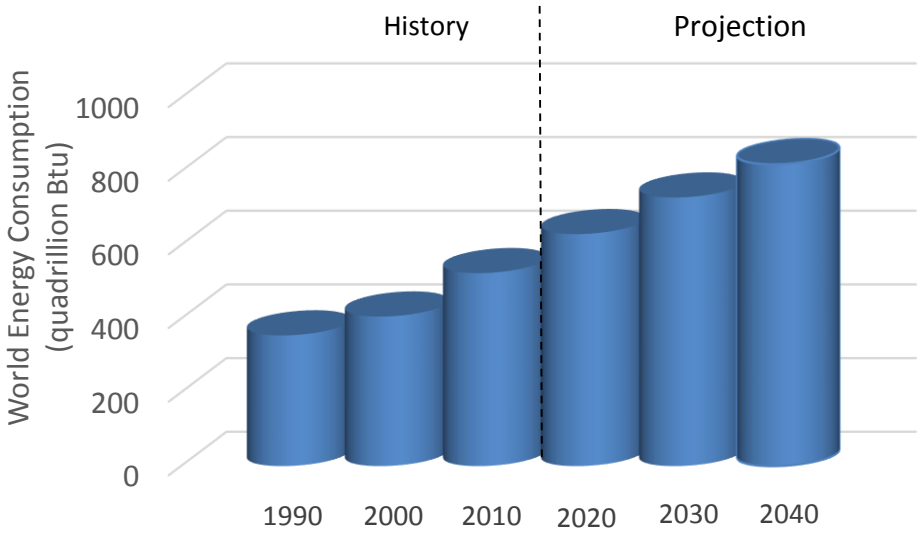

Figure 2.1 Past, current and projected world energy consumption between 1990-2040 (EIA, 2013).

High energy consumption and dependence on fossil fuels in industrialized countries of the world pose global sustainability challenges (Weidenhofer et al., 2013). Presently, United States has the highest per capita energy consumption. In the year 2013, U.S. consumed about 17.5% (96 quadrillion Btu) of the total world energy consumption (547 quadrillion Btu) (EIA, 2013) even though US is inhabited by only about 4.4% of the world population (USCB, 2014).

Fossil fuels (coal, natural gas and petroleum) play a major role in meeting U.S. energy requirements. Out of 95 quads energy consumed in 2012, 78 quads were derived from fossil fuels (EIA, 2013). More than 67% of the petroleum consumed (34.58 quadrillion Btu) in the U.S. was imported. United States therefore relies heavily on petroleum imports to meet its energy requirements.

In 2012, about 9.2% (8.8 quadrillion Btu) of the total energy consumed in United States was derived from renewable sources (EIA, 2013). About 50% (4.383 quadrillion Btu) of this renewable energy amount was derived from biomass (EIA, 2013).

2.2 Bioenergy

Bioenergy is energy derived from biomass which includes, but not limited to energy crops, agricultural crops, food, fiber, feed, forest products, aquatic plants, wood residues, industrial and residential waste, processing byproducts and non-fossil organic material (ASABE S593.1, 2011). Biomass has been used as main source of energy in rural areas for centuries (Mafakheri and Nasiri, 2014). It is the fourth largest source of global energy accounting for 10% to 14% of global energy

consumption (Kheshgi et al., 2000; Parrika, 2004; Balat and Ayar, 2005; Demirbas, 2005). Due to increasing interest in renewable and environment friendly energy sources, biomass has gained a lot of attention as a potential energy source. In addition, biomass is the only renewable resource of energy that can be converted into carbon based fuels and products. Bioenergy is also cleaner form of energy having lower impact on environment than energy derived from fossil fuels (McNew and Griffith, 2005; Rajagapol at al., 2009).

In United States, concerns about global climate change and air pollution has led to an increased interest in biomass as potential energy source because bioenergy is CO_2 neutral and less polluting than fossil fuels (Cook and Beyea, 2000). There is an abundance of biomass resources in United States. It is estimated that land resources of the U.S. will be capable of producing at least 1 billion dry tons (0.91 billion dry metric tonnes) of biomass feedstock per year by the mid-21st century (Perlack et al., 2005). This quantity has been estimated to replace at least 30% of the nation's petroleum consumption. Other benefits of using biomass include creation of employment opportunities, diversifying economic structure of rural communities and maintaining forest health (Mayfield et al., 2007; Gan and Smith, 2007).

2.3 Biomass Logistics and Dust Generation

Some of the challenges that will be faced by the emerging bioenergy industry for it to be viable, sustainable and mature includes supply logistics, a

continuous and large feedstock supply and residue handling (Tembo et al., 2003). Biomass supply logistics consists of biomass harvesting and collection, storage, transportation, pretreatment, storage, transport and energy conversion (figure 2.2).

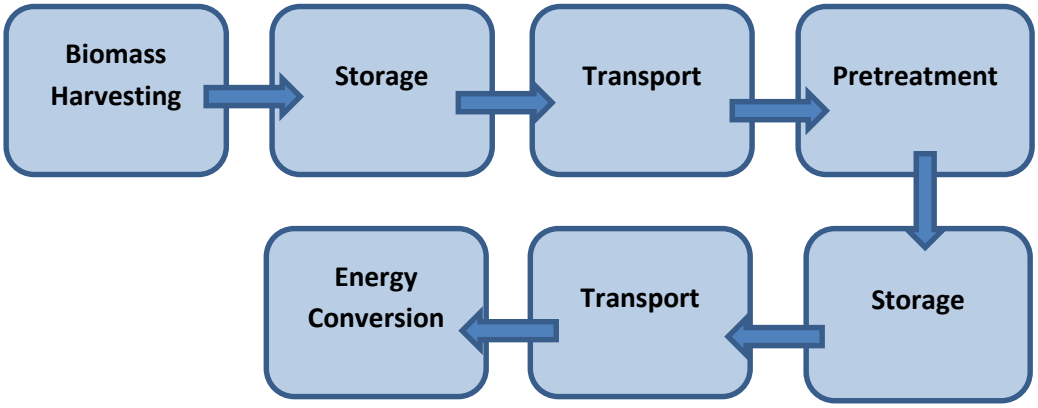

Figure 2.2 Operational components of biomass supply chain (Mafakheri and Nasiri, 2014).

Biomass feedstocks have low energy density, high moisture content and are geographically dispersed. Therefore there is high logistics cost incurred to deliver them from farms/forest land to conversion plants (An and Searcy, 2012). For example, the cost of silage or bale logistics was estimated to vary between \$40 Mg^{-1} and \$60 Mg^{-1} (U.S. Department of Energy, 2010). In addition, biomass has to be processed before using it for energy production. Processing and handling of biomass involves unit operations such as grinding, milling, conveying and densifying that also generate dust. For example, dust is generated when bulk material such as biomass undergo freefall as shown in figure 2.3 (Wypych et al., 2005). Dust generation while handling biomass can lead to dust fire or explosion and to health problems of workers (Khan et al., 2008).

Wood dusts was shown to cause allergic reactions (Hausen, 1981), nasal adenocarcinoma (Acheson et al., 1981) and pathological changes in the lungs of woodworkers (Michaels, 1967). Also, coal dust exposure can cause acute alveolar and interstitial inflammation that can lead to chronic pulmonary diseases (Pinho et al., 2004).

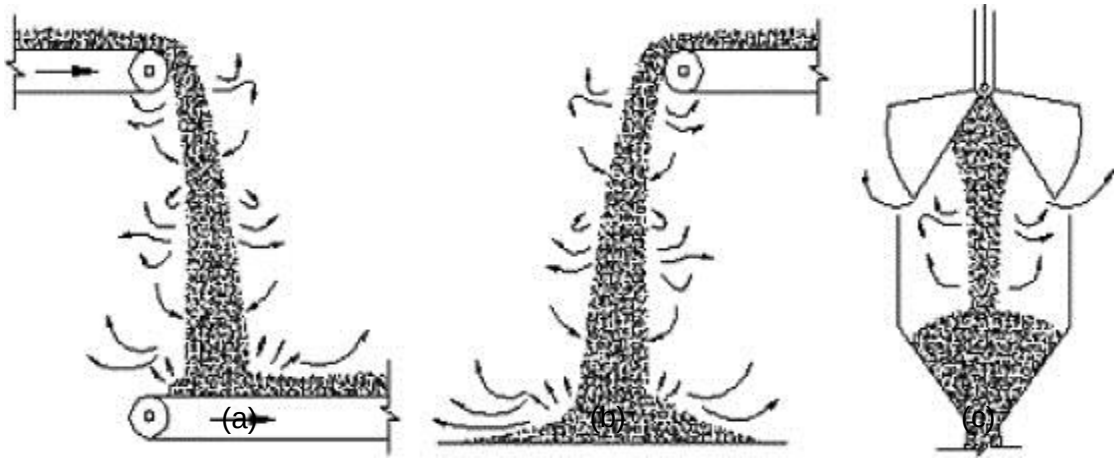

Figure 2.3 Dust generated during handling of biomass. Dust is generated as (a) material falls from one conveyor to another, (b) from conveyor to floor and (c) material falling into a silo (Wypch et al., 2005).

2.4 Combustible Dust

Particle size is the main criteria used for defining dust (Amyotte et al., 2007). Previous editions of NFPA 654 defined combustible dust as material capable of passing through a U.S. No. 40 standard sieve (420 µm) but 500 µm (U.S. No. 35 standard sieve) is now used as the new size criterion by NFPA 654 standard (NFPA, 2013). This is because particles of different shapes such as fiber

segments, flat platelets and agglomerates cannot readily pass through a U.S. No. 40 sieve, but may be combustible (Zalosh, 2005). Generally, combustible particulate solids with size greater than 500 μm have surface area to volume ratios that are not sufficient to cause a dust explosion hazard and may therefore not contribute significantly to dust explosions (Calle et al, 2005; NFPA, 2013).

2.5 Hazardous Area

The interior parts of a processing plant that have significant dust accumulation are classified as dust flash fire and/or dust explosion hazard area. This classification depends on the depth and mass of accumulated dust (NFPA, 2013). The critical 'layer depth' of combustible dust that causes an area to be hazardous for dust explosion or dust fire prone is given by equation 2.1 (NFPA, 2013).

$$LD = \frac{152527}{160000\ BD} \qquad (2.1)$$

where,

LD is layer depth (m),

BD is bulk density (kg m^{-3})

If the actual dust layer depth in an area is greater than the layer depth calculated in equation 2.1 (LD) then that area is considered as hazardous. Note that equation 2.1 is applicable to floor areas <1000 ft^2 (92.9 m^2) and for dust with bulk density <1201 kg/m^3.

On a mass basis, the mass of dust in a processing plant should be less than the value calculated in equation 2.2 and 2.3 (NFPA, 2013) respectively to minimize the risk for dust explosion and dust fire hazard.

$$M_{\text{basic explosion}} = 0.004\ A_{\text{floor}}\ \text{H} \qquad (2.2)$$

where,

$M_{\text{basic explosion}}$ is threshold dust mass (kg) based on building damage criterion,

A_{floor} is enclosure floor area (m^2) or 2000 m^2, whichever is less,

H is ceiling height (m) or 12 m, whichever is less.

$$M_{\text{basic fire}} = 0.02\ A_{\text{floor}} \qquad (2.3)$$

where,

$M_{\text{basic fire}}$ is threshold dust mass (kg) based on personnel fire exposure criterion,

A_{floor} is enclosure floor area (m^2) or 2000 m^2, whichever is less.

2.6 Dust Explosion

As discussed earlier, dust generated during handling of biomass can settle as dust layers on various sections of a processing plant such as on the floor, on process equipment and on storage structures. The accumulated combustible layer of dust can ignite and cause fire or explosion if these surfaces reach a critical high temperature. These dust layers may also be disturbed by an external event such as blowing air or mechanical action resulting in suspension of the dust to form dust

cloud. If the concentration of the dust cloud is high enough and in a confined space, dust explosion can occur when an ignition source such as electric spark, hot surface or a naked flame comes in contact with the cloud (Amyotte and Eckhoff, 2010) (figure 2.4).

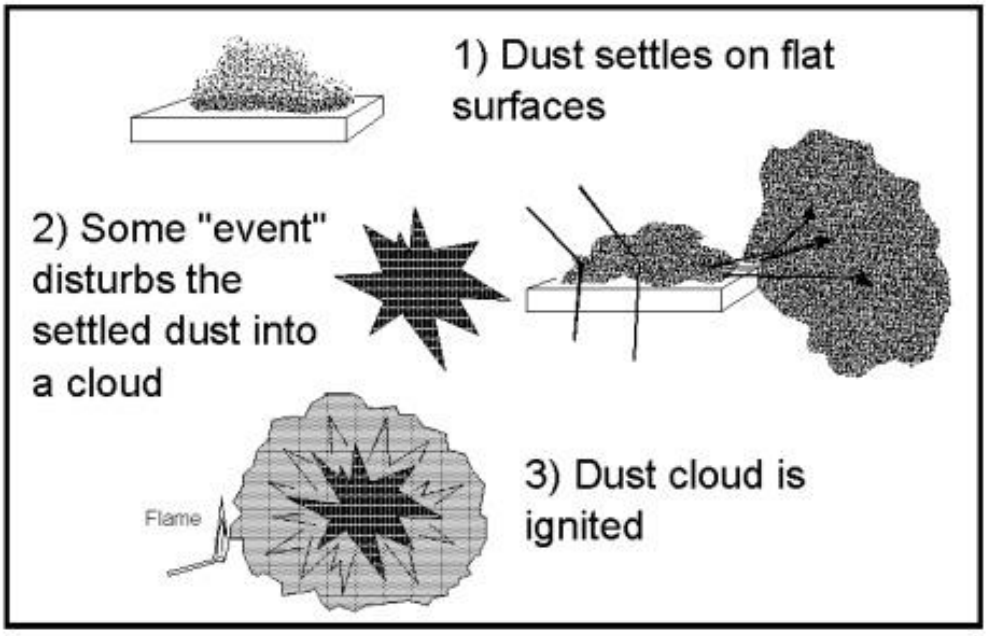

Figure 2.4 Dust explosion due to disturbance of a dust layer (Blair, 2012).

The three elements required for fire are fuel (in this case, dust), oxidizing medium (air) and heat (ignition source). Removal of any one of these would cause fire to cease. In the case of dust explosion, two other elements, dispersion or mixing and confinement are required along with the requirements for fire (figure 2.5).

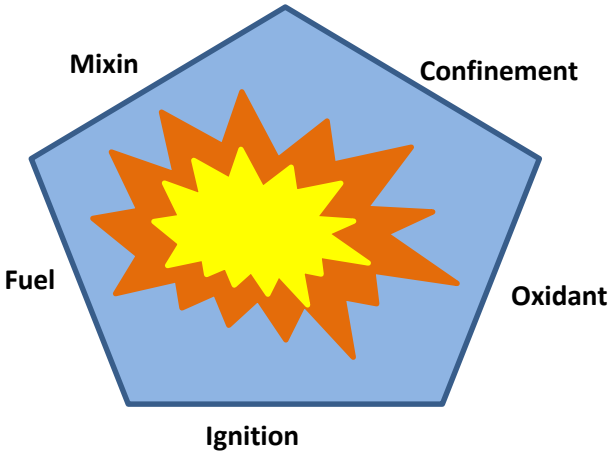

Figure 2.5 Dust explosion pentagon (Kauffman, 1982).

2.6.1 Primary and Secondary Dust Explosions

Primary dust explosion occurs in units and equipment (milling, grinding, etc.) of a process industry when all the conditions of the explosion pentagon are met. However, shock or blast wave from such an explosion may disturb the dust accumulated outside of this equipment or unit by creating a suspension and eventually a secondary explosion (Amyotte and Eckhoff, 2010). A weak primary dust explosion can cause a very powerful secondary dust explosion depending upon the amount and extent of accumulated dust. The secondary explosion may further disturb the accumulated dust in other areas and lead to a series of dust explosions. This phenomenon is referred to as *Domino effect* in dust explosions (Abbasi and Abbasi, 2007).

2.6.2 Dust Explosion Characteristics

The ability of dust to cause explosion is determined by parameters such as minimum ignition energy (MIE), minimum ignition temperature (MIT), and minimum explosion concentration (MEC). The maximum explosive pressure (P_{max}) and

maximum rate of explosion pressure rise ($(dP/dt)_{max}$) (Nifuku et al., 2005; Cashdollar, 2000) are used to quantify the severity of the explosion that a dust fire can cause (Eckhoff, 2003).

Minimum Ignition Energy (MIE)

MIE is the minimum spark energy that can ignite the most ignition sensitive concentration of dust-air mixture (NFPA, 2013). The value of MIE for combustible dust clouds range from 0.01 mJ to beyond 1 kJ (Eckhoff, 2002). Janes et al. (2008) found MIE for wood dust to lie between 45 and 58 mJ. They also reported MIE for crushed pea fiber, cocoa powder and coal to vary between 100-300 mJ, 300-1000 mJ and >1000 mJ respectively.

Minimum Ignition Temperature (MIT)

MIT for a dust cloud is the minimum air temperature at which flame is observed when the dust particles are combusted (Benedetto et al., 2007). Minimum ignition temperature is measured in a BAM oven or Godbert-Greenwald furnace. For most dust clouds, the minimum ignition temperature values ranges from 420˚C to 660˚C (Zalosh, 2008). Minimum ignition temperature values of dusts from wheat flour, corn starch and rye dust at relative humidity of 30-90% are 410-430˚C, 410-450˚C and 430-500˚C respectively (Zalosh, 2008). Polka et al. (2012) found MIE for hop, nettle, barley, corn starch and sunflower hull dusts to be 460˚C, 500˚C, 450˚C, 460˚C and 460˚C respectively.

Minimum Explosible Concentration (MEC)

Minimum explosible concentration (MEC) is defined as minimum concentration (mass of dust / volume of confined space) of explosible dust that is suspended in air and can support deflagration (a rapid burning slower than speed of sound) (NCDOL, 2012). MEC is typically measured with Hartmann tube apparatus or 20 liter sphere apparatus. Garcia-Torrent et al. (1998) measured minimum explosive concentration (MEC) of forest residue biomass including wood pieces and bark. At 6% moisture content, MEC as determined by Hartmann tube was 30 g/m^3, and MEC value of 20 g/m^3 was obtained from the 20 liter sphere apparatus. Amyotte et al. (2012), determined MEC of fibrous wood samples to be 100 g/m^3. When the samples were fractionated, those that passed through 35 mesh sieve (<500 µm) and 200 mesh sieve (<75 µm) had MEC values of 30 and 20 g/m^3 respectively.

2.7 Dust Explosion Incidents

The total number of dust explosions that occurred in USA and Germany between 1900 - 1956 are reported to be 1120 (Theimer, 1973). Nearly half of these cases occurred in grain, flour and feed handling industries with about 392 casualties and 1015 injuries. Financial losses were estimated to be over $75 million.

According to U.S. Chemical Safety and Hazard Investigation Board's report (2006), there were at least 281 dust fire and explosion incidents that caused 119 fatalities and over 718 injuries in the United States between 1980 and 2005. In

United Kingdom, a total of 571 dust explosion cases were reported in a period of ten (1968-1979) years (Lunn, 1992) that resulted in 247 fatalities and 324 non-fatal injuries. Between 1979 and 1988 in UK there were 36 dust explosions reported that lead to injuries and 123 dust explosions that did not cause injuries (Vijayaraghavan, 2004).

On an average, 10.6 agricultural grain dust explosions are reported per year in the U.S. resulting in 1.6 deaths, 12.6 injuries and millions of dollars of damages (Schoeff, 2006). In February 2008, a major dust explosion and fire incident occurred at a sugar refinery in Georgia, USA, which claimed 14 lives, injured 38 people and led to total destruction of the plant (CSB, 2013). Dust explosions are not only limited to agricultural and food processing facilities. Three combustible dust incidents occurred in a powdered iron producing facility (Hoeganaes Corporation) at Gallatin, TN over a period of 6 months that led to five fatalities and three injuries (CSB, 2013). In March 2011, two workers were killed and two seriously injured when fire and explosion occurred at Carbide Industries facility in Louisville, KY. This facility produced calcium carbide products. In April 2013, dust explosion caused a fire in two of the fuel storage silos of Koda Energy Plant (MN, USA) which continued for over a week. The facility uses wood chips, oat hulls and other organic materials to generate electricity (Biomass magazine, 2014). In August 2013, a combustible wood dust explosion ocuurred at ‘Inferno Wood Pellet Inc.’ – a wood pellet manufacturing unit at East Providence, RI (USA) which partially demolished the building and injured a worker (OSHA, 2014).

More than 70% of powders in processing facilities are combustible. This is why most of the dust explosion accidents start in areas where powder processing equipment (e.g. mills, grinders, filters, driers, silos, hoppers and ducts) are installed and operated (Vijayraghavan, 2011).

2.8 Dust Ignition

A combustible dust is ignited first before it causes explosion. Requirements for ignition of combustible dust whether suspended in air or deposited on surfaces include air or oxidizing medium, dust in sufficient quantity and ignition source such as electrostatic discharge, electric current arc or spark, glowing ember, hot surface, welding slag, frictional heat or a naked flame (NFPA, 2013). Ignition occurs when the rate of slow fuel oxidation changes to a rate of rapid oxidation either of the volatiles or the solid matrix of the material (Grotkjaer et al., 2003). This results in a sudden rise of sample/fuel temperature (Haykiri-Acma, 2003). Ignition of biomass can be of three types, viz. homogeneous ignition, heterogeneous ignition and hetero-homogenous ignition. Chen et al. (1996) defined homogeneous ignition as ignition of the volatile matter released from the material, whereas heterogeneous ignition is ignition of actual particles of the material. Hetero-homogeneous ignition is the simultaneous ignition of volatile matter and particles. Since, combustible dust layers when ignited can lead to dust explosion and associated financial losses and fatalities (Joshi et al., 2012), it is very important to

quantify the heating and ignition properties for combustible dusts. These properties are reviewed below.

2.8.1 Volatilization Properties

Volatilization properties are measured by conducting thermal decomposition study (with TGA) on dust samples exposed to constant or programmed heating rates. A mass loss vs. temperature and mass loss rate vs. temperature curves are obtained and are used to estimate parameters such as temperature of onset of volatilization, temperature at maximum rate of mass loss and oxidation temperature. Temperature of onset of volatilization signifies the temperature at which significant release of volatiles starts as the material is being heated. Temperature at maximum rate of mass loss can be attributed to rapid release of volatile matter due to pyrolysis and thus gives an indication of reactivity of the sample. In air stream, TG analysis loss of mass due to thermal degradation of sample occurs over a range of temperature making it difficult to assign a single oxidation temperature to the sample. Thus, O_2 stream TG analysis is used to obtain oxidation temperature which allows different dusts to be categorized based on their ignition risk (Ramirez et al., 2010). A dust with lower oxidation temperature value would be at a higher risk of ignition than a dust with higher oxidation temperature.

Ramirez et al. (2010), estimated temperature of onset of rapid volatilization (TORV) and temperature of maximum mass loss rate (TMML) for icing sugar to be 212ºC and 220 ºC respectively. For maize, wheat and barley TORV values were estimated at 268ºC, 252ºC and 242ºC respectively, while their TMML values were estimated at 279ºC, 283ºC and 271ºC. Both, TORV and TMML values for maize,

wheat and barley were more than that of icing sugar indicating that icing sugar has more ignition risk. Oxidation temperature (TOXY) values for icing sugar (239 ºC), was also smaller than those of maize (289 ºC), wheat (279 ºC) and barley (277 ºC). In addition, temperature of maximum mass loss rate for wheat straw in 20% O_2 environment was found to lie between 220-270˚C (Grotkjaer et al., 2003). Sahu et al. (2010) reported the temperature of maximum mass loss rate (TMML) for coal, sawdust and rice husk as 419.5˚C, 417.3˚C and 323.2˚C respectively. Haykiri-Acma (2003) measured the temperature of maximum mass loss rate (TMML) for sunflower shell, cozla seed, pine cone, cotton refuse and olive refuse as 300˚C, 262˚C, 292˚C, 325˚C and 264˚C respectively.

2.8.2 Exothermic Parameters

Exothermic parameters of samples are determined by measuring the heat flow of sample relative to inert reference material or empty crucible in a differential scanning calorimeter (DSC). Exothermic parameters are used to characterize the ignition characteristics of dust samples by obtaining maximum temperature reached during exothermic reaction (TME), temperature required for onset of rapid exothermic reaction (TRE) and exothermic energy from heat flow curves (Ramirez et al., 2010). Dust sample with lower TRE value would be easily ignited than the dust with higher TRE value. Samples with higher values of TME would promote secondary dust fire or ignition by providing sufficient energy for the reaction. Dusts with higher exothermic energy release greater amount of energy in form of heat during ignition or explosion than samples with lower exothermic energy value. The

heat energy released could lead to secondary dust explosions or fires in a processing plant or facility leading to further destruction.

Ramirez et al. (2010) estimated TME values for maize, wheat, barley and alfalfa as 386˚C, 283˚C, 311˚C and 288˚C respectively and TRE values for the given samples to be 242˚C, 252˚C, 257˚C and 240˚C respectively. Sahu et al. (2010), found TME values for coal, sawdust and rice husk as 423˚C, 422˚C and 454˚C respectively.

2.8.3 Minimum Hot Surface Ignition Temperature

One main cause of ignition of dust layers are hot surfaces that are commonly found in processing plants. Several studies have been conducted on the hot surface temperature requirements for ignition of dust layers (Park et al., 2009; Janes et al., 2008; Joshi et al., 2012; Sweis, 1998). Hot surface minimum ignition temperatures for Pittsburgh seam coal, paper dust, Arabic gum powder and brass powder was measured to be 220°C, 360°C, 270°C and >400°C respectively (Park, 2006). Minimum ignition temperature of dust layer for icing sugar, maize grain dust, wheat grain dust, barley grain dust, alfalfa, bread-making wheat and soybean dust was reported to be 400°C, 420°C, 510°C, 480°C, 460°C, 440°C and 560°C respectively (Ramirez et al., 2009). The hot surface ignition temperature is determined by ASTM E2021 standard (2010). A hot plate is used to heat the sample placed on a metal plate (200 mm in diameter and 20 mm thick) confined at the sides by a metal ring (12.7 mm in diameter and 10 mm high). Temperature of metal plate and sample is recorded by a data logger through

thermocouples. The minimum temperature of the hot plate that ignites the sample is the minimum hot surface ignition temperature.

2.9 Factors Affecting Dust Ignition

2.9.1 Particle Size

Dust particles are readily combustible because the surface area to volume ratio is significantly higher than the bulk material they are derived from (figure 2.6). Higher surface area to volume ratio means more oxygen interacts with the material during combustion. Oxygen is a prerequisite for combustion and combustion starts at surface of the particle. In addition, the energy required is smaller for smaller sized material since there is limited conductive heat transfer when compared to combustion of bulk solids (Eckhoff, 2003).

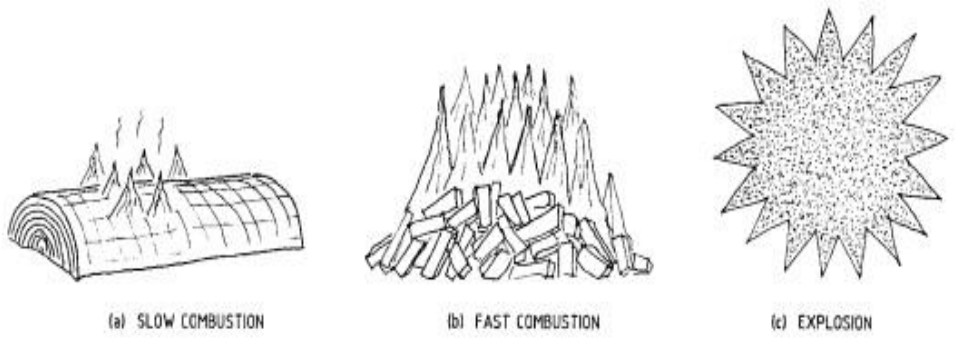

Figure 2.6 Increase in rate of combustion with increasing surface area (Eckhoff, 2003).

Particle size of dust particles also affects the dust burning rate and ignition front speed. Ryu et al. (2006), in their experiment with willow, miscanthus and pine

(M.C. <8%) showed that the burning rate for samples reduced from about 185 kg/m^{3}hr to about 165 kg/m^{3}hr as the size of the samples increased from 5 mm to 35 mm. Ignition front speed was also affected adversely with increase in particle size. It decreased from 0.93 m/hr to about 0.7 m/hr as the size increased from 5 mm to 20 mm. Mass loss during ignition propagation also decreased from about 87% to 80% as size increased from 5 mm to 35 mm. In summary, as the size of particles increases, burning rate and ignition front speed decreases.

Chen et al. (1996) also showed that heterogeneous ignition temperature for Kaipin (bituminous) coal and Hongay coal samples shifted to higher temperatures as particle size increased. This is because as particle size increases, the rate of heating of particle surface becomes slower. For samples with sizes 105-149 µm, 350-500 µm, 1410-2000 µm, and 4000 µm, heterogeneous ignition temperatures were found to be 500°C, 535°C, 600°C and 630°C respectively. Also, the ignition temperatures of Hongay coal samples of particle sizes 350-500 µm, 1410-2000 µm and 4000 µm, were measured to be 515°C, 560°C and 625°C respectively.

Vamvuka and Sfakiotakis (2011), showed that particle size had effect on ignition temperature and temperature of maximum mass loss rate for sewage sludge samples which were air dried, and separated into three different size fractions viz. <250 µm, <500 µm and <1000 µm. Ignition temperature for the samples increased from 229°C to 242°C whereas, the temperature of maximum mass loss rate increased from 515°C to 527°C as the particle sieve size increased from <250 µm to <1000 µm respectively.

2.9.2 Moisture Content

Shi and Chew (2011) in their study showed that moisture content had little effect on ignition temperatures for different types of wood samples (pine, beech, cherry, oak and maple wood). Correlation coefficient between moisture content and ignition temperature was obtained to be 0.12. Range of ignition temperatures for dry and wet woods (11% moisture) were recorded as 267-525°C and 264-558°C respectively. The ignition time however increased with increase in moisture content as more energy is required to reach ignition in a wet sample. Range of ignition time for dry wood samples was obtained as 7-49 s whereas for wet wood samples it was 10-119 s.

2.9.3 Volatile Content

Ignition temperature is dependent upon volatile matter content because released volatiles further fuels the ignition of unignited particles. Chen et al. (1995) found that ignition temperature of coal increases with decreasing volatile matter. Thus, they concluded that volatile matter is the most important factor affecting ignition. Grotkjaer et al. (2003), measured the ignition temperature for poplar wood (volatile content: 75% d.b.) and eucalyptus wood (volatile content: 64% d.b.) to be 235˚C and 285˚C respectively. Using data for coal from previous studies (Tognotti et al., 1985; Zhang and Wall, 1994; Chen et al., 1995; Chen et al., 1996), they showed that ignition temperature decreases with increase in volatile matter (figure 2.7).

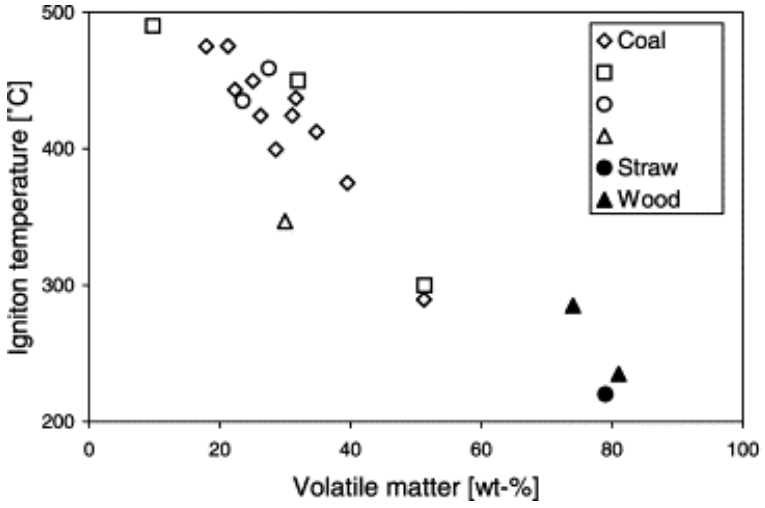

Figure 2.7 Relationship between volatile content (dry basis) and ignition temperature for biomass and coal samples (Grotkjaer et al., 2003).

2.9.4 Ash Content

Ash largely comprises of inorganic materials such as Al_2O_3, NaCl, SiO_2, KCl, MgO and $CaSO_4$, (Wang et al., 2011). Ash act as inhibitors to ignition as they are incombustible and therefore do not contribute towards ignition and act as heat sink. High ash content in biomass can cause ignition and combustion problems during bioenergy conversion processes such as gasification and pyrolysis (Demirbas, 2004). For example, the presence of alkali metals in biomass can cause fouling, slagging and ash agglomeration (Ryu et al., 2006). Liodakis et al. (2002), in their study with ground (0.3-0.5 mm) forest plant species (*Pistacia lentiscus, Cupressus sempervirens, Olea europaea* and *Cistus incanus*) showed that ignitability of samples decreases with increase in ash contents (i.e. the ignition delay increases). Samples of different species with ash contents of 3.51, 3.52, 5.64, 5.06 and 4.41% (% mass dry basis) had ignition delay values at 500˚C of 30

s, 36 s, 47 s, 48 s and no ignition respectively. Species with ash content 4.41-5.64% were classified as least flammable whereas species with ash content 2.96-3.52% were classified as most flammable species.

Vuthaluru (2004) showed that addition of coal (ash content 9.7% on dry basis) to wheat straw (ash content 3.3% on dry basis) and wood waste (ash content 0.1% on dry basis) increased the temperature of onset of rapid mass loss. The temperature of onset of rapid volatilization for 0:100, 70:30, 90:10 and 100:0 (blend coal:wheat straw mass/mass), were found to be 260˚C, 316˚C, 366˚C and 426˚C respectively. Coal and wood waste blends (ratio 0:100, 70:30, 90:10 and 100:0), had temperatures of onset of rapid volatilization to be 291˚C, 345˚C, 350˚C and 426˚C respectively. This shows that the presence of ash retards oxidation/ignition process of biomass.

2.10 NIR Spectroscopy (NIRS)

2.10.1 Introduction

Near Infrared (NIR) spectroscopy is an inexpensive and quick method for predicting the concentration of the constituents of a sample (Foley et al., 1998). This spectroscopy method involves measuring the amount of light reflected from a sample within the wavelength range of 750 to 2500 nm (13333 cm^{-1} to 4000 cm^{-1}) (Lu and Bailey, 2005). Amount of near infrared light reflected is a function of the chemical composition and microstructure of the material. Absorbance of the NIR radiation by a material is governed by Beer-Lambert's law. Beer-Lambert law

relates the radiant power in a beam of electromagnetic radiation to length of path of beam travel within a material and concentration of the absorbing material (Swinehart, 1962) (equation 2.4). Some other advantages of NIRS include non-destructive measurement; ease of sample preparation, ability to be used by low skilled operator and high data/spectrum acquisition rates (Vergnoux et al., 2009).

$$A = -log_{10}\frac{P}{P_0} = abc \qquad (2.4)$$

Where A is absorbance (Absorbance units, Au),

P is radiant power of reflected light,

P_0 is radiant power of incident light,

a is absorptivity (coefficient),

b is length of the beam in absorbing medium

c is concentration of absorbing medium.

The first application of NIRS was for measuring the moisture content of grains (Norris, 1964). NIRS is now widely used in many applications, such as measuring the solid content, firmness of fruits and post-harvest quality of fruits (Nicolai et al., 2008; Bobelyn et al., 2010), moisture content, water activity and salt content of meat (Collell et al., 2011), quality control of potato chips (Shiroma and Rodriguez-Saona, 2009), taste characterization of fruits (Jamshidi et al., 2012), proximate analysis and heating values of torrefied biomass (Via et al., 2013). Multivariate techniques such as principal component analysis (PCA) and partial least square (PLS) regression are used to analyze the complicated NIRS raw spectra.

Quantifying heating and ignition properties requires expensive equipment such as thermogravimetric analyzer (TGA) and differential scanning calorimeter (DSC) and is also time consuming. Thus, we attempted to use NIRS to develop prediction models for quick prediction of heating and ignition properties of biomass dusts.

2.10.2 Analysis Techniques

2.10.2.1 Principal Component Analysis

Principal component analysis (PCA) is the most widespread multivariate statistical technique used in chemometrics (Brereton, 2007). PCA is used to obtain systematic variations in a given data set (Kettaneh et al., 2005) and for classification, description and interpretation of NIR spectral data (Vergnoux et al., 2009). The PCA method involves the modeling of the variance or covariance structure of a given data set by obtaining principal components. This makes it possible to reduce large number of data points or variables to a few principal components that are then used for model development. Principal components are assumed to be independent of each other with no correlation amongst them.

2.10.2.2 Partial Least Square Regression Analysis

Partial least square regression analysis is based on the relationship between signal intensity and sample properties (Martens, 1979). PLS was first proposed by Herman Wold (a Swedish statistician) who used it as a tool for economic forecasting (Brereton, 2007). It takes into account the full spectral region rather than unique and isolated absorption bands (Vergnoux et al., 2009). The

algorithm involved in the analysis helps to mathematically correlate the spectral data and properties of the material while accounting for all significant factors (Liang and Kvalheim, 1996). Samples with known or measured properties are used to formulate a calibration model and the samples with unknown parameters are then employed in the model to calculate the unknown properties.

The values for properties estimated using developed models are compared with real or actual values. The comparison gives rise to the standard error of prediction (RMSEP) which gives an idea of the performance of prediction (equation 2.5).

$$RMSEP = \sqrt{\left(\frac{\sum_{i=1}^{N}(C_i - C_i{}')^2}{dof}\right)} \qquad (2.5)$$

Where, C_i is the actual value,

C_i' is the estimated value (as determined by calibration model),

dof is the 'degrees of freedom' value.

The degrees of freedom value is usually equal to N-1 where N is the number of samples. Relative error of prediction (REP) (equation 2.6) is also a useful parameter which quantifies the ability of the model to predict (Vergnoux et al., 2009).

$$REP = 100\left(\frac{RMSEP}{\bar{Y}}\right) \qquad (2.6)$$

Where, $\bar{Y}$ is the mean of known values.

2.10.3 Predictions Using NIRS

Vergnoux et al. (2009) used NIRS to predict physiochemical (age, moisture, pH, composting time, temperature and organic carbon) and biochemical parameters (soluble fraction, hemicellulose, cellulose and lignin) of industrial compost. In principal component analysis, 100% of the spectral variation was explained by two principal components (PCs). PC1 accounted for 98% variation whereas PC2 accounted for the remaining 2%. PC1 vs. PC2 (spectral data) plot was used to distinguish between different stages of composting (figure 2.8). Loading graph for PC1 was in accordance with the drying of the compost as the spectrum resembled the water spectra. The compost dried with time and this trend was clearly shown in PC1 vs. PC2 plot. In the physiochemical and biochemical parameters PCA, PC1 explained 42% of the total variation and PC2 explained 17% of variation. Correlation loading plot was used to estimate the correlations between PCs and compost parameters to be predicted. Best results obtained for physiochemical and biochemical parameters were tabulated along with *RMSEC,* $R^2_{calibration}$, *RMSEP,* $R^2_{prediction}$ and number of PCs used. Most of the models had good R^2 values (above 0.90). It was concluded that NIRS and PCA can be used to estimate the stages of composting.

Lu and Bailey (2005) performed experiment for prediction of soluble solids content (SSC) and firmness of apple as affected by postharvest storage. Samples (apple) were divided into three groups based on different post storage times. Actual vs predicted values were plotted for the model developed to predict SSC in these three groups. R^2 values obtained for the three models were between 0.771

and 0.853 whereas standard error of validation (SEV) for these models was found to be between 0.42 and 0.55. R^2 value obtained from model used to predict SSC from the samples of all the groups was 0.818 with SEV as 0.50. Model was also developed to predict firmness using NIR spectrometer. A good R^2 value of 0.839 was obtained with SEV as 4.81 showing that NIRS is capable of developing efficient prediction models.

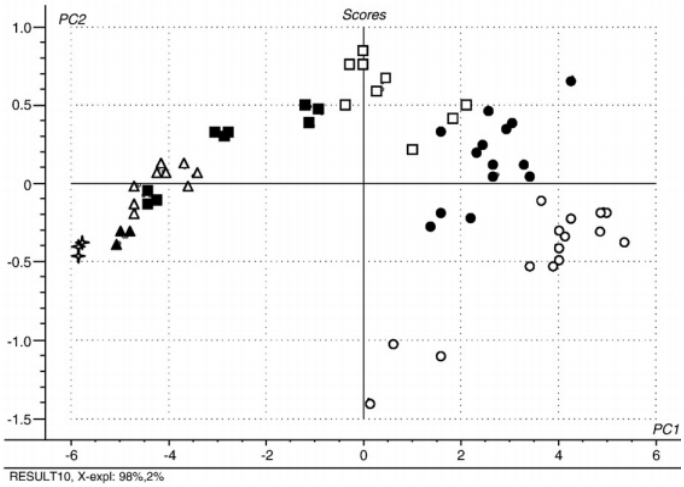

Figure 2.8 Example of principal component score plot showing PC1 vs. PC2 (Vergnoux et al., 2009).

FTNIR spectroscopy was used to develop prediction models for total soluble solids (TSS), total acidity (TA), sugar to acid ratio, firmness and weight for three South African plum cultivars - Pioneer, Laetitia and Angeleno (Louw and Theron, 2010). Figure 2.9 shows absorbance vs. wavelength NIR spectra for the three cultivars. The TSS prediction models (single and all cultivars combined) performed well with coefficient of determination (R^2) values ranging from 0.817 to 0.959 and root mean square error of prediction (RMSEP) values ranging from 0.4453 to 0.610 (% brix). The TA, sugar to acid ratio, firmness and weight prediction models

performed well with R^2 values of 0.608-0.830, 0.718-0.896, 0.623-0.791 and 0.577-0.817 respectively. RMSEP values for the above parameters were found out to be 0.110-0.194, 0.608-1.590, 12.459-22.760 and 7.700-12.800 respectively.

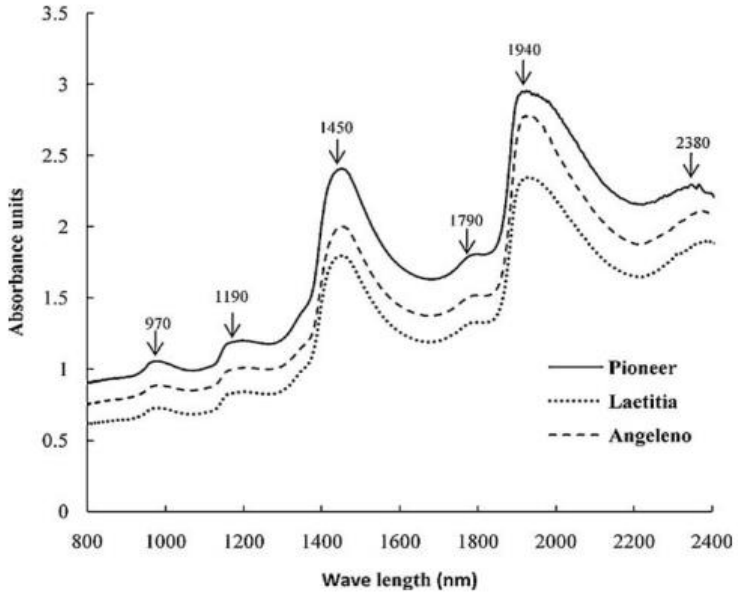

Figure 2.9 Typical NIR spectra for three different Japanese plum fruit taken at start of fruit ripening (Louw and Theron, 2010).

The NIR spectra for different plums followed similar trend with difference in absorbance values at different wavelengths. This shows that similar materials will show similar NIR spectral trend. The peaks in the NIR spectral graph corresponded to the wavelengths associated with the specific chemical composition or components of the material which caused variation in the spectra of the three samples. For example, the peaks at 970, 1190, 1450 and 1940 nm (10309, 8403, 6897 and 5155 cm^{-1}) are due to pure water (Rambala et al., 1997) and peaks at 970 and 1190 nm (10309 and 8403 cm^{-1}) may also be due to sugar content

(Osborne et al., 1993). Thus, water and sugar content apart from other constituents of the fruit were the causes of variation in the spectra (figure 2.9). Actual vs predicted values for given properties were also plotted for all-cultivar model to validate the developed model (figure 2.10).

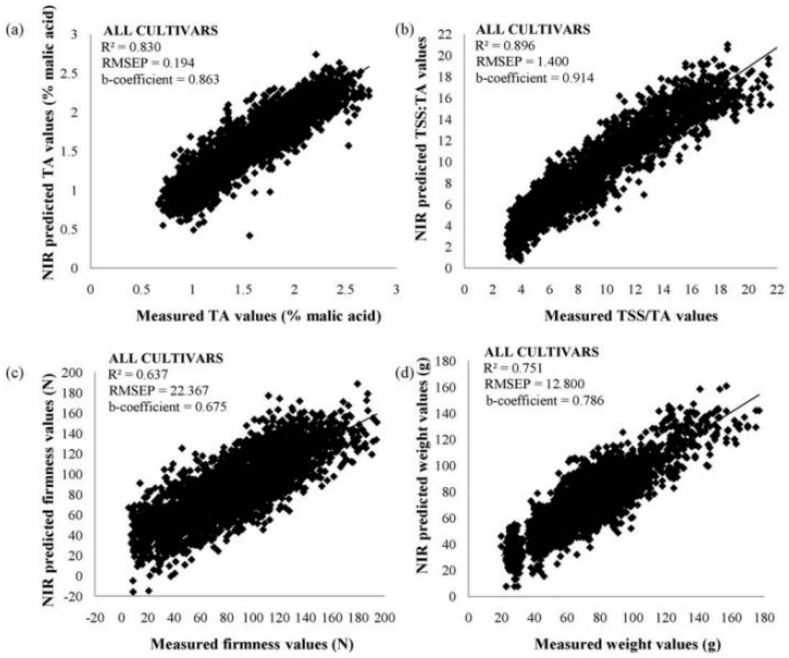

Figure 2.10 Actual vs. predicted values for TA (a), TSS (b), firmness (c) and weight (d) for multi cultivar NIR model (Louw and Theron, 2010).

Via (2013) developed models for predicting load capacity and deflection for oriented strand construction board in presence of phenol formaldehyde resin using NIRS. Models for prediction of load capacity were found to be better with R^2 value of 0.69 than the model for deflection prediction which had R^2 value of 0.59.

Via et al. (2013) collected NIR spectra between 10000 and 4000 cm^{-1} and mid IR (FTIR) spectra at a different wavenumber range (4000 and 650 cm^{-1}) for quick determination of proximate analysis and heating value of torrefied biomass

(pine, sweetgum and switchgrass). PCA technique was used to develop NIR and FTIR models. Actual vs. predicted values obtained from NIRS was also plotted for different parameters. R^2, adjusted R^2, RMSEC and RMSEP values obtained for NIR and FTIR models were tabulated and used to compare prediction efficiency of different models. It was concluded that NIR performed well for most of the multivariate models than FTIR. The R^2 values obtained for prediction of moisture, ash, volatiles, fixed carbon and HHV of the samples were 0.85, 0.92, 0.99, 0.99 and 0.92 respectively.

Summary

The United States and other countries rely heavily on fossil fuels which are available for a limited period of time and which have a negative impact on the environment. Thus, the focus is shifting towards renewable sources of energy such as biomass, solar energy and wind energy to meet the future world energy demand. The advantage that biomass has over other forms of renewable energy is that it is the only renewable source which can be used for producing liquid fuels, chemicals and other products. However, biomass have to be processed and handled before it could be converted into biofuels. Equipment such as mills, grinders, silos, hoppers and conveyors that are used to process and handle biomass can lead to dust generation. If dust is combustible, the presence of ignition source will ignite the dust that can result in a fire or explosion incident. It is therefore important to determine the ignition properties of biomass (e.g. minimum hot surface ignition temperature, temperature of onset of rapid volatilization, temperature of maximum rate of mass loss, oxidation temperature, temperature of rapid exothermic reaction and maximum temperature reached during exothermic reaction). Furthermore, study on physical properties of dust such as moisture content and particle size is also important as it affects dust ignition behavior and can be beneficial in designing dust removal and fire suppression systems.

Our review of literature shows that dusts with smaller particle are more susceptible to ignition. Similarly, dusts with high volatile content and low ash content have higher in terms of risk associated with ignition. Near infrared spectroscopy (NIRS) has been used to analyze and predict a wide range of properties for different materials in the past. It is a quick and inexpensive way to analyze effect of chemical and physical properties of biomass on different parameters. NIRS can be combined with statistical techniques such as principal component analysis (PCA) and partial least squares (PLS) regression analysis to develop prediction models for heating and ignition characteristics of biomass dusts.

Chapter 3 Physical, Chemical and Heating and Ignition Properties of Biomass and Coal Dusts

3.1 Abstract

Plants and refineries utilizing biomass to produce energy have to preprocess, store and handle biomass several times using milling, grinding, sieving and conveying equipment. These operations lead to dust generation and the dust settling on floor and equipment surfaces in the plant or refinery. Accumulated layer of dust on hot surfaces can ignite that can lead to fire and explosion. Therefore, this study was conducted to characterize heating and ignition properties of dusts from 10 biomass feedstocks and three types of coal. The range of values obtained for these properties were 240°C-335°C (MIT), 266°C-448°C (TORV), 304°C-485°C (TMML), 242°C-423°C (TOXY), 206°C-249°C (TRE) and 354°C-429°C (TME). Physical and chemical properties of ground biomass and coal feedstock as well as dusts were also quantified. The effects of these properties on heating and ignition parameters of dusts was also studied. For grassy biomass, dusts with higher ash content had significantly higher MIT ($p<0.0001$). Also, grassy biomass dust with higher volatile matter have lower MIT ($p=0.025$). TORV and TMML of coal dusts were found to decrease with increase in their volatile contents. Grassy biomass dusts with higher ash content and lower volatile matter had significantly higher activation energy values ($p<0.0001$) whereas, woody biomass dusts with

higher energy content had significantly higher TME values (p=0.0013). Based on TORV and TMML values, biomass dusts were found to be at higher risk of ignition than coal dusts. Based on the exothermic energy values, most of the biomass dusts (all except poultry litter dust) are associated with higher release of energy during a dust explosion or fire event than coal dusts.

3.2 Introduction

The world population is currently estimated to be about 7.2 billion and projected to increase to about 9.4 billion by the year 2050 (USCB, 2014). Since energy is needed for sustenance, energy consumption will increase 524 quads in 2010 to 820 quads in 2040 because of this projected increase in population (EIA, 2013). Most of the energy requirement of the world is currently met from nonrenewable fossil fuels (EIA, 2013) that also pose environmental challenges. To meet the increasing energy requirement, more focus is being given to renewable sources of energy such as wind energy, solar energy, hydroelectric power and bioenergy. This is partly responsible for the increase in consumption of renewable energy in U.S. from 3.0 quadrillion Btu in 1950 to 8.8 quadrillion Btu in 2012 (EIA, 2013).

Bioenergy is the energy derived from biomass which includes, but not limited to energy crops, agricultural crops, food, fiber, feed, forest products, aquatic plants, wood residues, industrial and residential waste, processing byproducts and non-fossil organic material (ASABE S593.1, 2011). Bioenergy is the only renewable source of energy that can supply the liquid fuels needed in the industrial

and transportation sectors. In 2012, about 50% (4.4 quadrillion Btu) of the 8.8 quads of renewable energy consumed was derived from biomass (EIA, 2013).

Biomass supply logistics is one of the challenges that has limited its conversion to energy. Biomass logistics consists of biomass harvesting, collection, storage, transportation, pretreatment, and storage. Biomass is low in energy density, high in moisture content and has to be harvested from geographically dispersed locations. As a result there are high logistics costs involved in delivering biomass to conversion plants (An and Searcy, 2012). The various operations involved in the delivery logistics may lead to dust generation (Abbasi and Abbasi, 2007; Eckhoff, 2003). Since biomass feedstocks are combustible (McKendry, 2002), the dust generated from them can cause fire and explosion in process plants. Workers exposed to biomass dusts can also develop health problems (Khan et al., 2008).

The National Fire Protection Association standard 654 defines combustible dusts as “particles passing through a 500 µm sieve which presents a dust fire or dust explosion hazard” (NFPA, 2013). Accumulated layer of combustible dust on hot surfaces can ignite and cause fire hazard or explosion. These dust layers may also be disturbed by an external event such as blowing air or mechanical disturbance resulting in suspension of the dust to form dust cloud. If the concentration of the dust cloud surpasses a critical limit, and the dust cloud is formed in a confined space, dust fire and explosion can occur when an ignition source such as electric spark, hot surface or a naked flame comes in contact with the cloud (Amyotte and Eckhoff, 2010).

Particle size of dust plays an important role in dust ignition. Materials with less particle size has large surface area to volume ratio as compared to material with higher particle size which leads to more oxygen availability for combustion at the surface making the material more readily combustible (Eckhoff, 2003). As the dust particle size decreases in a layer of dust, its ignition temperature also decreases making the material easier to ignite (NFPA, 2013). Chen et al. (1996) found out that ignition temperatures of Kaipin (bituminous) coal and Hongay coal increased as particle size of the samples increased. Kaipin coal samples with size fractions of 105-149 µm, 350-500 µm, 1410-2000 µm and 4000 µm were found to have ignition temperatures of 500°C, 535°C, 600°C and 630°C respectively. Hongay coal samples with size fractions of 350-500 µm, 1410-2000 µm and 4000 µm were found to have ignition temperatures as 515°C, 560°C and 625°C respectively.

Chemical properties of dust material such as volatile matter and ash contents also affect ignition temperature. Volatile matter acts as fuel for combustion with ignition temperature decreasing as volatile content increases (Tognotti et al., 1985; Zhang and Wall, 1994; Chen and Mori, 1995; Chen et al., 1996). Grotkjaer et al. (2003) measured the ignition temperatures of poplar wood (volatile content: 75% d.b.) and eucalyptus wood (volatile content: 64% d.b.) to be 235˚C and 285˚C respectively - an increase in ignition temperature with decreasing volatile matter. Ash largely comprises of the inorganic material which do not contribute towards ignition and therefore act as heat sink and hindering the ignition process (Wang et al., 2011). Vuthaluru (2004) showed that addition of coal (ash

content 9.7% d.b.) to wheat straw (ash content 3.3% d.b.) and wood waste (ash content 0.1% d.b.) samples increased the temperature of onset of rapid mass loss. For 0:100, 70:30, 90:10 and 100:0 (blend coal:wheat straw mass/mass), the temperature of onset of rapid volatilization were found to be 260˚C, 316˚C, 366˚C and 426˚C respectively. Coal and wood waste blends (ratio 0:100, 70:30, 90:10 and 100:0), had temperatures of onset of rapid volatilization to be 291˚C, 345˚C, 350˚C and 426˚C respectively. This shows that the presence of ash retards oxidation/ignition process of biomass.

The study of volatilization properties of biomass is needed to understand the ignition behavior of biomass and coal. Thermal degradation of biomass includes release of moisture and volatiles followed by char oxidation. Gil et al. (2010) in their experiment with pine sawdust showed that temperature ranges for release of water, release and combustion of volatiles, and char oxidation are 25-105˚C, 196-364˚C and 364-487˚C respectively. The lower the temperature of release and combustion of volatiles in a biomass would be, the higher risk of its ignition. Ramirez et al. (2010), estimated temperature of onset of rapid volatilization (TORV) and temperature of maximum mass loss rate (TMML) for icing sugar to be 212ºC and 220 ºC respectively. For maize, wheat and barley TORV values were estimated at 268ºC, 252ºC and 242ºC respectively whereas TMML values were estimated at 279ºC, 283ºC and 271ºC. Both, TORV and TMML values for maize, wheat and barley were more than that of icing sugar indicating that icing sugar has more ignition risk. Oxidation temperature (TOXY) values for

icing sugar (239 ºC), was also smaller than those of maize (289 ºC), wheat (279 ºC) and barley (277 ºC).

Exothermic properties are also used to characterize the ignition behavior of combustible material. This includes determination of the maximum temperature reached during exothermic reaction (TME), temperature required for onset of rapid exothermic reaction (TRE) and exothermic energy from heat flow curves (Ramirez et al., 2010). Dust sample with lower TRE value would be easily ignited than the dust with higher TRE value. Samples with higher values of TME would promote secondary dust fire or ignition by providing sufficient energy for the reaction. Dusts with higher exothermic energy release greater amount of energy during ignition or explosion than samples with lower exothermic energy value. The heat energy released could lead to secondary dust explosions or fires in a processing plant or facility leading to further destruction. Ramirez et al. (2010) estimated TME values for maize, wheat, barley and alfalfa as 386˚C, 283˚C, 311˚C and 288˚C respectively and TRE values for the given samples to be 242˚C, 252˚C, 257˚C and 240˚C respectively.

Determination of heating and ignition properties of biomass dusts is important in order to quantify their ignition risk. It is also important to measure the physical and chemical properties of biomass dusts as they affect the heating and ignition behavior. Therefore, the objective of this study was to characterize the heating and ignition properties, and the physical and chemical properties of biomass dusts.

3.3 Methods and Materials

3.3.1 Raw Material

The ten biomass feedstocks, and the three coal types used in this study are listed in table 3.1. Moisture content of the raw samples was measured (in triplicates) using ASTM E871-82 standard (ASTM E871-82, 2006). About 2 g of raw sample was placed in a conventional oven at 105ºC for 24 hours (VWR International model 1370FM, Sheldon Mfg., OR, USA) (figure 3.1). Sugarcane bagasse and sweetgum chips were dried prior to grinding because of their high moisture content. Sweetgum chips were air dried under a shed at Agricultural Land and Resource Management Center using fans for a week (figure 3.2a). Sugarcane bagasse was dried at 45°C with a food dehydrator (Excalibur Food Dehydrator, Sacramento, CA, USA) (figure 3.2b). Moisture contents of dried samples were also determined. Moisture content measurements are presented on wet basis.

3.3.2 Grinding and Dust Collection

The samples were ground with a hammer mill (C.S. Bell Co., model 10HBLPK, Tiffin, OH, USA) (figure 3.3 a) fitted with a 3.175 mm (1/8th inch) screen. Dust was obtained from the ground material by passing it through #35 market grade (437 μm) screen using a vibratory sieve shaker (Kason Corp., model K30-2-8S, NJ, USA) (figure 3.3 b). This is the closest screen size to the NFPA 654 standard's 500 μm size definition of dust (NFPA, 654). Pecan shell and lignite coal samples obtained were already in dust form and were not ground using hammer mill. Dust collected from each feedstock was stored in three 80 oz. air tight containers for

further analysis that includes characterization of physical, chemical, heating and ignition properties and near infrared spectroscopy (NIRS) analysis. Ground material (1/8th inch hammer mill screen size) for biomass feedstock and coal samples was also stored in air tight containers for further analysis of physical and chemical properties.

Table 3.1 List and sources of biomass feedstocks and coals used in the study.

Sample	Source
Corn Stover	Purdue University
Corn Cobs	Purdue University
Sugarcane Bagasse	Louisiana State University
Sweetgum	Auburn University
Poultry Litter	Department of Poultry Science, Auburn University
Loblolly Pine	South Alabama forests
Eucalyptus	Auburn University
Bermuda Grass	North Alabama
Pulverized river bed (PRB) coal (sub-bituminous)	National Carbon Capture Center, Wilsonville
Bituminous Coal	Alabama Power, Birmingham
Lignite Coal	National Carbon Capture Center, Wilsonville
Pecan Shells	Louisville Pecan Company
Switchgrass	E.V. Smith Research Station

Figure 3.1 Conventional oven used for moisture content determination.

(a) **(b)**

Figure 3.2 Air drying of sweetgum wood chips (a) and drying sugarcane bagasse in food dehydrator (b).

(a) **(b)**

Figure 3.3 Hammer mill used for grinding biomass feedstock (a) and vibratory screen used for collection of dust (b).

3.3.3 Physical and Chemical Properties

3.3.3.1 Moisture Content

Moisture content of the ground material and dust collected from each biomass feedstock and coal type was measured using a moisture content analyzer (IR 200, Denver Instrument, Avrada, CO) according to ASTM E871-82 standard (ASTM E871-82, 2006). This involved about 2g sample on the sample pan of the analyzer and exposing the sample to temperature of 105°C until the balance of the moisture meter did not detect a change in sample mass greater than 0.05% per minute. The experiment was carried out in triplicates and equation 3.1 was used to estimate moisture content of samples.

$$MC_{wb} = \frac{M_{wet} - M_{dry}}{M_{wet}} X\ 100 \qquad (3.1)$$

where,

MC_{wb}= moisture content - wet basis (%),

M_{wet} = initial mass of sample (g), and

M_{dry} = final mass of sample (g).

3.3.3.2 Bulk Density

Bulk density was measured in triplicates with a bulk density apparatus (OHAUS, Burrows Co., Evanston, IL) (figure 3.4) on all ground and dust samples using the ASABE standard S269.5 (ASABE, 2012). All the samples were dried for

24 hours at 105°C to nullify the effect of moisture. Sample was poured from a set height of 610 mm (above top edge of container) through a funnel into a container of known volume (1137 ml). The mass of the dust sample required to fill the container was recorded and bulk density was calculated as follows:

$$\rho_{bulk} = \frac{M}{V} \qquad (3.2)$$

Where,

ρ_{bulk} = bulk density (kg/m^3),

M = mass of sample (kg) and,

V = volume of container (m^3).

3.3.3.3 Particle Density

A gas pycnometer (AccuPyc 1330, Micrometrics Instrument Corp., Norcross, GA, USA) (figure 3.5) was used to estimate average volume of the particles (based on three replications). The pycnometer estimates the volume of particles by passing helium gas through the chamber containing known mass of sample and measuring the change in pressure. Particle density was calculated as ratio of mass of dust sample to the volume obtained from pycnometer. All the samples were dried for 24 hours at 105°C before measuring the particle density to reduce the effect of moisture content.

Figure 3.4 Apparatus for measuring bulk density.

Figure 3.5 Gas pycnometer used for estimation of particle density.

3.3.3.4 Particle Size Distribution

A particle size analyzer that uses digital imaging system (CAMSIZER, model D-4278, Haan, Germany) (figure 3.6) was used to estimate volume based particle size distribution of the ground and dust sample. All samples (ground and

dusts) were dried for 24 hours at 105°C before analyzing the particle size distribution. Geometric mean diameter and geometric standard deviation was calculated according to ASABE S319.3 standard (ASABE, 2003) from the data obtained from the imaging system (equations 3.3 – 3.5).

$$d_{gw} = log^{-1}\left[\frac{\sum_{i=1}^{n}\left(M_i log\bar{d}_i\right)}{\sum_{i=1}^{n} W_i}\right] \quad (3.3)$$

$$S_{log} = \left[\frac{\sum_{i=1}^{n} M_i\left(\log\ \bar{d}_i - log\ d_{gw}\right)^2}{\sum_{i=1}^{n} W_i}\right]^{1/2} \quad (3.4)$$

$$S_{gw} = \frac{1}{2}\ d_{gw}\ \left[log^{-1}S_{log} - \left(log^{-1}S_{log}\right)^{-1}\right] \quad (3.5)$$

Where,

d_{gw} is geometric mean diameter of particles (mm),

S_{log} is geometric standard deviation of log-normal distribution by mass in base 10 logarithm (dimensionless),

S_{gw} is geometric standard deviation of particle diameter by mass (mm),

n is the number of sieves + 1 (pan),

$\overline{d_i} = (d_i \times d_{i+1})^{1/2}$,

d_i is nominal sieve aperture size of the i^{th} sieve (mm),

d_{i+1} is the nominal sieve aperture size of the i^{th} + 1 sieve (mm),

M_i is the mass of the sample retained on the i^{th} sieve (g).

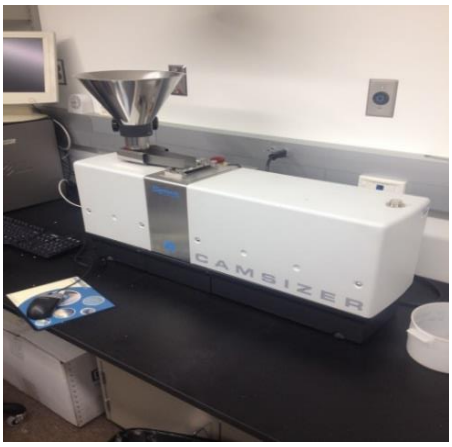

Figure 3.6 Digital imaging particle size analyzer.

3.3.3.5 Ash Content

The ash content of the ground and dust samples was determined according to National Renewable Energy laboratory (NREL, 2005) laboratory analytical procedure. Porcelain crucibles were marked and kept in a muffle furnace (Thermoscientific, model F6020C, Dubue Iowa, USA) (figure 3.7) at 575ºC for four hours. Crucibles were then removed and placed directly into the desiccator till they cooled down for about an hour. The mass of the dried crucibles was recorded and known amount of sample (within a range of 0.5-2 g) was placed into crucibles. Crucibles were placed back into the furnace set at 105ºC and furnace was held at that temperature for 12 minutes. Furnace was then ramped to 250ºC at 10ºC/min and was held at this temperature for 30 minutes. Furnace was again ramped to 575ºC at 20ºC/min and was held at that temperature for 180 minutes. Furnace was allowed to cool to 105ºC and the samples were removed. Ash content was

calculated according to ASTM standard (ASTM D 3174-04, 2004) using equation 3.6. Experiment was triplicated for each sample.

$$Ash = \left[\frac{M_{ca} - M_c}{M_s}\right] X \left(\frac{100}{100 - M_{wb}}\right) \quad (3.6)$$

where,

Ash = estimated percentage of ash in biomass (%),

M_{ca} = final mass of crucible with ash after completion of experiment (g),

M_c = mass of empty crucible (g) and,

M_s = initial mass of biomass sample (g), and

M_{wb} = moisture content of biomass sample on wet basis (%)

Figure 3.7 Muffle furnace used for ash content determination.

3.3.3.6 Volatile Matter Content

The volatile matter content of ground and dust samples of the biomass and coal samples were measured using ISO 562 standard (ISO 562, 2002). Crucibles and their lids were cleaned and placed in the volatile matter furnace (VMF Carbolite, model 10/6/3216P, England) (figure 3.8) that was at a temperature of 900ºC for an hour. They were then placed in a desiccator until they cooled down to room temperature. About 1±0.1 g of sample was added into each crucible. Crucibles with lids containing samples were placed in the furnace at 900ºC for seven minutes. They were then taken out and allowed to cool in the desiccator. They were weighed again and volatile matter content was determined using equation 3.7 (ISO 562, 2002). Three replications were performed for each dust sample.

$$VM = \left[\frac{100\ (M_3 - M_1)}{M_2 - M_1}\right] X \left(\frac{100}{100 - M_{wb}}\right) \qquad (3.7)$$

Where,

VM= volatile matter content on dry basis (%),

M_1= mass of empty crucibles and lid (g),

M_2= initial mass of crucible, lid and sample (g),

M_3= final mass of crucible, lid and sample (g) and,

M_{wb}= moisture content on (w.b. %)

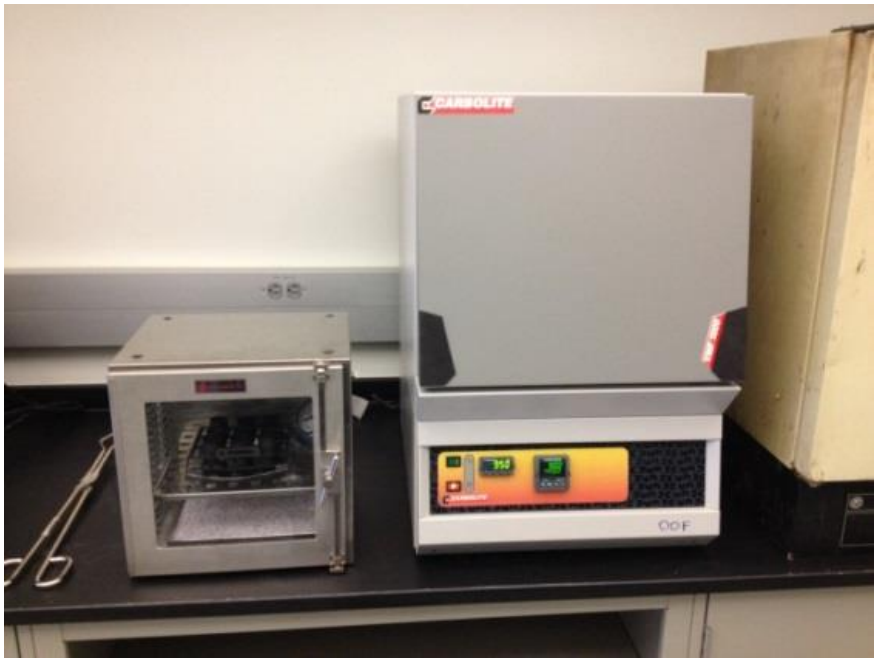

Figure 3.8 Volatile matter determination furnace.

3.3.3.7 Energy Content

A bomb calorimeter (IKA Works Inc., model C200, Wilmington, NC, USA) (figure 3.9) was used to estimate the energy content of the ground and dust samples. About 0.5 to 1 g of sample was compressed to a pellet form using a press (IKA Works Inc., model C21, Wilmington, NC, USA) and was weighed. The pellet was connected to the ignition wire using a thread and was placed in a pressurized (with oxygen) decomposition chamber. The decomposition chamber was placed inside the bomb calorimeter where the sample was combusted completely and energy content was recorded. Experiment was performed in triplicates.

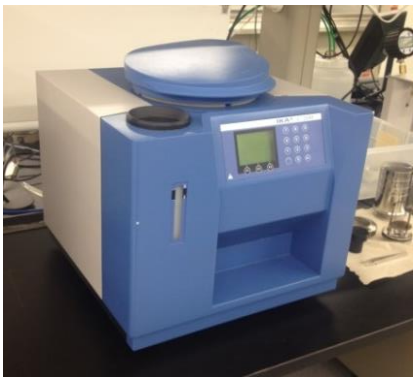

Figure 3.9 Bomb calorimeter used for energy content determination.

3.3.4 Heating and Ignition Properties

3.3.4.1 Hot Surface Ignition Temperature

Hot surface ignition temperature of dust samples was determined according to ASTM E2021 standard (2010). A hot plate (VMWare, Thorofore, NJ, USA) (figure 3.10) was used to heat the dust sample and to estimate hot surface ignition temperature. Apparatus consisted of a hot plate, a cylindrical metal plate (200 mm in diameter and 20 mm thick), a metal ring (12.7 mm in diameter and 10 mm thick) and a bare wire type-K thermocouple wire (0.20 mm dia) connected to a datalogger. The metal plate rested on the hot plate and the metal ring was placed on top of the metal plate. The bare type thermocouple was installed through the holes in the metal ring at a height of 5 mm. Another K-type thermocouple (insulated, 0.25 mm dia) was also connected to the metal plate to measure its temperature. Temperatures from both thermocouples were recorded using a datalogger (Fuji Electric Systems Co., Ltd., Tokyo, Japan) at 5 s intervals. Desired temperature was set initially on the temperature controller of the hot plate. Once

the desired temperature was reached, the metal ring was filled with the dust sample. Sample was leveled with the top of metal ring. Temperature of the dust layer was monitored and recorded continuously. If ignition did not occur, a new dust sample layer is used and the test was repeated with a new set temperature 5ºC higher than the previous one. Tests were repeated until ignition occurred and was confirmed by running two more tests, at maximum temperature where ignition did not occur and at minimum temperature at which ignition occurred.

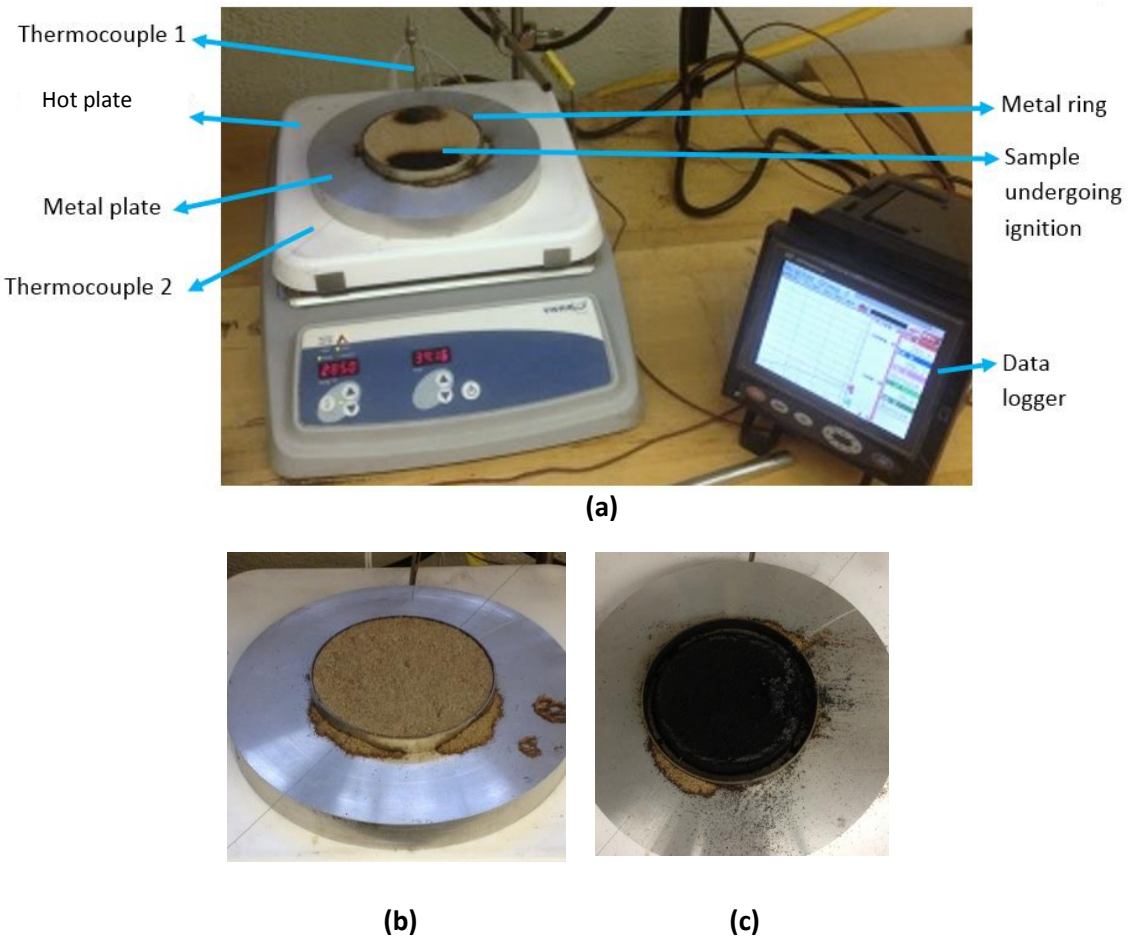

Figure 3.10 Apparatus to measure minimum hot surface ignition temperature (a), metal ring filled with dust sample before ignition (b), dust sample after ignition (c).

3.3.4.2 Volatilization Properties

Temperature of onset of rapid volatilization (TORV), temperature of maximum rate of mass loss (TMML) and oxidation temperature (TOXY) were estimated using mass loss curves obtained from thermogravimetric analyzer equipment (TGA, model Pyris1, PerkinElmer, Shelton, CT, USA) (figure 3.11). About 5 mg of sample was heated in air and oxygen environments from 30ºC to 800ºC at 20ºC/min. TORV and TMML temperatures were obtained from mass loss data of samples heated in air environment while TOXY was estimated from mass loss data of samples heated in oxygen environment since a single oxidation temperature could not be obtained when sample is heated in air (Ramirez et al., 2010). The desired temperatures were estimated with the software supplied by TGA equipment manufacturer. Experiments were conducted in triplicate.

Figure 3.11 Thermogravimetric analyzer (TGA) used to measure volatilization properties.

Isoconversional method was applied to the air atmosphere mass loss data to estimate activation energies associated with biomass dust volatilization. This method has been widely used to estimate kinetic parameters during thermal decomposition of biomass (Park et al., 2009; Biagini et al., 2008; Ramirez et al., 2010). The mass loss data was used to calculate conversion (α) at any time t, using equation 3.8 (SSCHE, 2009; White et al., 2011; Park et al., 2009).

$$\alpha = \frac{m_0 - m}{m_0 - m_\infty} \tag{3.8}$$

where,

m_0 is initial mass of the sample (mg),

m is actual sample mass (mg),

m_∞ is residual mass at the end of TGA experiment (mg).

Rate of decomposition $\left(\frac{d\alpha}{dt}\right)$ is a function of temperature and conversion (equation 3.9) (White et al., 2011; Friedman, 1963).

$$\frac{d\alpha}{dt} = k(T)g(\alpha) \tag{3.9}$$

where,

k(T) is a function of temperature,

g(α) is a function of conversion.

Temperature dependent function is expressed by Arrhenius equation (equation 3.10) whereas the conversion function is given by equation 3.11 (White et al., 2011; Friedman, 1963).

$$k(T) = A\ exp\left(\frac{-E}{RT}\right) \quad (3.10)$$

$$g(\alpha) = (1-\alpha)^n \quad (3.11)$$

Where,

A is pre-exponential factor (1/s),

E is activation energy (J/mol),

R is universal gas constant (8.314 J K^{-1} mol^{-1}).

Using natural logarithmic function equation 3.9 can be rewritten as equation 3.12 (Ramirez et al., 2010).

$$ln\left(\frac{d\alpha}{dt}\right) = lnA + n * \ln(1-\alpha) - \frac{E}{RT} \quad (3.12)$$

A graph of $ln\left(\frac{d\alpha}{dt}\right)$ vs inverse of absolute temperature (1/T) was plotted. The activation energy (E) was obtained from the slope $(-\frac{E}{R})$.

3.3.4.3 Exothermic Parameters

A differential scanning calorimeter (TA Instruments, model Q200, New Castle, DE, USA) (figure 3.12) was used to estimate temperature of rapid exothermic reaction (TRE), maximum temperature reached during exothermic reaction (TME) and exothermic energy. This involved measuring heat flow required to heat about 5 mg of sample from 30ºC to 550ºC at the rate of 20ºC/min. The sample was held at 550ºC for ten minutes. A plot of heat flow vs. temperature was

obtained from the software provided by the manufacturer of the equipment. The exothermic reaction parameters were also obtained using the same software.

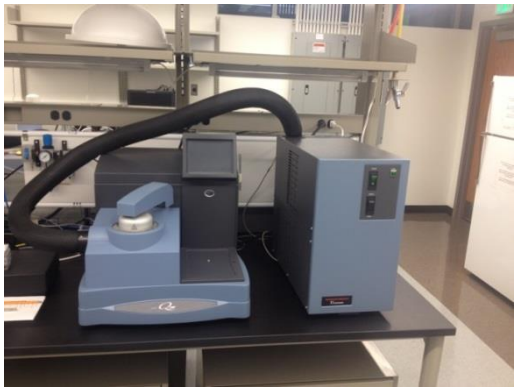

Figure 3.12 Differential scanning calorimeter (DSC) equipment used to determine exothermic parameters of dust samples.

3.3.5 Data Analysis

Tukey tests were performed on the measured physical, chemical, heating and ignition properties for biomass and coal dusts that were significantly different from others (95% significance level) using Statistical Analysis Systems (SAS,2009). Tukey test was also performed on measured physical and chemical properties for ground biomass and coal samples. Biomass dust samples were categorized into grassy biomass (switchgrass, Bermuda grass, corn stover and sugarcane bagasse) and woody biomass (eucalyptus, pine, sweetgum) groups because of similar nature of the samples in a group before carrying out correlation analysis for physical, chemical, heating and ignition properties of the dust samples. Graphs were plotted using Microsoft Excel (Microsoft Excel, Redmond, WA). Each experimental run was triplicated.

3.4 Results and Discussion

3.4.1 Physical and Chemical Properties

Geometric mean diameter and geometric standard deviation values for biomass and coal ground samples and dust samples are given in table 3.2 and table 3.3 respectively. Values of other physical and chemical properties (bulk density, particle density, volatile matter, ash content and energy content) obtained for all the ground samples and dust samples are given in table 3.4 and table 3.5 respectively. These results are discussed in more details below.

Table 3.2 Geometric mean diameter and geometric standard deviation values of ground (through 3.175 mm screen size) samples.

Sample	Geometric mean size, d_{gw} (μm)	Geometric Standard deviation, S_{gw} (μm)
Bermuda grass	1013	680
Bituminous coal	274	179
Corn cobs	636	512
Corn stover	568	481
Eucalyptus	596	512
Pine	846	668
Poultry litter	526	524
PRB coal	302	200
Sugarcane bagasse	554	445
Sweetgum	847	702
Switchgrass	1074	590

Pecan shell and lignite coal samples were received in dust form

Table 3.3 Geometric mean diameter and geometric standard deviation values of dust samples (passing through 437 µm screen).

Sample	Geometric mean size, d_{gw} (µm)	Geometric Standard deviation, S_{gw} (µm)
Bermuda grass	526	520
Bituminous coal	237	128
Corn cobs	398	246
Corn stover	337	208
Eucalyptus	278	178
Lignite coal	319	221
Pecan shell	261	126
Pine	516	349
Poultry litter	204	126
PRB coal	216	107
Sugarcane bagasse	282	175
Sweetgum	420	388
Switchgrass	598	575

3.4.1.1 Moisture Content

Moisture contents for the biomass feedstock before and after grinding operation are depicted in figure 3.13. Moisture contents of the ground samples was found to be significantly (α=0.05) less than initial moisture content except for bituminous coal, sugarcane bagasse and sweetgum. Loss of moisture can be attributed to the heat generated due to particle-particle and particle-hammer friction during the grinding process. Also, the higher surface area ground samples facilitated the drying process (Probst et al., 2013). Probst et al. (2013) measured initial and post-grinding (hammer mill) moisture content for corn and corncobs samples.

Table 3.4 Measured physical and chemical properties of ground biomass and coal samples

Sample	Bulk Density (kg/m^3)	Particle Density (kg/m^3)	Volatile Matter (% db)	Ash Content (% db)	Energy Content (MJ/kg)
Biomass Samples					
Bermuda grass	127.01 ± 1.65^{f}	1106.60 ± 3.1^{h}	$84.51\pm0.48^{c,d}$	4.02 ± 0.15^{d}	$19.42\pm0.06^{c,d}$
Corn cobs	160.24 ± 1.06^{d}	1359.03 ± 1.77^{e}	$88.57\pm0.85^{a,b}$	1.06 ± 0.01^{e}	19.25 ± 0.05^{d}
Corn stover	93.61 ± 1.35^{g}	1267.00 ± 2.51^{g}	81.24 ± 2.02^{d}	7.58 ± 1.59^{b}	18.16 ± 3.2^{e}
Eucalyptus	196.34 ± 0.91^{b}	1427.47 ± 2.84^{d}	$88.36\pm1.36^{a,b}$	0.66 ± 0.52^{e}	$19.80\pm0.06^{b,c}$
Pine	184.44 ± 1.37^{c}	1465.47 ± 2.08^{c}	$85.44\pm1.02^{b,c}$	0.48 ± 0.13^{e}	20.68 ± 0.04^{a}
Poultry litter	271.10 ± 2.70^{a}	1501.27 ± 1.86^{b}	84.83 ± 0.76^{c}	9.43 ± 0.15^{a}	18.35 ± 0.33^{e}
Sugarcane bagasse	92.20 ± 1.44^{g}	1535.27 ± 5.12^{a}	$83.81\pm0.22^{c,d}$	5.84 ± 0.52^{c}	19.01 ± 0.08^{d}
Sweetgum	166.42 ± 0.71^{d}	1461.40 ± 0.75^{c}	89.86 ± 1.75^{a}	0.66 ± 0.06^{e}	19.88 ± 0.24^{b}
Switchgrass	142.13 ± 1.41^{e}	1319.43 ± 3.57^{f}	$84.16\pm0.74^{c,d}$	$4.94\pm0.31^{c,d}$	19.13 ± 0.14^{d}
Coal Samples					
Bituminous coal	651.74 ± 1.67^{a}	1385.03 ± 1.88^{b}	38.87 ± 0.24^{b}	10.47 ± 0.95^{a}	31.75 ± 0.58^{a}
PRB coal	615.41 ± 1.60^{b}	1490.57 ± 3.00^{a}	53.71 ± 0.54^{a}	7.82 ± 0.24^{a}	27.11 ± 0.07^{b}

***Superscripts with same letters in a column are not significantly different from each other ($\alpha=0.05$)**

Table 3.5 Measured physical and chemical properties of biomass and coal dust samples

Sample	Bulk Density (kg/m^3)	Particle Density (kg/m^3)	Volatile Matter (% db)	Ash Content (% db)	Energy Content (MJ/kg)
Biomass Samples					
Bermuda grass	159.28 ± 1.43^{f}	1167.33 ± 1.65^{h}	$78.61 \pm 0.85^{c,d}$	4.68 ± 0.16^{d}	19.14 ± 0.06^{c}
Corn cobs	164.86 ± 2.00^{f}	$1481.43 \pm 0.17^{e,f}$	81.51 ± 1.51^{b}	2.62 ± 0.08^{e}	19.08 ± 0.05^{c}
Corn stover	126.52 ± 1.76^{h}	1500.90 ± 4.56^{d}	72.97 ± 0.58^{e}	14.33 ± 0.26^{b}	17.17 ± 0.07^{e}
Eucalyptus	217.60 ± 2.08^{c}	$1490.30 \pm 2.19^{d,e}$	$81.27 \pm 0.14^{b,c}$	1.40 ± 0.12^{f}	19.51 ± 0.06^{b}
Pecan shell	403.95 ± 2.61^{a}	1521.93 ± 0.95^{c}	64.93 ± 0.19^{f}	2.68 ± 0.04^{e}	20.31 ± 0.17^{a}
Pine	173.06 ± 3.43^{e}	1471.87 ± 3.80^{f}	84.97 ± 0.82^{a}	1.10 ± 0.14^{f}	20.55 ± 0.07^{a}
Poultry litter	360.74 ± 3.71^{b}	1539.23 ± 1.51^{b}	71.43 ± 0.21^{e}	13.74 ± 0.07^{b}	17.43 ± 0.06^{e}
Sugarcane bagasse	112.34 ± 1.74^{i}	1585.27 ± 2.42^{a}	72.41 ± 1.18^{e}	15.52 ± 0.27^{a}	16.69 ± 0.07^{f}
Sweetgum	183.57 ± 1.37^{d}	$1480.47 \pm 2.85^{e,f}$	86.82 ± 0.55^{a}	1.41 ± 0.22^{f}	19.71 ± 0.07^{b}
Switchgrass	141.01 ± 0.63^{g}	1366.17 ± 5.59^{g}	77.86 ± 0.73^{d}	7.57 ± 0.35^{c}	18.77 ± 0.12^{d}
Coal Samples					
Bituminous coal	651.75 ± 3.88^{a}	1406.20 ± 13.98^{c}	33.00 ± 0.05^{b}	10.27 ± 1.81^{b}	32.26 ± 0.02^{a}
Lignite coal	503.40 ± 3.34^{b}	1672.20 ± 2.38^{a}	53.69 ± 7.14^{a}	20.84 ± 0.16^{a}	26.78 ± 0.57^{b}
PRB coal	655.66 ± 3.19^{a}	1505.13 ± 0.66^{b}	47.06 ± 0.53^{a}	8.14 ± 0.07^{b}	27.41 ± 0.16^{b}

Superscripts with same letters in a column are not significantly different from each other (α=0.05)

The author also reported that the mean moisture of corncobs with initial moisture contents of 10.04%, 14.65% and 20.13% (w.b.%), reduced to 8.53%, 9.19% and 12.93% (w.b.%) respectively after grinding. We however found that samples with moisture content less than 6% before grinding showed a significant (α=0.05) increase in moisture content after grinding. This can be attributed to the hygroscopic nature of the material as material with low moisture content (less than atmospheric moisture content) tends to absorb moisture from the environment. Samples with initial moisture content less than 6% were the ones that were dried after receiving.

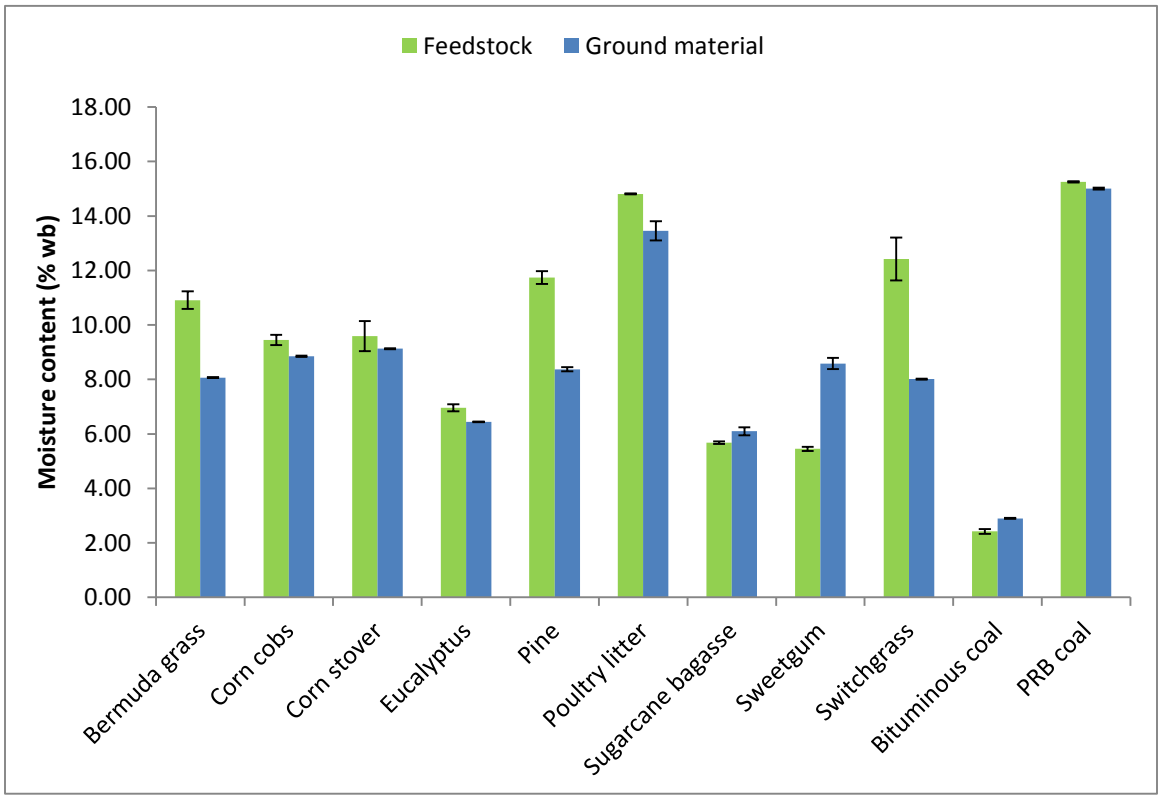

Pecan shell and lignite coal samples were received in dust form

Figure 3.13 Moisture content before and after grinding biomass and coal.

3.4.1.2 Particle Size Distribution

Geometric mean diameter and geometric standard deviations obtained for the ground samples are given in table 3.2. Geometric mean particle size of ground material (3.175 mm screen size) for all the feedstock varied from 274 µm (bituminous coal) to 1074 µm (switchgrass) and as expected were greater than the geometric mean size for their respective dust samples (table 3.3).

Particle size distributions for the different dust samples are shown in figure 3.14. All the dust samples showed skewness in particle size distribution (log-normal distribution) which is typically obtained for naturally occurring particle populations (Rhodes, 1998; Fasina, 2008). Geometric mean diameter and geometric standard deviations obtained for all the dust samples are given in table 3.2. The geometric mean diameter of particles for the dust samples varied from 204 µm (poultry litter) to 598 µm (switchgrass). The sieve size assigned by NFPA (NFPA, 2013), 500 µm falls within this range. As expected, the geometric mean diameter for most dusts was smaller than the sieve size (437 µm) used to fractionate them from ground material. However, in case of switchgrass and Bermuda grass, the geometric mean diameter of the dust samples was greater than that of sieve size as many long and thin particles managed to pass through the sieve (figure 3.15).

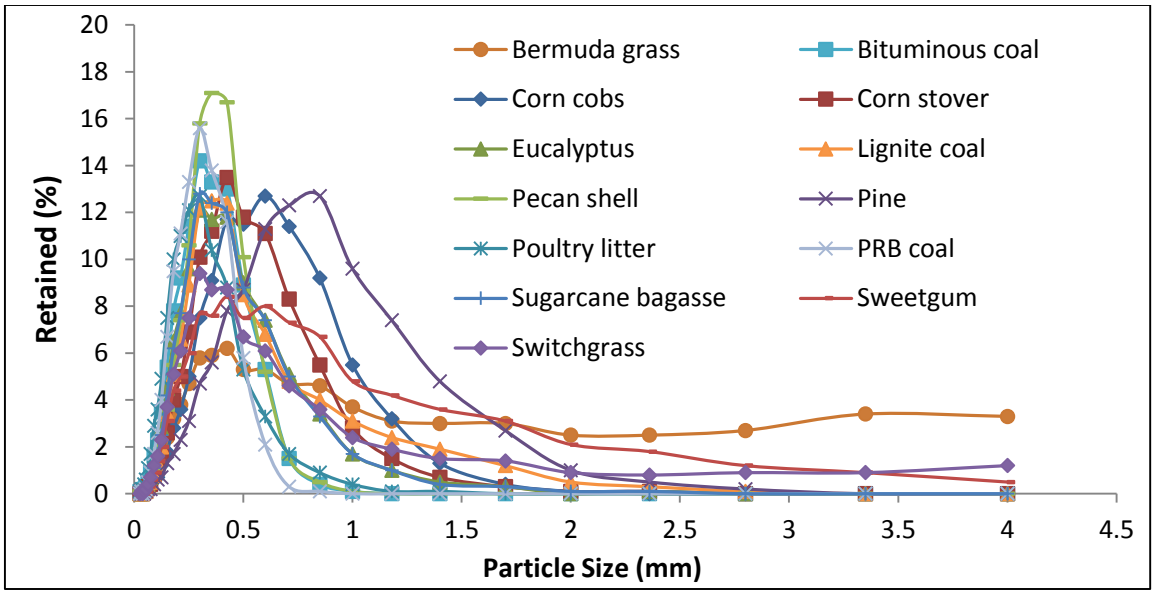

Figure 3.14 Particle size distribution of dust samples.

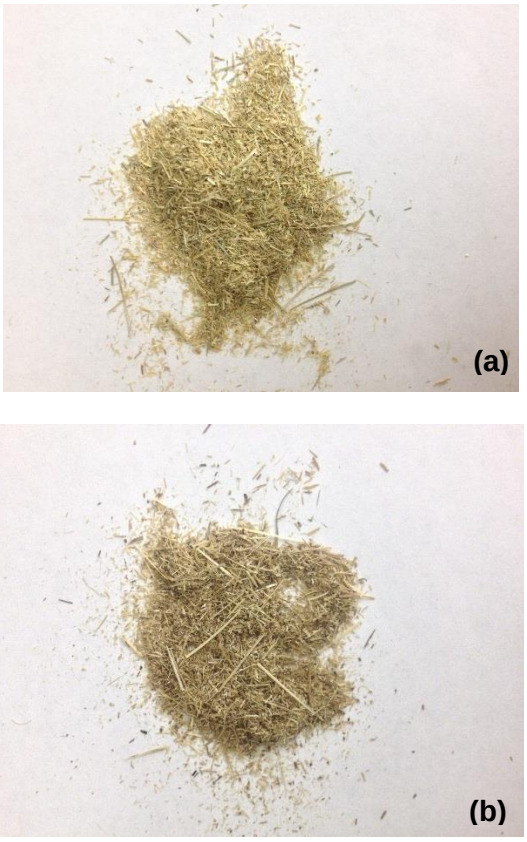

Figure 3.15 Elongated particles in Bermuda grass dust (a) and switchgrass dust (b) samples.

3.4.1.3 Bulk Density

Bulk density of ground material varied from 92.20 kg/m^3 (sugarcane bagasse) to 651.74 kg/m^3 (Bituminous coal) whereas for dust samples it varied from 112.34 kg/m^3 (sugarcane bagasse) to 655.66 kg/m^3 (PRB coal). Bulk density of ground Bermuda grass, corn stover, eucalyptus, poultry litter, PRB coal, sugarcane bagasse and sweetgum was found to be significantly (α=0.05) less than bulk density of corresponding dust samples for (figure 3.16). This is because larger particles have larger void spaces between them which occupy more volume whereas finer particles tend to rearrange themselves to fill the voids between coarser/larger particles resulting in more mass per unit volume and thus higher bulk density (Mani et al., 2003; Tabil, 1996). Also, higher ash content of dusts leads to higher bulk density because of higher particle density of ash (see section 3.4.1.5). For example, the particle density of ash obtained from sugarcane bagasse dust sample was measured to be 2781.5±3.46 kg/m^3. Bulk density of wheat straw grinds increased from 77 kg/m^3 to 115 kg/m^3 as geometric mean particle diameter decreased from 1.43 mm to 0.25 mm (Mani et al., 2004). Bulk density of ground corn cobs and corn cobs dust was not significantly different. This can be attributed to the heavier particles (which did not reduce in size below a certain size during hammer mill operation) in ground corn cobs sample which passed through the 3.175 mm hammer mill screen but could not pass through the 437 µm screen used to collect dust.

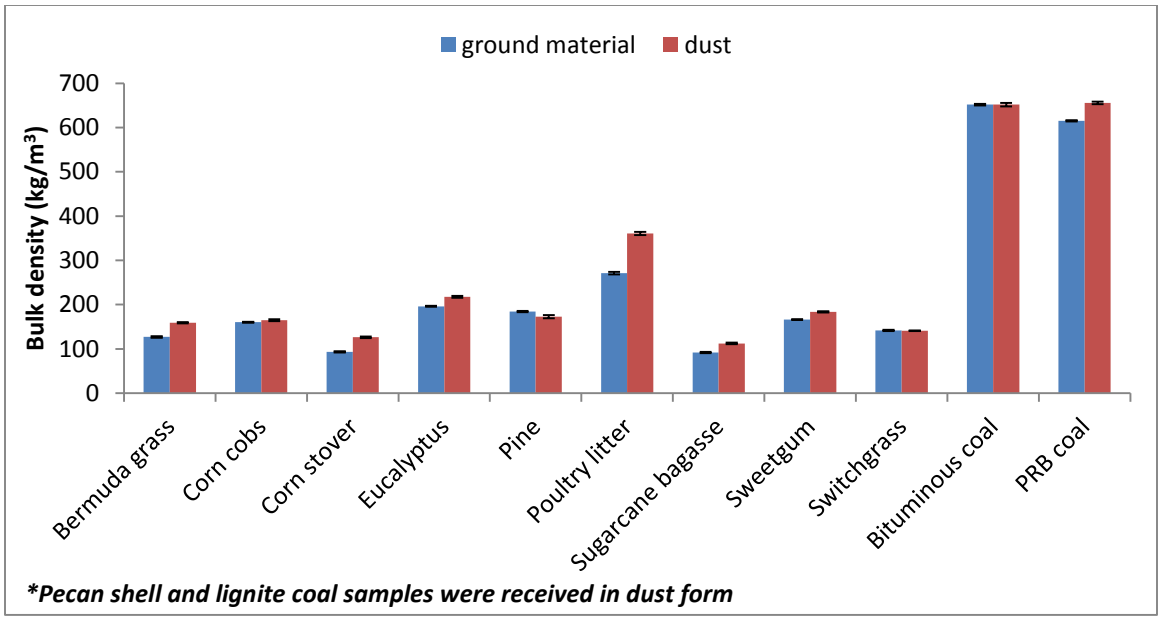

Figure 3.16 Bulk density of ground and dusts from biomass and coal.

3.4.1.4 Particle Density

Particle density for ground material varied from 1106.6 kg/m^3 (Bermuda grass) to 1535.3 kg/m^3 (sugarcane bagasse) whereas for dust samples, it varied from 1167.33 kg/m^3 (Bermuda grass) to 1585.27 kg/m^3 (sugarcane bagasse). Mean particle density for ground material was found to be less than that of the dusts for all feedstocks (figure 3.17). This is because individual particles become less dense as the particle size increases (Littlefield et al., 2011) as there is reduction in porosity within a particle with decrease in particle size (Mani et al., 2004). Particle densities of ground bituminous coal and pine were not significantly (α=0.05) different from their respective dust samples. Mean particle density for corn stover dust was measured to be 1500.90 kg/m^3. Mani et al. (2006) reported the particle density of corn stover ground through hammer mill screen size of 0.8 mm to be 1399.16 kg/m^3.

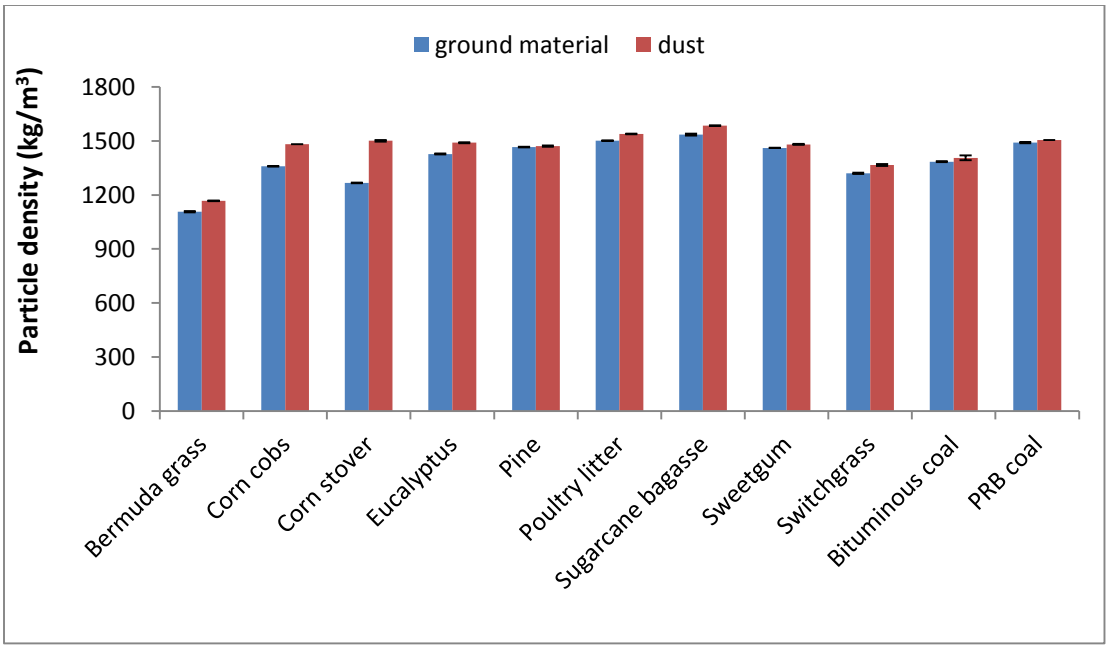

Pecan shell and lignite coal samples were received in dust form

Figure 3.17 Particle densities of ground and dusts from biomass and coal.

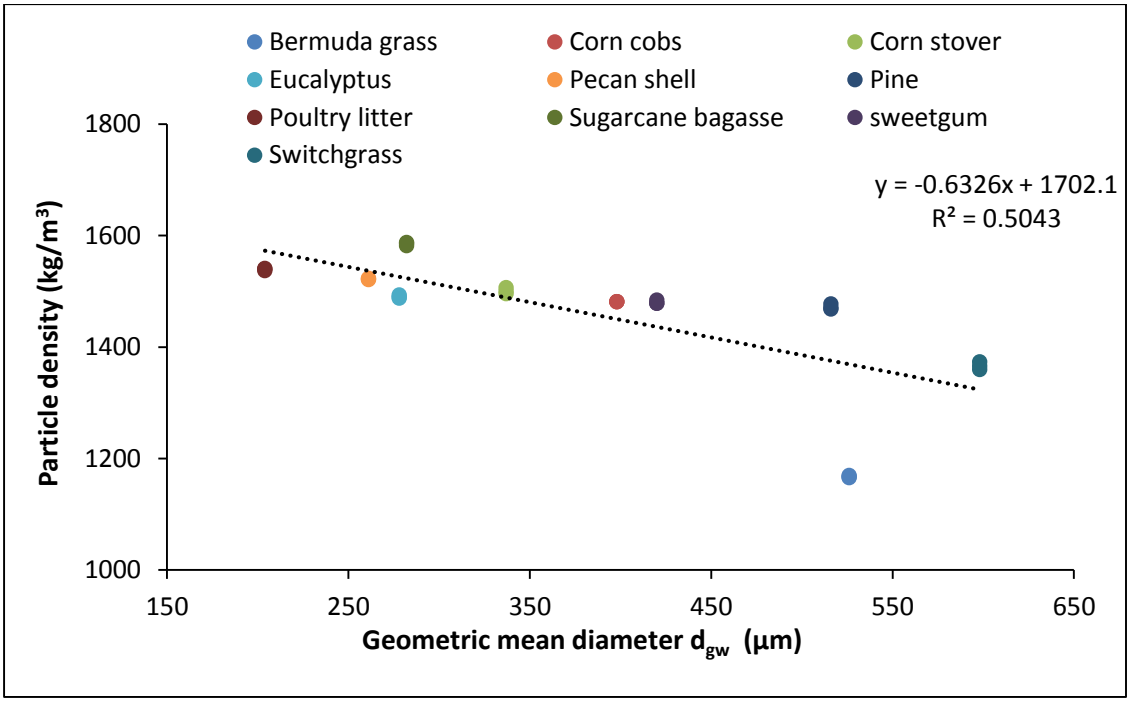

Figure 3.18 Particle density dependence on geometric mean particle size in case of all biomass dusts.

The geometric mean particle diameter of biomass dusts had a significant effect on particle density ($p<0.0001$). Particle density was found to be higher in dusts with smaller geometric mean diameter (Pearson's correlation coefficient, r=-0.71) (figure 3.18). This is because in large biomass particles, there are voids within the particles that do not contribute to the mass of the particle. As the particle size becomes small (due to grinding), internal particulate voids are reduced leading to increase in particle density (Mani et al., 2004; Esteban and Carrasco, 2006). In their experiment with raw pecan shells divided into three different sieve size fractions (>1.885 mm, 1.295-1.885 mm and <1.295 mm), Littlefield et al. (2011) showed that with decrease in size, particle density increased. Mani et al. (2006) also showed that particle density increased for ground wheat straw, barley straw, corn stover and switchgrass as the hammer mill screen size decreased from 3.2 mm to 0.8 mm. Dusts with smaller particle sizes also have higher particle densities because of more ash content in finer fractions of material (Hehar, 2013), which have higher particle densities (1760 – 2760 kg/m3) (Ghosal and Self, 1995) than biomass or coal dusts.

3.4.1.5 Ash Content

Ash content of ground material varied from 0.48% d.b. (pine) to 10.47% d.b. (bituminous coal) whereas, ash content of the dust samples varied from 1.10% d.b. (pine) to 20.84% (lignite coal) where. Ash content of ground biomass samples was found to be significantly ($\alpha=0.05$) less than the ash content of dusts except eucalyptus (figure 3.19) that had lower ash content in ground sample but was not significantly different from ash content of the dust. Ground biomass material had

less ash content than dusts because the inorganic content is more grindable and are easily separated into finer fractions from lignocellulosic structure of biomass during grinding (Hehar, 2013). Liu and Bi (2011) also obtained similar results with switchgrass sample milled to obtain size less than 1 mm. Ash content of switchgrass sample increased from 4.31% to 10.53% as the sieve size of the fraction decreased from >0.95 mm to <0.15 mm. Ash content of ground bituminous coal and PRB coal was not significantly (α=0.05) different from their respective dust samples. This can be due to smaller geometric mean particle size of ground samples for these two coal types as compared to other ground samples.

Ash content for woody biomass dusts - pine, eucalyptus, sweetgum (1.10% - 1.41%) was found to be lower than ash content in grassy biomass dusts – Bermuda grass, corn stover, sugarcane bagasse and swithcgrass (4.68% - 15.42%). This is similar to the results that have been documented for woody and grass like biomass. McKendry (2002) reported the ash contents of Danish pine and willow wood (woody biomass) to be 1.60% while Jenkins et al. (1998) measured the ash content of switchgrass to be 8.97%. Also, Cuiping et al. (2004) reported that the ash contents of corn stover are in the range of 4.33-21.91%.

For grassy biomass, geometric mean diameter had a significant effect on ash content ($p<0.0001$). Ash content was found to be higher in grassy biomass dust samples with smaller geometric mean diameter (Pearson's correlation coefficient, r=-0.91) (figure 3.20a). Also, for grassy biomass, ash content was found to be higher in dusts with higher particle density (Pearson's correlation coefficient, r=0.97) (figure 3.20b). This is because ash consists of inorganic

mineral particles which have high particle densities (1760 – 2760 kg/m^3) (Ghosal and Self, 1995). Also, particle density of ash from sugarcane bagasse sample used in this study was found out to be 2781.5±3.46 kg/m^3 which is higher than particle densities of most biomass and coal dusts.

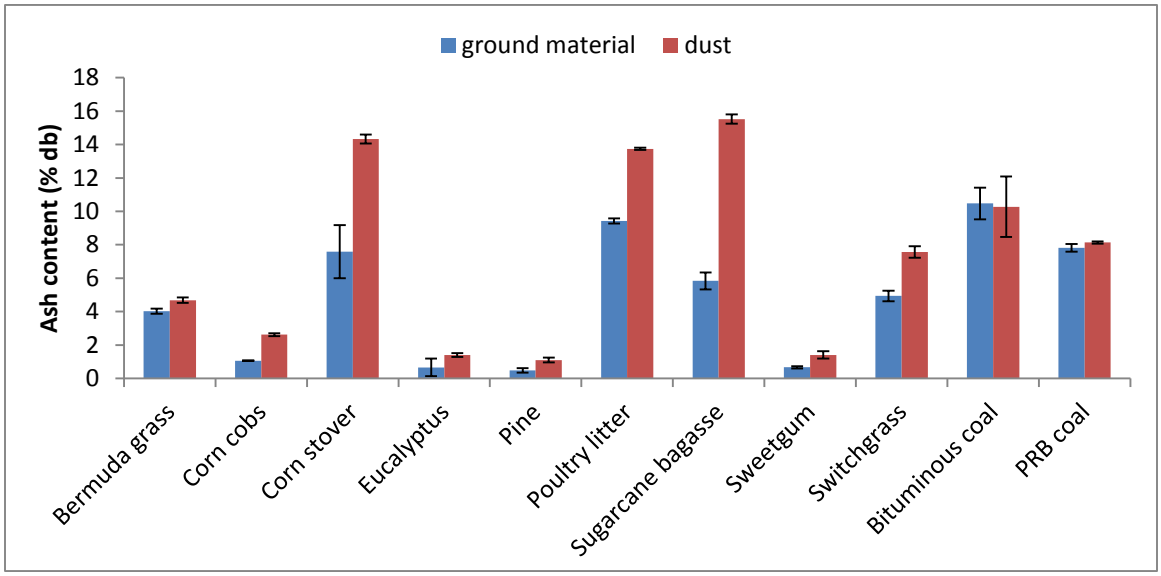

Pecan shell and lignite coal samples were received in dust form

Figure 3.19 Ash content of ground and dusts from biomass and coal.

Ash content of coal dusts were measured to vary between 8.14%-10.27% (dry basis). These values are higher than the ash contents (1.10% - 1.41%) of woody biomass – an indication of higher amount of inorganic compounds in coal (Demirbas, 2004; Hehar, 2013). McKendry (2002) measured ash content of bituminous coal to be 8.0% which is comparable to the ash content value obtained in this study for bituminous coal (10.27% d.b.). Samaras et al. (1996) reported the ash content for lignite coal to be 22.1% (d.b.). This is also comparable to the ash content of lignite coal used in this study (20.84 d.b.%).

Mean ash content (dry basis) for poultry litter was obtained as 13.74% which is comparable to the mean ash content of poultry litter (14.1 d.b.%) found by Tiqui and Tam (2000). Ash content of poultry litter was also found to be higher than that of woody biomass because poultry birds use up a significant amount of nutrients (carbohydrates, protiens, fat and minerals) from feed for bodily functions (Chiba, 2014). Thus, mineral content of poyltry excreta is also high leading to higher ash content in poultry litter.

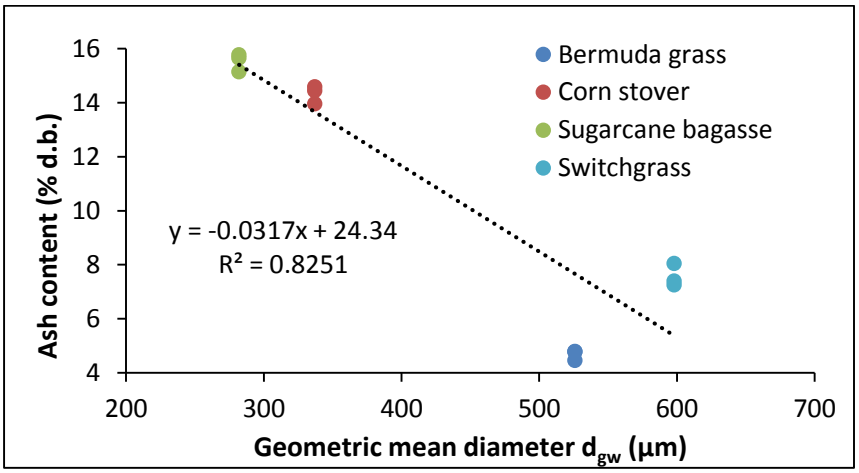

(a)

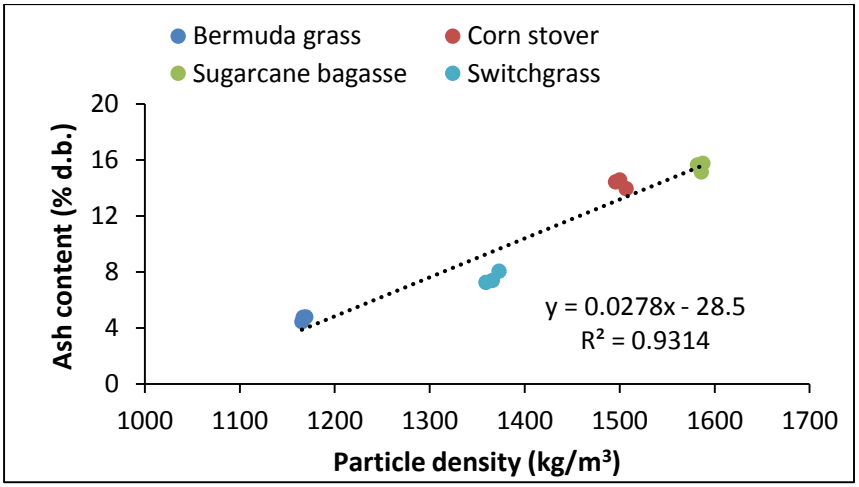

(b)

Figure 3.20 Ash content dependence on geometric mean particle size (a) and particle density (b) for grassy biomass dusts.

3.4.1.6 Volatile Matter

Volatile content of ground biomass samples ranged from 81.24% (d.b.) (corn stover) to 89.86% (d.b.) (sweetgum) whereas ground bituminous coal and PRB coal had volatile content of 38.87% (d.b.) and 53.71% (d.b.) respectively. Mean volatile matter values for all dusts samples varied from 33.00% (d.b.) (bituminous coal) to 86.82% (d.b.) (sweetgum). Volatile content of coal dusts was in the range of 33.0 d.b.% (bituminous) to 53.69 d.b.% (lignite) which was lower than the volatile content range of biomass dusts that varied from 64.93 d.b.% (pecan shell) to 86.82 d.b.% (sweetgum). Volatiles are generated due to thermal decomposition of organic compounds present in biomass and coal. Since biomass have generally higher hydrogen to carbon and oxygen to carbon ratios than coal (Jenkins et al. 1998), the volatile matter of biomass is generally higher than that of coal.

Mean values of volatile matter of ground material for all biomass and coal feedstocks were higher than volatile matter contents of respective dust samples (figure 3.21). This difference was found to be significant (α=0.05) for all samples except pine. Higher volatile matter in ground material as compared to dusts is due to higher ash content of dusts (Hehar, 2013; Gani and Naruse, 2007). Volatile matter of grass like biomass dusts (Bermuda grass, corn stover, sugarcane bagasse and switchgrass) was found to reduce significantly ($p<0.0001$) with increase in ash content (Pearson's correlation coefficient, r=-0.94) (figure 3.22). Similar results were not obtained for woody biomass dusts because of their narrow range of ash content (1.10% - 1.41% d.b.).

Mean volatile matter value for bituminous coal dust was obtained to be 33.00% (d.b.). These values are comparable to the volatile matter of bituminous coal that have been reported in literature: 35% (McKendry, 2002) and 28.33% (Cuiping et al., 2004). Jenkins et al. (1998) also found out volatile matter of switchgrass as 76.69%, which is comparable to the value for switchgrass used in this study (77.86% d.b.). Cuiping et al. (2004) found volatile matter for corn stover as 67.36% (d.b.) which is comparable to the value obtained in this study (72.97% d.b.).

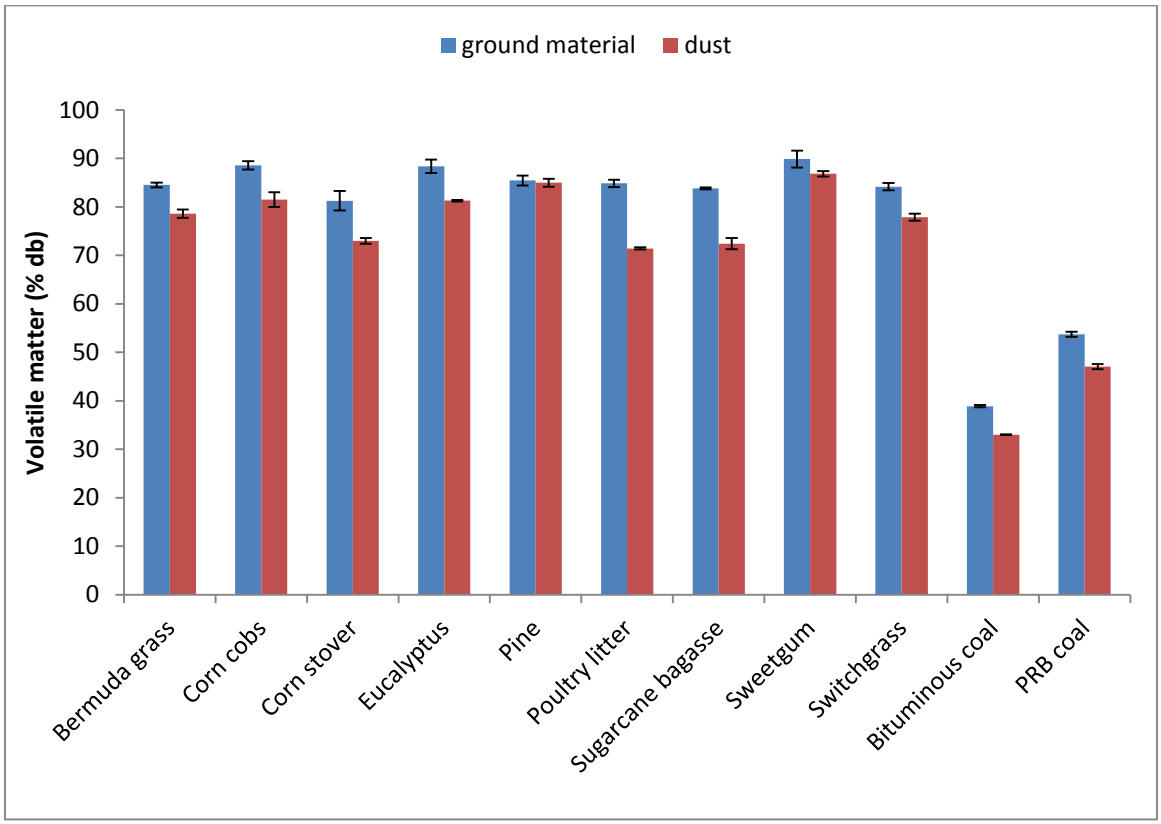

Pecan shell and lignite coal samples were received in dust form

Figure 3.21 Volatile matter of ground and dusts from biomass and coal.

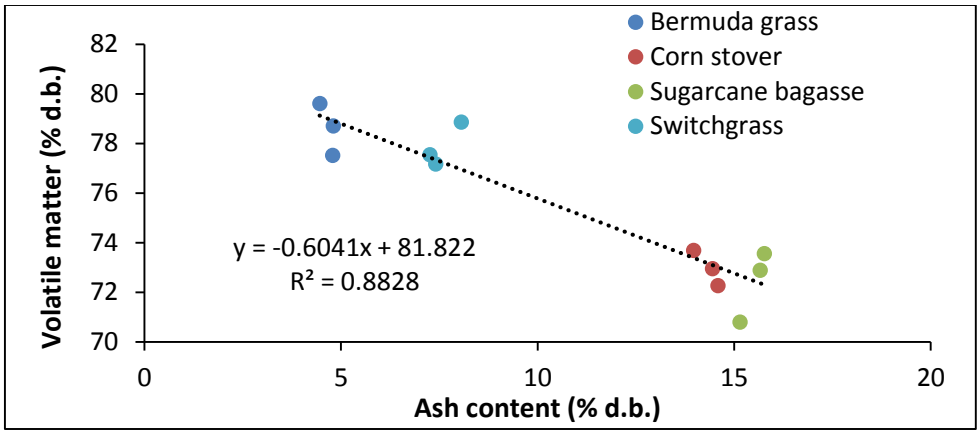

Figure 3.22 Effect of ash content on volatile matter content of grassy biomass dusts.

3.4.1.7 Energy Content

Energy content of ground material varied from 18.16 MJ/kg d.b.(corn stover) to 31.75 MJ/kg d.b. (Bituminous coal) whereas, energy contents for dust samples varied from 16.69 MJ/kg d.b. (sugarcane bagasse) to 32.26 MJ/kg d.b.(bituminous coal). Energy contents of coal dust samples (27.41 MJ/kg – 32.26 MJ/kg d.b.) were found to be higher than those of biomass dust samples (18.77MJ/kg - 20.55MJ/kg d.b.). This is because biomass has less carbon and more oxygen (Demirbas, 2004). Material with more carbon will have higher energy content (Jenkins et al., 1998). According to Jenkins (1989), each 1% increase in carbon concentration elevates the higher heating value by 0.39 MJ/kg.

Mean value of energy content for all ground biomass samples was found to be higher than the respective dust samples (figure 3.23). This difference was significant (α=0.05) for all biomass feedstock except pine and sweetgum. Ground material had higher energy content than dusts due to higher ash content in dusts as compared to ground material. Mani et al. (2004) also confirmed that biomass

with higher ash content value has lower heating value. Similar results were also obtained by Ebling and Jenkins (1985) in their study on wheat and barley straws. Also, for biomass dusts, ash content had a significant ($p<0.0001$) effect on energy content of the samples. Samples with higher ash content were found to have lower energy content values (Pearson's correlation coefficient, r=-0.95) (figure 3.24). Mean energy content of pine was found out as 20.55 MJ/kg which is comparable to the values obtained in earlier studies. Energy content for Danish pine and pine (*Pinus tabulaeformis*) samples was reported to be 21.2 MJ/kg (McKendry, 2002) and 19.38 MJ/kg (Cuiping et al., 2004) respectively. Mean energy content (dry basis) for switchgrass was found out as 18.77 MJ/kg which is comparable to values found out in earlier studies by McKendry (2002) (17.40 MJ/kg), Jenkins et al. (1998) (18.06 MJ/kg) and Mani et al. (2004) (17.61 MJ/kg).

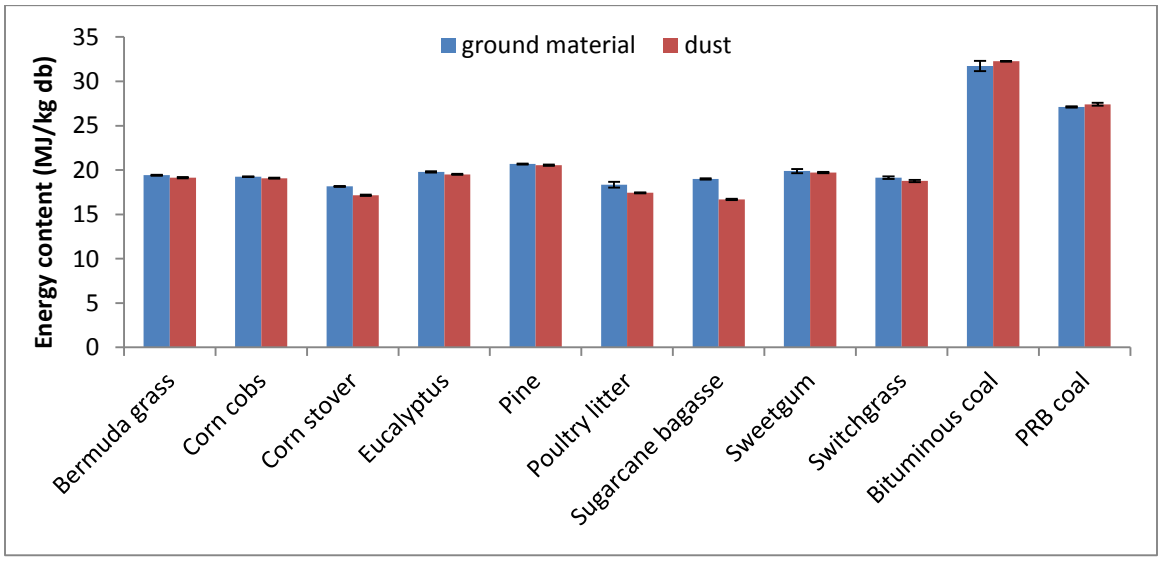

Pecan shell and lignite coal samples were received in dust form

Figure 3.23 Energy content of ground and dusts from biomass and coal.

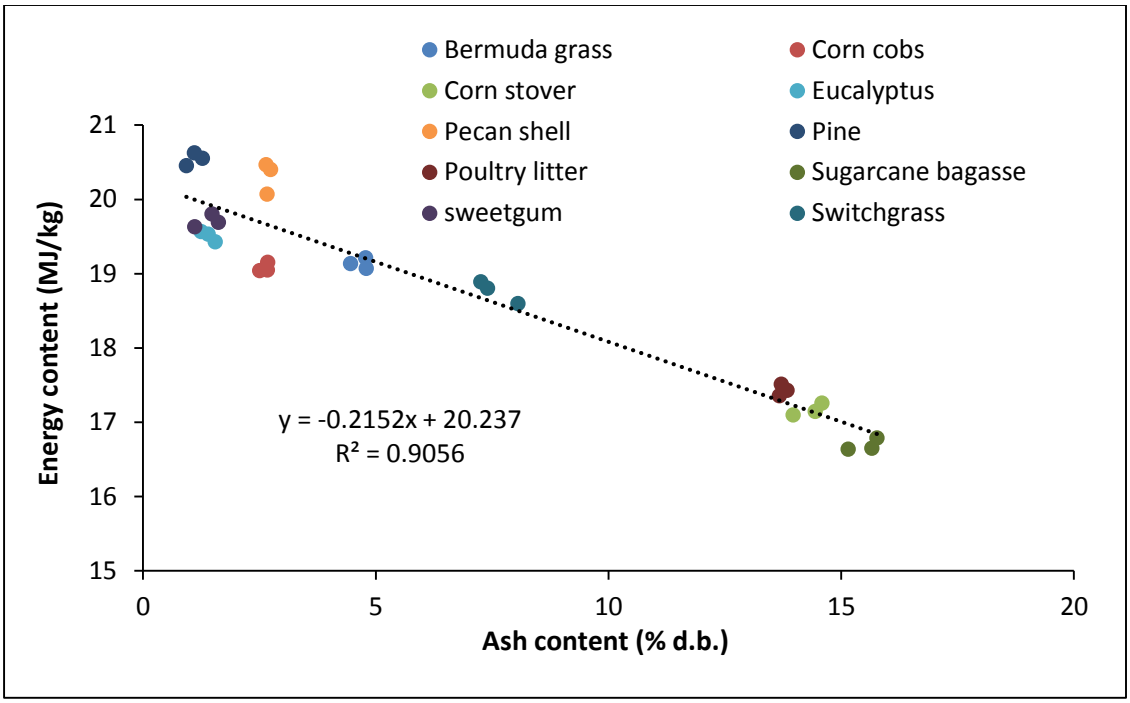

Figure 3.24 Effect of ash content on energy content for all biomass dusts.

3.4.2 Heating and Ignition Properties

Minimum hot surface ignition temperature (MIT) values for biomass and coal dusts are given in table 3.6. Volatilization properties (TORV, TMML, TOXY and activation energy) and exothermic parameters (TRE, TME and exothermic energy) for biomass and coal dust samples are given in table 3.7.

3.4.2.1 Minimum Hot Surface Ignition Temperature

Hot surface ignition temperature of dust samples was determined according to ASTM E2021 standard (2010). Figure 3.25 shows a typical temperature profile obtained when a dust layer is heated on a hot plate. For this sample (corn cobs), there was no ignition because temperature of the dust layer increased to about

200°C and then became essentially constant. Also, the temperature of the dust layer did not cross the constant hot plate temperature profile (figure 3.25a). In figure 3.25b, there was ignition of the corn cobs dust sample with the temperature of the dust sample increasing at a rapid rate to about 575°C. The hot plate temperature that caused the ignition of dust sample was taken as the minimum hot surface ignition temperature (MIT).

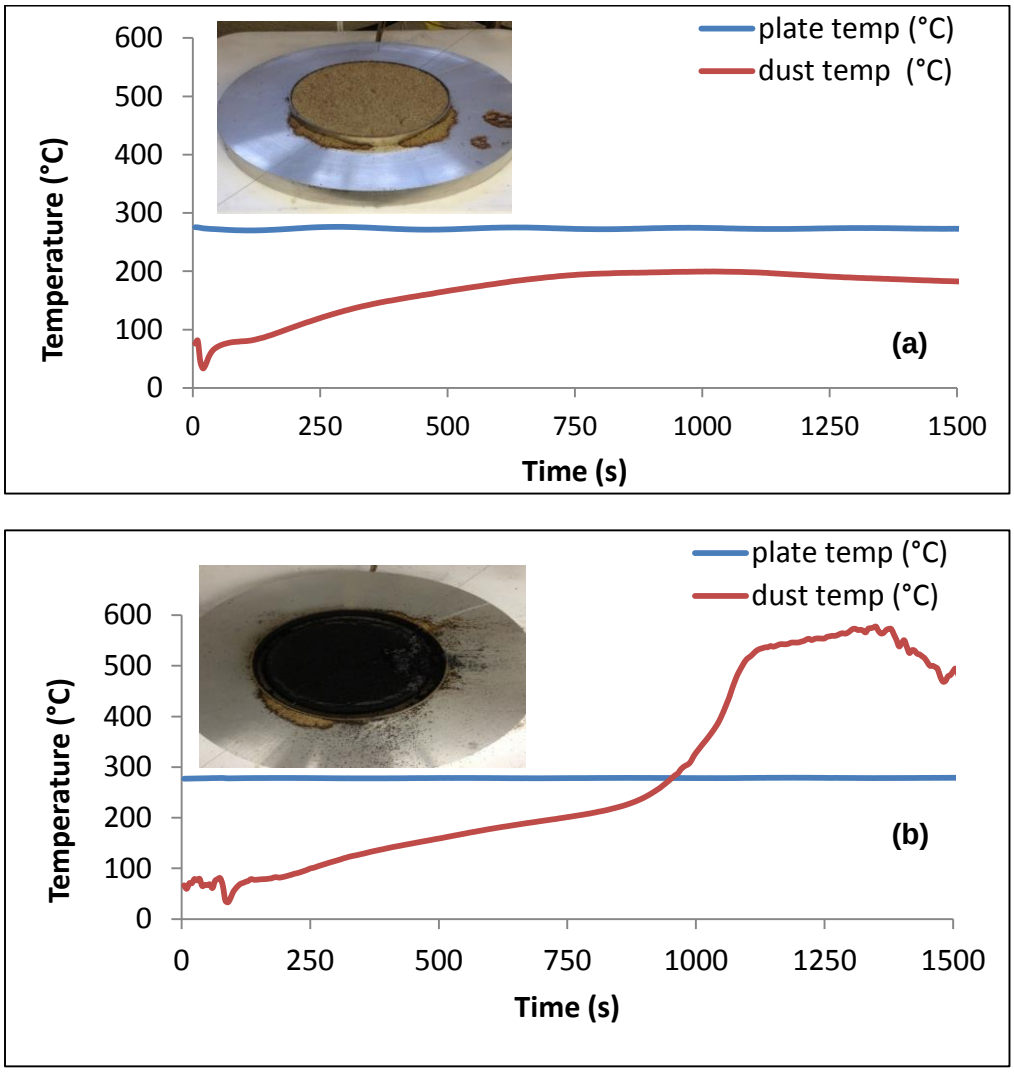

Figure 3.25 Plots of temperature vs. time showing maximum temperature of no ignition, 275ºC (a) and minimum temperature of hot surface at which ignition occurred (MIT), 280ºC (b) for corn cobs sample.

MIT values were measured to be between 240°C (PRB coal and lignite coal) and 335°C (Bituminous coal). Bituminous coal had higher MIT than PRB or lignite coal because it has lower volatile content (33.00% wt. d.b.) than the other two coal dust samples. Volatile matter of coal is an important factor that affects ignition temperature. Higher volatile matter of coal would result in lower ignition temperatures (Miron and Lazzara, 1988). Hot surface minimum ignition temperatures for Pittsburgh seam coal was reported by Park (2006) to be 220°C. Reddy et al. (1998) measured the ignition temperatures for Prince and Pittsburgh coal samples to be 250°C and 270°C respectively.

Similarly, lower ash content of grass like biomass significantly reduced the MIT (Pearson's correlation coefficient, r=0.75, p=0.0049) (figure 3.26a). This is because ash content retards the oxidation process and acts as a heat sink (Vuthaluru, 2004; Hehar, 2013). This trend was not seen in case of woody biomass (eucalyptus, pine, sweetgum) since ash content values were very close to each other (1.10% - 1.41% db) for these samples, and were not significantly different. Grassy biomass dusts with higher volatile matter had significantly lower MIT values (Pearson's correlation coefficient r=-0.64, p=0.025) (figure 3.26d). This is because volatiles escape the solid biomass fuel upon heating and ignite while in gas phase leading to ignition. This trend was not observed in case of woody biomass since the volatile matter values for them were not significantly different from each other.

Bulk density of grass like biomass dusts had a significant effect on its MIT (p=0.0001). Samples with higher value of bulk density had lower MIT (Pearson's

correlation coefficient, r=-0.89) (figure 3.26b). Similarly, MIT-bulk density relationship was also obtained for woody biomass (Pearson's correlation coefficient r=-0.99, $p<0.0001$) (figure 3.26c). This is due to increase in the thermal conductivity of the dust layer with increase in bulk density (Bowes and Townshend, 1962).

Table 3.6 Minimum hot surface ignition temperature (MIT) of dust layer for all samples.

Sample	Temperature of no ignition of dust layer (°C)	Minimum temperature of ignition of dust layer (°C)
Bermuda grass	270	275
Bituminous coal	330	335
Corn cobs	275	280
Corn stover	285	290
Eucalyptus	280	285
Lignite coal	235	240
Pecan shell	260	265
Pine	310	315
Poultry litter	280	285
PRB coal	235	240
Sugarcane bagasse	300	305
Sweetgum	300	305
Switchgrass	290	295

The MIT values for duplicate runs were the same

Table 3.7 Measured volatilization and exothermic properties of biomass and coal dust samples.

Sample	TORV (°C)	TMML (°C)	TOXY (°C)	E_a (kJ/mol)	TRE (°C)	TME (°C)	Exothermic Energy (MJ/kg)
Biomass Samples							
Bermuda grass	266.1±1.0^{g}	312.4±1.6^{d}	274.0±3.8^{d}	48.3±0.6^{f}	237.5±3.5^{b,c}	379.3±11.7^{c,d}	7.95±0.01^{a}
Corn cobs	276.52±0.62^{e,f}	313.67±1.60^{d}	276.51±4.02^{d}	63.15±2.45^{d}	235.2±1.0^{c}	394.6±4.9^{a,b,c}	8.15±0.11^{a}
Corn stover	277.5±1.1^{e}	316.4±0.8^{d}	286.1±1.7^{c,d}	71.3±0.5^{c}	239.7±0.4^{a,b,c}	395.8±3.2^{a,b}	7.78±0.24^{a}
Eucalyptus	291.88±0.88^{b}	315.69±1.76^{d}	285.87±4.23^{c,d}	72.35±1.55^{c}	243.5±1.0^{a,b,c}	385.4±1.0^{b,c,d}	7.52±0.22^{a,b}
Pecan shell	290.0±1.7^{c,d}	331.2±4.7^{c}	283.5±11.4^{c,d}	55.6±0.3^{e}	206.0±2.5^{d}	407.7±2.6^{a}	5.61±0.15^{c}
Pine	306.08±1.78^{a}	348.75±2.09^{a}	319.08±2.79^{a}	64.43±0.11^{d}	244.5±1.4^{a,b,c}	401.1±3.3^{a,b}	6.14±0.46^{c}
Poultry litter	272.8±0.5^{f}	304.1±0.5^{e}	277.8±0.4^{d}	71.1±1.1^{c}	241.2±4.6^{a,b,c}	354.4±1.9^{e}	4.48±0.26^{d}
Sugarcane bagasse	285.2±0.4^{d}	345.21±1.33^{a,b}	309.57±6.34^{a,b}	77.08±0.54^{b}	245.3±4.7^{a,b}	377.3±4.5^{d}	7.55±0.73^{a,b}
Sweetgum	290.23±0.75^{b,c}	338.8±1.5^{b}	297.2±2.2^{b,c}	95.2±1.9^{a}	248.9±3.1^{a}	392.8±0.8^{a,b,c,d}	6.57±0.05^{b,c}
Switchgrass	285.0±1.8^{d}	329.76±0.49^{c}	315.28±4.61^{a}	61.6±1.3^{d}	249.0±0.8^{a}	389.0±1.6^{b,c,d}	7.69±0.16^{a}
Coal Samples							
Bituminous coal	447.6±2.2^{a}	485.1±4.4^{a}	423.1±16.7^{a}	91.6±6.3^{a}	223.4±1.5^{b}	395.6±2.2^{b}	3.51±0.10^{a}
Lignite coal	311.6±4.5^{b}	349.77±6.17^{c}	241.80±3.33^{b}	56.82±0.48^{b}	221.2±2.4^{b}	428.0±1.3^{a}	5.16±0.87^{a}
PRB coal	317.3±1.6^{b}	379.4±1.6^{b}	258.7±18.4^{b}	49.8±0.8^{b}	244.9±2.4^{a}	429.1±3.0^{a}	4.64±0.86^{a}

Superscripts with same letters in a column are not significantly different from each other (α=0.05)

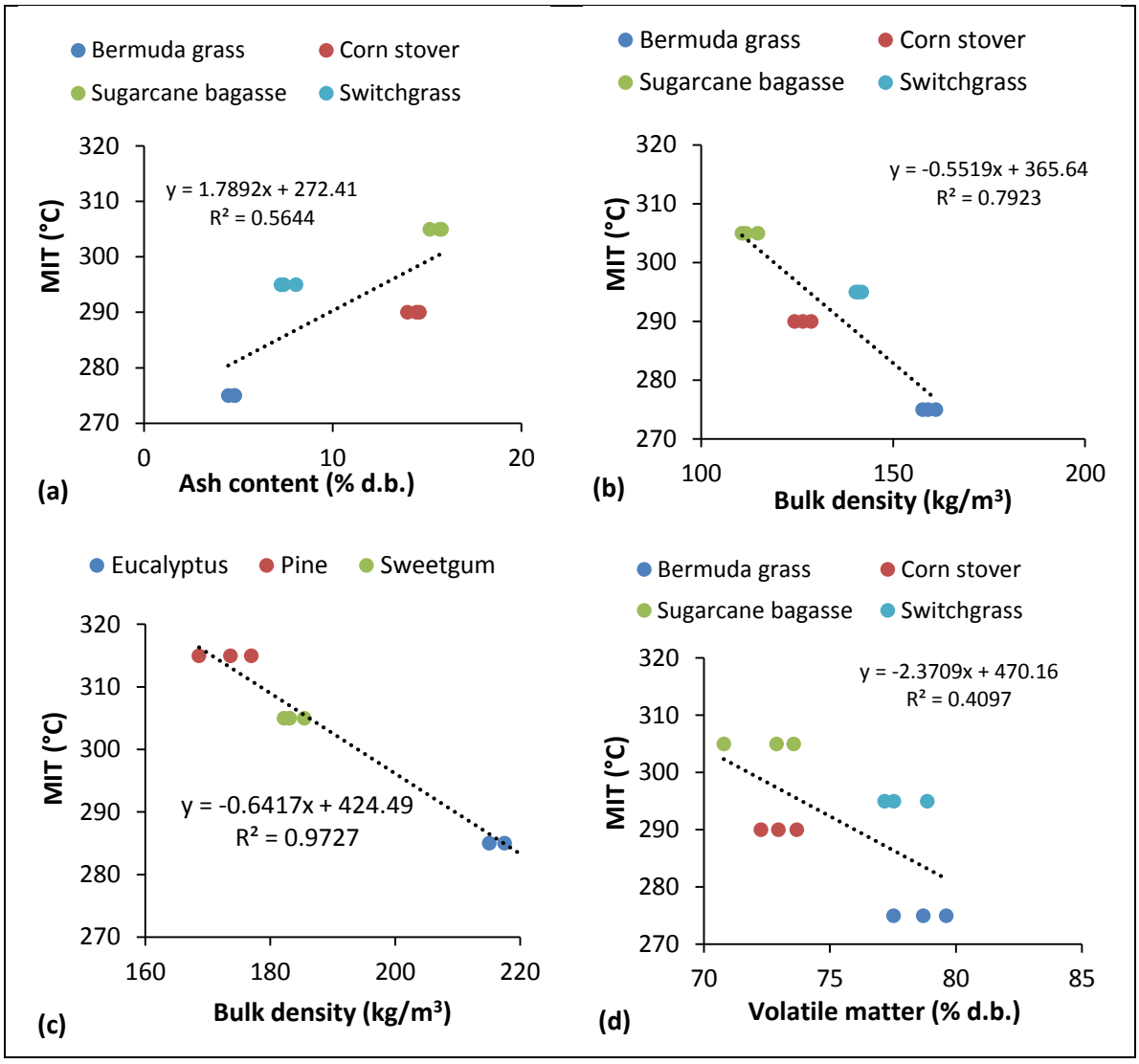

Figure 3.26 Minimum hot surface temperature (MIT) dependence on ash content of grassy biomass dusts (a), bulk density of grassy biomass dusts (b), bulk density of woody biomass dusts (c) and volatile matter of grassy biomass dusts (d).

3.4.2.2 Volatilization Properties

TGA mass loss curves for all the dust samples when heated in air and oxygen atmosphere are depicted in figure 3.27. Figure 3.28 shows mass loss curve for switchgrass dust heated in air and oxygen atmospheres as an example of how

temperature of onset of rapid volatilization (TORV), temperature of maximum rate of mass loss (TMML) and oxidation temperature (TOXY) were estimated. As shown in figure 3.28a, TORV was obtained by drawing tangents to the parts of the curve corresponding to the onset of significant mass loss of sample due to devolatilization. TMML was obtained from the peak of the mass loss rate curve (figure 3.28a). Similarly, the peak of mass loss rate curve when sample is heated under oxygen atmosphere gives the TOXY value (figure 3.28b).

The initial mass loss in all the dust samples when heated (in air and oxygen atmospheres) from ambient to about 110°C is due to the loss of moisture. Initial mass loss curve for lignite coal is prominent than the rest of the samples because of the high initial moisture content of lignite coal (29.4 w.b.%). After initial moisture loss from the sample, mass loss for biomass dust samples occurred in two parts. A rapid mass loss starts after 200°C (Vamvuka et al., 2003). After about 350°C, this major loss is followed by a slow rate of mass loss.

The maximum rate of mass loss in biomass generally occurred between the temperatures of 200°C to 400°C due to release of the volatiles (Jenkins et al., 1998) from hemicellulose decomposition. From figure 3.27a, it can be seen that every biomass dust sample lost mass rapidly in this temperature range. The slow mass loss that typically occurs after the rapid mass loss has been attributed to the decomposition of cellulose in biomass (Yang et al., 2006). Lignin decomposes with difficulty in comparison to hemicellulose and therefore decomposes over a wide range of temperatures (Yang et al., 2006; Vamvuka et al., 2003; Gronli et al., 1999; Orfao et al., 1999; Sorum et al., 2001). However, since coal is not a lignocellulosic

material, mass loss in case of coal dust samples did not follow the two stage decomposition of biomass

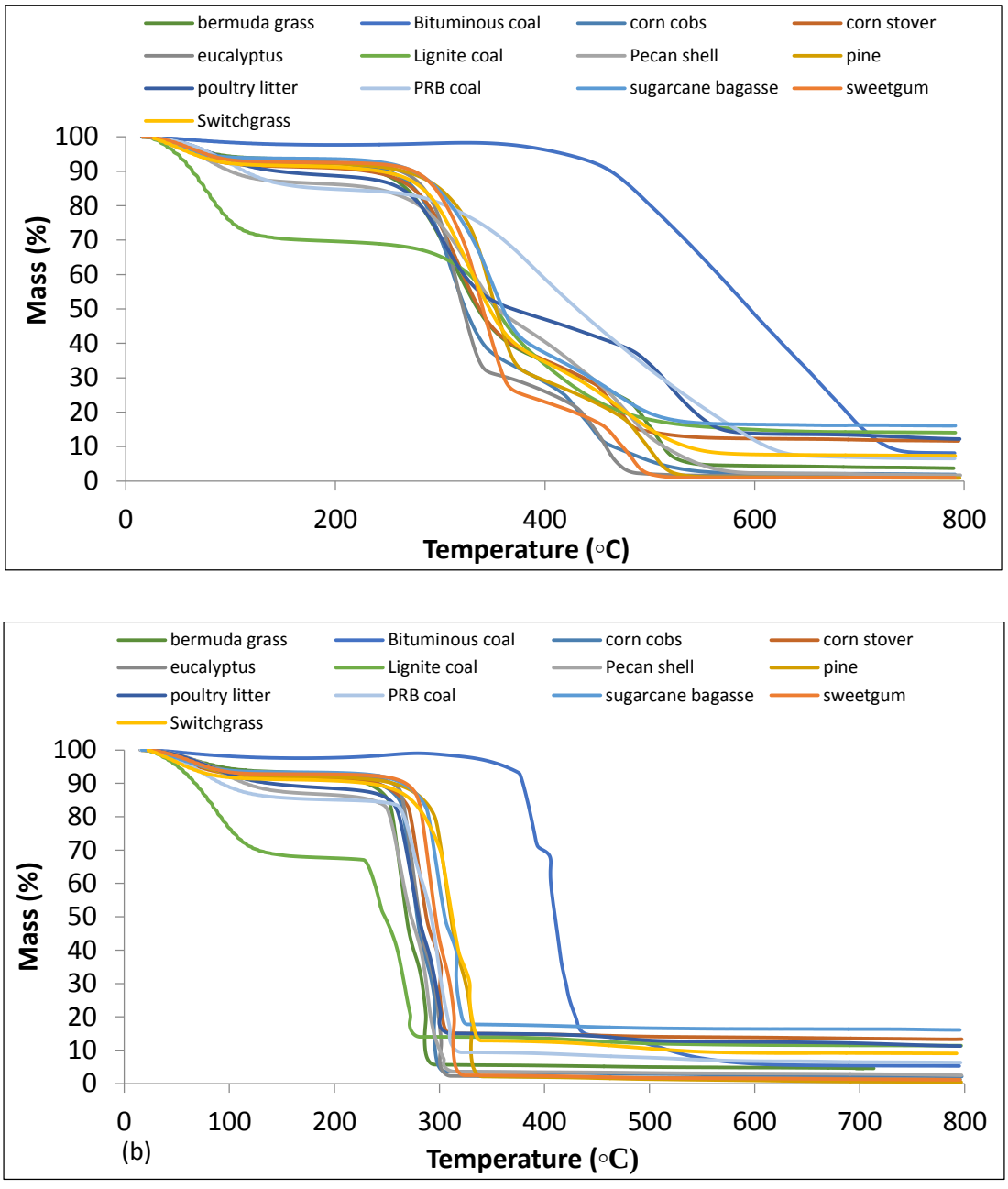

Figure 3.27 TGA mass loss curves for dust samples heated in air environment (a) and oxygen environment (b).

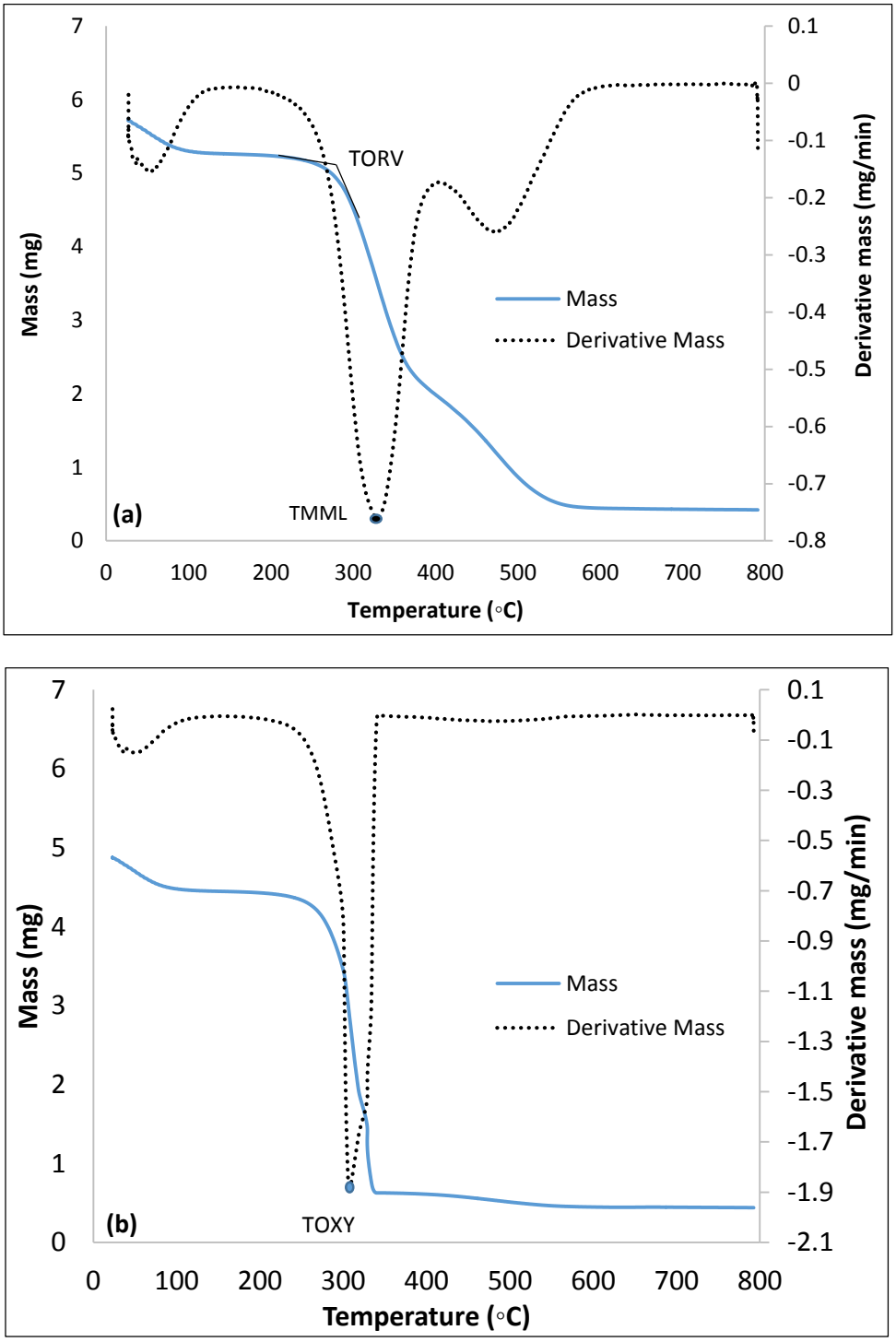

Figure 3.28 Example of how TORV and TMML were estimated. Mass loss curves are for switchgrass dust sample heated in air atmosphere (a) and heated in oxygen atmosphere (b).

Data obtained from oxygen atmosphere decomposition was used to obtain the single point oxidation temperature (TOXY). The TG data showed rapid mass loss in the dust samples for both coal and biomass due to presence of excess oxygen for combustion (Ramirez et al., 2010). TOXY for biomass dusts varied from 274.0°C (Bermuda grass) to 319.1°C (pine) whereas for coal dusts it varied from 241.8°C (lignite coal) to 423.1°C (bituminous coal). TOXY value for bituminous coal was significantly higher than the other two coal samples because of its lower volatile content which acts as fuel and is easily oxidized as compared to carbon. Based on TOXY values it can be said that bituminous coal dust is at lower risk of ignition than lignite and PRB coal dusts.

Value of TORV of bituminous coal dust sample (447.6°C) was significantly higher than that of PRB coal dust (317.3°C) and lignite coal dust (311.6°C). This is due to the low volatile content of bituminous coal dust than the other two dust samples. TORV indicates the ease with which a material will release volatiles upon heating. The lower the TORV value, the more easily volatiles are released from the solid fuel matrix.

For coal dusts, TORV values (311.6°C - 447.6°C) were significantly higher than that of biomass dusts (266.1°C - 306.1°C) which again can be attributed to the low volatile content of the coal dust samples. Thus, based on TORV values, biomass dusts are at higher risk of ignition than coal dusts. According to Muthuraman et al. (2010), coal requires a higher temperature to release its

volatiles than compared to biomass like wood, which is in accordance to the findings in this study.

Similarly, TMML value for bituminous coal dust (485.1°C) was significantly higher than that of PRB coal (379.4°C) and lignite coal dusts (349.8°C). This again can be said due to low volatile content of bituminous coal than other types of coal. Also, TMML values for coal dusts (349.8°C - 485.1°C) was significantly higher than those of biomass dusts (304.1°C - 348.8°C) because of low volatile content of coals. This is because volatile release and ignition corresponds to maximum mass loss rate as compared to char oxidation (Jenkins et al., 1998). Thus, based on TMML values, biomass dust is at higher risk of ignition and dust explosion than coal dusts.

An example of determination of activation energy is shown in figure 3.29. Only a section of the conversion data corresponding to the maximum mass loss rate was used in estimation of activation energy (Ramirez et al., 2010). Activation energy value for grassy biomass dusts with higher ash content was found to be significantly higher (Pearson's correlation coefficient $r=0.96$, $p<0.0001$) (figure 3.30a). This is again because ash acts as heat sink and effects ignition as it hinders the oxidizer-fuel contact (Porteiro et al., 2010).

Grassy biomass dust samples with higher amount of volatile matter had significantly lower activation energy values (Pearson's correlation coefficient $r = -0.89$, $p<0.0001$) (figure 3.30b). This is because of combustion of volatiles in gas phase as it escapes biomass particles upon heating. Higher volatile matter leads to lower ignition temperature (Grotkjaer et al., 2003).

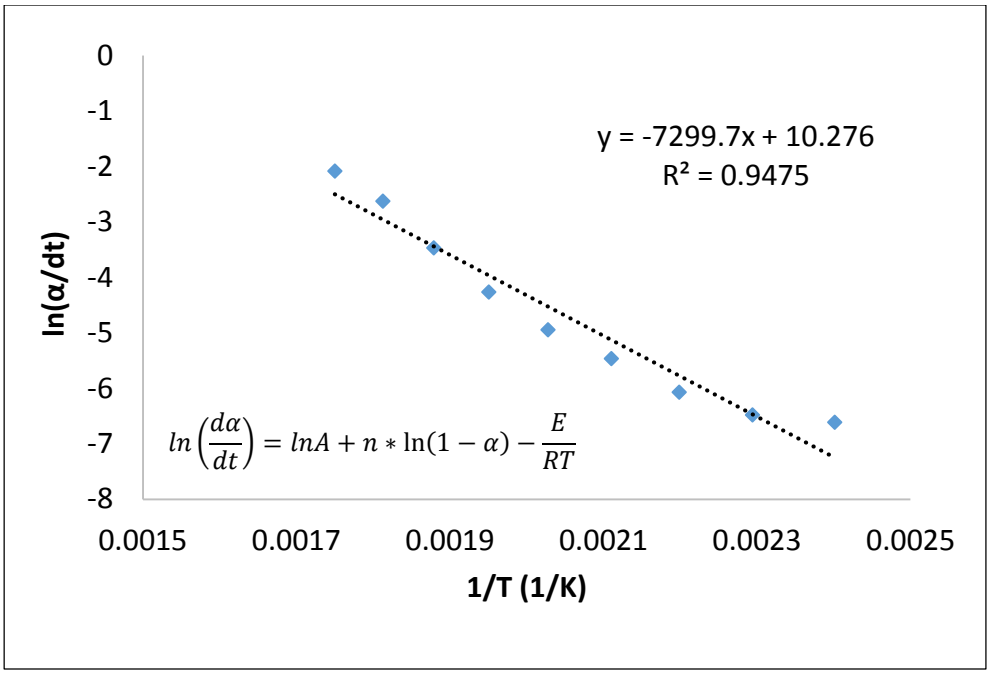

Figure 3.29 Example for determination of apparent activation energy (switchgrass dust sample).

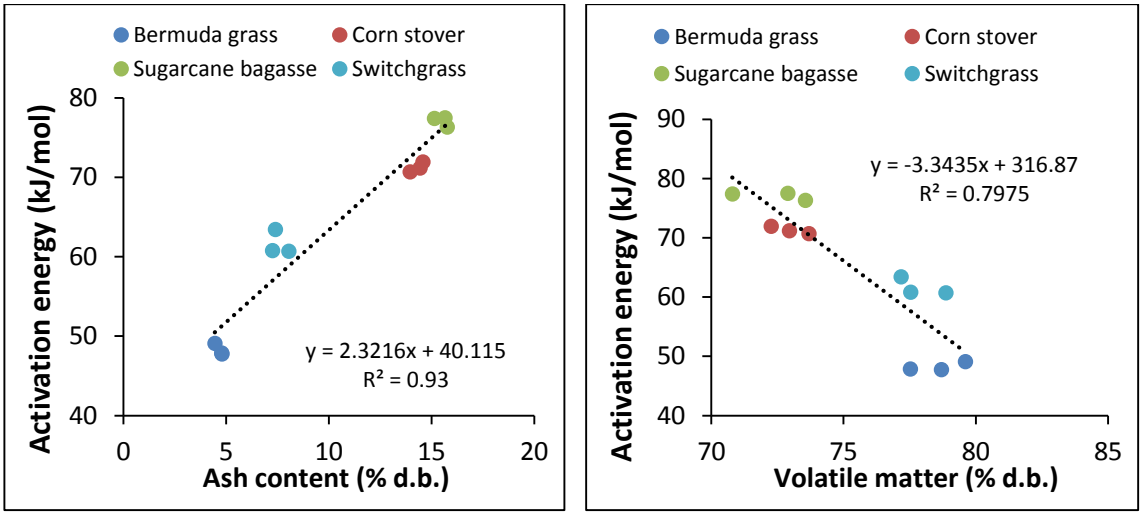

(a) **(b)**

Figure 3.30 Effect of ash content on activation energy (a) and effect of volatile matter on activation energy (b) for grassy biomass dusts.

3.4.2.3 Exothermic Parameters

DSC parameters (temperature of rapid exothermic reaction (TRE), maximum temperature reached during exothermic reaction (TME) and exothermic energy) obtained for all dust samples are tabulated in table 3.7. DSC heat flow vs. temperature curves for all the dust samples heated in air atmosphere are depicted in figure 3.31. Figure 3.32 shows DSC curve for switchgrass dust heated in air atmosphere as an example of how TRE and TME were estimated. The intersection point of the tangents drawn at parts of the curve corresponding to rapid increase in heat flow and end of rapid exothermic reaction gives the TRE and TME values respectively. Exothermic energy was obtained by integrating the area under part of the heat flow vs. time curve corresponding to exothermic reaction. Negative value of heat flow in a DSC curve represents endothermic reaction taking place. An endothermic peak is observed for every dust sample at around 100°C due to the loss of moisture from the sample. This is the temperature at which water vaporizes upon heating. After the moisture loss, sample reacts with oxygen in presence of heat resulting in an exothermic reaction (positive heat flow) (Ramirez et al., 2010). Exothermic energy was estimated by calculating area under the DSC heat flow curve (calculated by the software provided along with the DSC equipment).

Rapid exothermic reaction occurs for all the dusts between temperatures of 200°C and 250°C (figure 3.31). TRE for biomass dust varied from 206.1°C (pecan shell) to 248.96°C (switchgrass) whereas for coal dusts it varied from 221.2°C (lignite coal) to 244.9°C (PRB coal). In a separate study, Ramirez et al. (2010)

measured the TRE for bituminous and sub bituminous coal to be 240.0°C and 220.0°C respectively. A value of 223.4°C was obtained as TRE for bituminous coal used in this study.

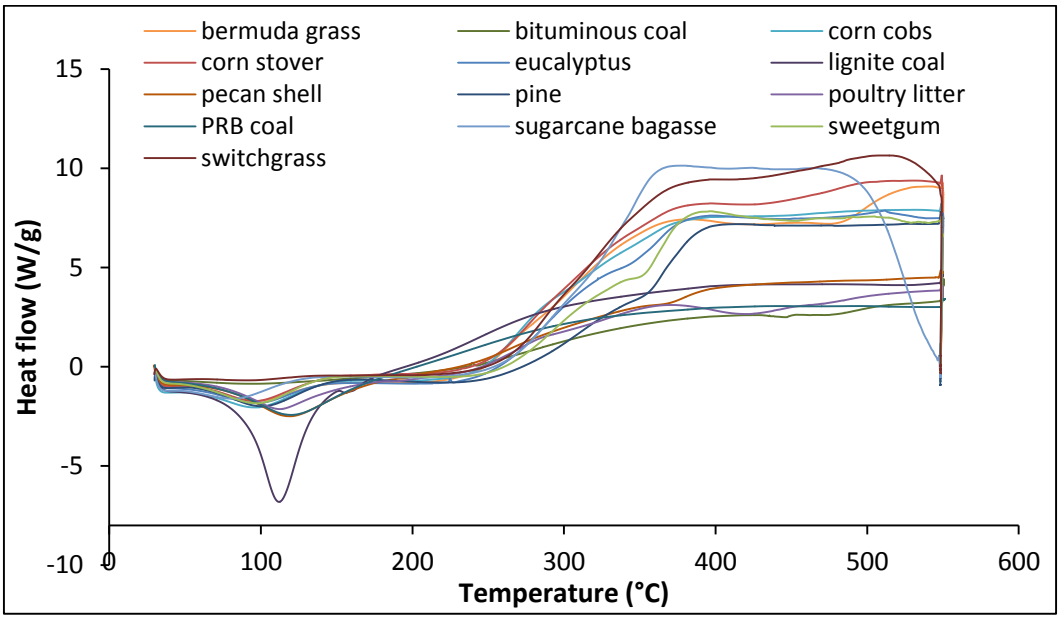

Figure 3.31 Heat flow curves of biomass and coal dusts heated with DSC in air atmosphere.

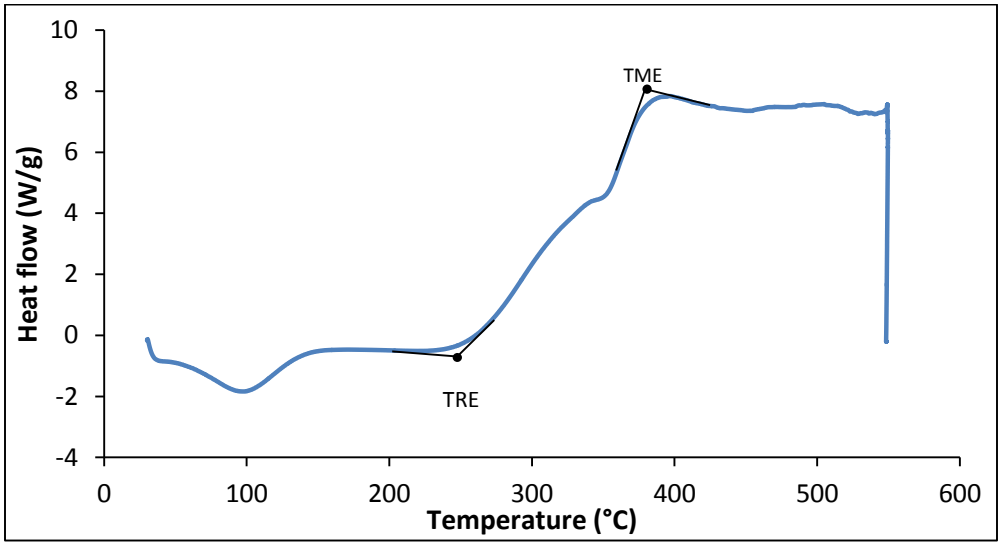

Figure 3.32 Example of how TRE and TME were estimated from heat flow vs. temperature curve for switchgrass sample when heated under air environment.

Mean value of maximum temperature reached during an exothermic reaction (TME) for bituminous coal, lignite coal and PRB coal were measured to be 395.6°C, 428.0°C and 429.1°C respectively whereas, for biomass, it varied from 354.4°C (poultry litter) to 407.7°C (pecan shell). Sahu et al. (2010) also found out DSC curve peak temperature (TME) for coal as 423.0°C. In general, TME was found to be higher in case of coal samples than biomass as coal had higher energy content than biomass dusts. For woody biomass, dust samples with higher energy content had significantly higher TME value (Pearson's correlation coefficient r=0.89, p=0.0013) (figure 3.33).

Exothermic energy is the measure of quantity of heat evolved upon heating a material. Exothermic energy of the dust samples varied from 3.51 MJ/kg (bituminous coal) to 8.15 MJ/kg (corn cobs). The exothermic energy released during the DSC process is less than the calorific value (energy content) of the dust samples because of the incompletely burned volatiles (Jiricek et al., 2012). While measuring heating value, oxygen atmosphere was provided to the sample which led to complete burning of the sample whereas, samples were heated in air atmosphere during DSC experiments which lead to incomplete combustion (char residue). This caused exothermic energy value to be less than the heating value of the dust samples.

Exothermic energy of bituminous coal was found to be less than that of biomass. This can be attributed to low volatile content of bituminous coal. Dust samples were heated only up to temperature of 550.0°C in DSC experiments, and from TG analysis of bituminous coal, it is evident (figure 3.27a) that the coal sample

still continued to show slight mass loss, thus release energy via oxidation process beyond 550.0°C, which was not accounted for in DSC experiment due to limitations of the equipment, resulting in low exothermic energy value.

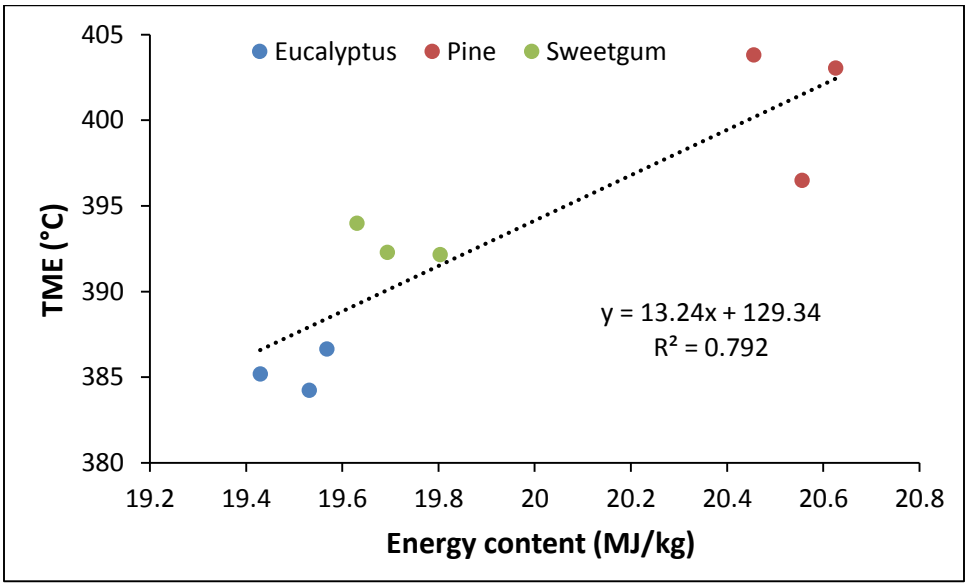

Figure 3.33 Effect of energy content on maximum temperature reached during exothermic reaction (TME) for woody biomass dusts.

Lignite and PRB coal dusts were found to have higher TME values (428.0°C and 429.1°C respectively) than biomass dusts (354.4°C – 407.7°C). Although, TRE values for bituminous and lignite coal dusts is lower than that of all the biomass dusts except pecan shell, the exothermic energy of all biomass dusts except poultry litter was higher than that of coal dusts in a given range of temperature (30°C-550°C). Thus, biomass dusts in general are associated with higher destruction capability during a dust explosion than coal dusts.

3.5 Conclusion

Physical and chemical properties were measured for ground material and dust samples. Heating and ignition parameters were also measured for dusts. Range of values obtained for MIT, TORV, TMML, TOXY, TRE and TME for all the dusts were 240.0°C-335.0°C, 266.1°C-447.6°C, 304.1°C-485.1°C, 274.0°C-423.1°C, 206.1°C-249.0°C and 354.4°C-429.1°C respectively. Grassy biomass dusts with higher ash contents had significantly lower volatile matter ($p<0.0001$). All biomass dusts with higher ash content had significantly lower energy content ($p<0.0001$). Grassy and woody biomass dusts with higher bulk density had significantly lower MIT value ($p=0.0001$ and $p<0.0001$ respectively). Also, MIT values of grassy biomass with higher ash contents and lower volatile matter was significantly higher ($p=0.0049$ and $p=0.025$ respectively). Grassy biomass dusts with higher ash contents and lower volatile matter had significantly higher activation energy values ($p<0.0001$). Woody biomass dusts with higher energy content had significantly higher TME values ($p=0.0013$). Based on TORV and TMML values, biomass dusts are at higher risk of ignition than coal dusts. Based on TOXY values it can be said that bituminous coal dust is at lower risk of ignition than lignite and PRB coal dusts. Based on the exothermic energy values, most of the biomass dusts (all except poultry litter dust) are associated with higher destruction capability during a dust explosion than coal dusts.

Chapter 4 Prediction of Heating and Ignition Properties Using Near Infrared Spectroscopy (NIRS)

4.1 Abstract

Dusts (i.e. particles of size less than 500 μm) are often generated during handling and processing of biomass feedstock. More than 70% of dusts generated in process industries are combustible (Vijayraghavan, 2004) and can lead to dust fire and/or explosion hazards if ignited. Fire and explosion due to dust ignition cause damage to plants or units and injuries to personnel and fatalities (Eckhoff, 2009). In addition to structural damage, dust explosions can result in loss of income by a plant due to down time and time required to repair the damaged portion of the plant (Sapko et al., 2000). Thus, heating and ignition of biomass dusts plays a critical role in development of safety guidelines and standards for process industries handling biomass and coal. This research aims at developing near infrared spectroscopy (NIRS) models to predict the heating and ignition properties of dusts from ten biomass feedstocks. The heating and ignition properties predicted are minimum hot surface ignition temperature of dust layer (MIT), temperature of onset of rapid volatilization (TORV), temperature of maximum rate of mass loss (TMML), oxidation temperature (TOXY), temperature of rapid exothermic reaction (TRE) and maximum temperature reached during an exothermic reaction (TME). Principal component analysis (PCA) was used on NIR

spectral data for dusts to develop prediction models for heating and ignition parameters. Coefficient of determination (R^2) values for internal validation of models developed using PCA on raw spectral data for MIT, TORV, TMML, TOXY, TRE and TME were 0.994, 0.984, 0.963, 0.737, 0.931 and 0.901 respectively, whereas, use of first derivative NIR spectral data yielded R^2 for these properties as 0.976, 0.964, 0.943, 0.798, 0.923 and 0.895 respectively.

Dusts from four biomass samples that were obtained from sources different than those used to develop models were used to validate the prediction models externally. Coefficient of determination (R^2) values for all models was obtained less than 0.28. Poor performance of models under external validation was attributed to small sample sizes of the biomass feedstocks that were used during building of prediction models.

4.2 Introduction

Fossil fuels such as coal and petroleum products are non-renewable sources of energy even though all the countries in world rely mainly on fossil fuels for energy. In the year 2013, more than 80% of all the energy consumed in USA was derived from fossil fuels such as petroleum, coal and natural gas (EIA, 2013). Due to negative impact of fossil fuel extraction and usage on environment and its long term availability issues, a lot of focus is being given to obtaining energy from renewable sources such as solar energy, wind energy and bioenergy. The main advantage that biomass has over other renewable energy sources is that energy derived from biomass can be converted into liquid fuels, chemicals and products.

These fuels can be directly used in sectors such as transportation, industries and power generation.

Biomass has to be preprocessed before it can be used to produce fuels chemicals and products. Preprocessing operations involves grinding, sieving, conveying and storage which could lead to dust generation. The National Fire Protection Association standard 654 defines combustible dusts as “particles that pass through a 500 µm sieve and are a dust fire or dust explosion hazard” (NFPA, 2013). Combustible dust, if ignited can cause fire hazard or dust explosion. Dust explosions lead to injuries and loss of life and property (Sapko et al., 2000; CSB, 2006; Amyotte and Eckhoff, 2010). Ignition sources that are present in processing and biomass handling facilities include hot bearings, hot surfaces, flames and sparks from electric motors that can ignite dusts and thus cause fire or explosion hazard. Thus, knowledge of heating and ignition properties of combustible dusts is very important in order to incorporate safety measures in process industries and other facilities processing biomass.

However, the methods used to quantify biomass heating and ignition properties are time consuming and require the use of expensive pieces of equipment such as thermogravimetric analyzer (TGA) and differential scanning calorimeter (DSC). NIRS can be used to develop prediction models for quick estimation of these properties. Near Infrared (NIR) spectroscopy has been used as a quick method of indirectly quantifying the properties of biological samples such as grain moisture content (Norris, 1964), dry matter content and fruit firmness (Nicolai et al., 2008), post-harvest quality of fruits (Bobelyn et al., 2010), moisture

content, water activity and salt content of meat (Collell et al., 2011), quality control of potato chips (Shiroma and Rodriguez-Saona, 2009), taste characterization of fruits (Jamshidi et al., 2012) and proximate analysis and heating values of torrefied biomass (Via et al., 2013). Some of the advantages of NIRS include non-destructive measurement, ease of sample preparation, ability to be used by low skilled operator and high data/spectrum acquisition rates (Vergnoux et al., 2009).

NIRS involves exposing a sample to near infrared light (light of wavelength 750 to 2500 nm) (13333 cm^{-1} to 4000 cm^{-1}) and measuring the amount of light reflected from the sample (Lu and Bailey, 2005) which is typically a function of chemical composition and microstructure of a sample (Vergnoux et al., 2009). Multivariate statistical techniques such as principal component analysis (PCA) or partial least squares (PLS) regression analysis are used to analyze the complex raw spectral data obtained from NIR equipment. PCA is the most widely used statistical approach used in chemometrics (Brereton, 2007). PCA involves modeling of variance or covariance structure of a given data set to reduce the number of variables to a fewer number of principal components. Principal components are independent of each other with no correlation amongst them. The objective of this study was to predict heating and ignition characteristics of biomass dusts using near infrared spectroscopy (NIRS).

4.3 Methods and Materials

4.3.1 Raw Material

Thirteen feedstock (10 biomass and 3 coal types) were obtained for this study from various sources as listed in table 3.1. Four other biomass samples were used for external validation of the prediction models (table 4.1). Wet biomass samples were either air dried or dried at low temperature (45°C) before they were further utilized for analysis. The samples were ground with a hammer mill (C.S. Bell Co., model 10HBLPK, Tiffin, OH, USA) (figure 3.3 a) fitted with a 3.175 mm (1/8 “) screen. Dust was obtained from the ground material by passing it through #35 market grade (437 μm) screen using a vibratory sieve shaker (Kason Corp., model K30-2-8S, NJ, USA) (figure 3.3 b). This is the closest screen size to the NFPA 500 μm size definition of dust (NFPA, 2013).

Pecan shell, lignite coal and switchgrass (external validation set) samples obtained were already in dust form and were not ground using hammer mill. Dust collected from each feedstock was stored in three 80 oz. air tight containers for further analysis and characterization of physical, chemical, heating and ignition properties which was performed in Chapter 3. Only heating and ignition properties were measured for samples used for external validation to check performance of developed prediction models.

Table 4.1 List of different biomass feedstock used for external validation of prediction models along with their sources.

Biomass	Source
Eucalyptus	Auburn University, AL
Loblolly pine	West Fraser Mills, AL
Sweetgum	Tuskegee (private forest), AL
Switchgrass	University of Tennessee, TN

4.3.2 Near Infrared Spectroscopy (NIRS)

FT-NIR spectrophotometer (FT-NIR 100, PerkinElmer, Shelton, CT, USA) (figure 4.1) was used to collect absorbance vs. wavelength data for the dust samples. Glass plate sample holder was filled completely with dust and sample was exposed to NIR wavelength. The equipment performed 40 scans for each run. NIR spectra from each sample were collected in triplicates. Data was collected at 2 cm^{-1} resolution scans and wavelengths ranging between 10000 and 4000 cm^{-1} but was processed to 10 cm^{-1} resolutions as Statistical Analysis Systems (SAS, 2009) was unable to process larger data matrices (Via et al., 2011). A standard reference check was performed after about every four readings for consistency. Absorbance vs. wavelength data was obtained from the software provided by the equipment manufacturer and the data was imported to Microsoft Excel (Microsoft Excel 2010, Redmond, WA, USA).

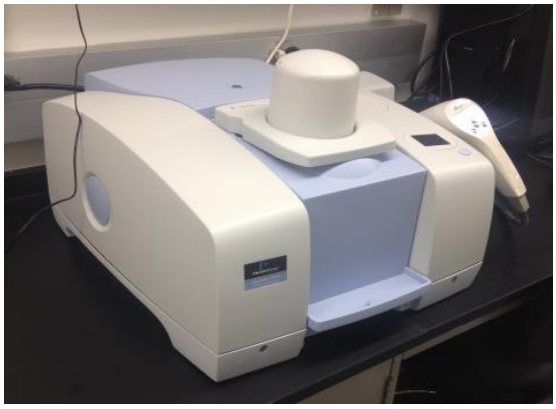

Figure 4.1 FT-NIR spectrophotometer used to collect spectral data of dust samples.

4.3.3 Data Analysis

Data analysis consisted of developing linear regression models for prediction of heating and ignition parameters of dusts with principal components analysis (PCA) using SAS (2009) software. Prediction models were developed for each heating and ignition parameter based on raw spectral data and first derivative data using only the 10 biomass dusts listed in table 3.1. Absorbance vs. wavelength spectral data was imported to Microsoft Excel (Microsoft Excel 2010, Redmond, WA, USA) and average absorbance value corresponding to each wavelength were calculated. Raw spectral graph showing average absorbance vs. wavenumber and first derivative graph was plotted using Microsoft Excel. Important wavelengths (wavelengths corresponding to peaks) were obtained from first derivative spectral plot. Heating and ignition properties prediction models were developed only for biomass dusts since the properties (physical, chemical, heating and ignition) of coal dusts were significantly different thereby causing a leverage point during developing of the models. Tukey test was also performed on principal component values of each selected PC to check if difference among them is significant (α=0.05) for different dust samples.

Raw and 1st-derivative spectra was standardized to a t-distribution with zero mean and standard deviation as 1, so that PCA could be performed by mean centering the spectral data. Principal component score plots and eigenvector loadings plots for significant PCs were obtained from the SAS results and were plotted using Microsoft Excel. Regression diagnostics such as coefficient of determination (R^2), adjusted R^2, root mean square error of calibration (RMSEC) and were employed to determine the best predictive model. A leave one out cross validation (LOOCV) strategy was used to validate the model using standard routines in SAS. For model validation, diagnostics such as root mean square error of prediction (RMSEP) was estimated form predicted sum of squares (PRESS) as shown in equation 4.2 (Via 2013).

$$PRESS = \sum_{i=1}^{N} \left(Y_i - Y_p\right)^2 \qquad (4.2)$$

$$RMSEP = \sqrt{\frac{PRESS}{N}} \qquad (4.3)$$

where,

N is number cases in validation data set,

Y_i is the actual value of i_{th} sample,

Y_p is the predicted value of Y for i_{th} sample.

Ten principal components (PC) were computed for each dust sample from NIR raw and first derivative spectra using SAS. Stepwise selection technique was chosen to decide the number of PC in a predictive model. Significant wavelengths associated with each PC were obtained from eigenvector loading graphs and the

wavelengths were considered significant if the peaks associated with wavenumbers exceeded the 'two standard deviation' mark along the loading distribution for a particular PC. Actual vs. predicted values were plotted for raw spectra models and first derivative models for each heating and ignition parameter. Calibration and validation statistics were tabulated. More information about various formulae involved in statistical analysis and their interpretation can be found in literature (Neter et al., 1996).

Similarly, principal component analysis was also performed for the four dust samples used for external validation (table 4.1). Principal component values thus obtained were used in the equations derived from prediction models to get predicted values for each heating and ignition property for these four dust samples. Plot of actual vs. predicted temperatures were plotted for each heating and ignition property and coefficient of determination (R^2) values were obtained using Microsoft Excel.

4.4 Result and Discussion

4.4.1 Raw NIR Spectra

Figure 4.2 shows average absorbance vs. wavenumber plot for biomass dust samples used for developing prediction models and coal dusts. It can be seen that average absorbance vs. wavenumber curve for all the biomass dust samples follow a similar trend. Coal dust spectra are however different from that of biomass dust spectra. This can be attributed to the difference in chemical nature of biomass and coal. In addition the spectra of bituminous coal was different from that of PRB

and lignite coal. This can be due to the low volatile content (chemical nature) of bituminous coal (33.00%) as compared to that of PRB coal (47.06%) and lignite coal (53.69%) samples.

A baseline shift between the raw NIR spectra of dusts, corresponding to different absorbance values was observed (figure 4.2). This difference in absorbance values can be attributed to variation in densities of the material (Via et al., 2003; Via et al., 2010). According to Beer Lambert's law, apart from absorptivity and length of NIR beam inside the sample, a material with higher density (concentration) will exhibit higher absorbance (Swinehart, 1962).

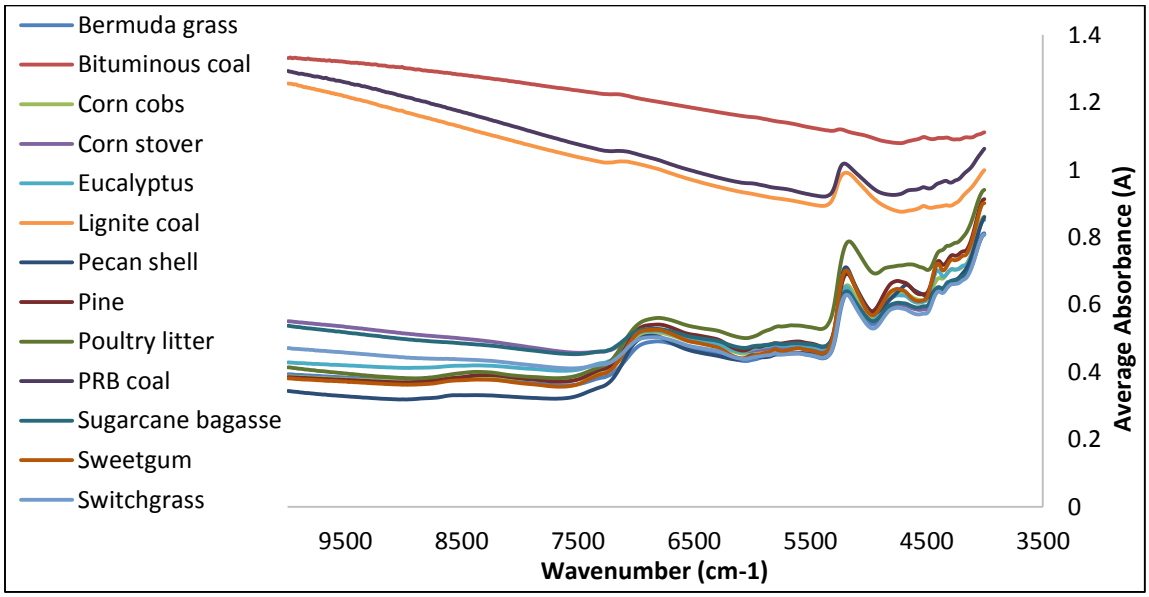

Figure 4.2 NIR spectra showing average absorbance vs. wavenumber plot for different dusts.

4.4.2 First Derivative NIR Spectra

Figure 4.3 shows the first derivative NIR spectral plots for the dust samples. First derivative analysis was carried out on the given samples so that the cause of

variation in spectra can be deciphered. First derivative treatment to the NIR spectra narrows down the peaks associated with important wavenumbers which may be responsible for variation in spectra. It also helps removing the baseline shift between spectra of different dust samples (Breitkreitz et al., 2003). The major disadvantage of first derivative treatment is the addition of noise to the data (Moes et al., 2008).

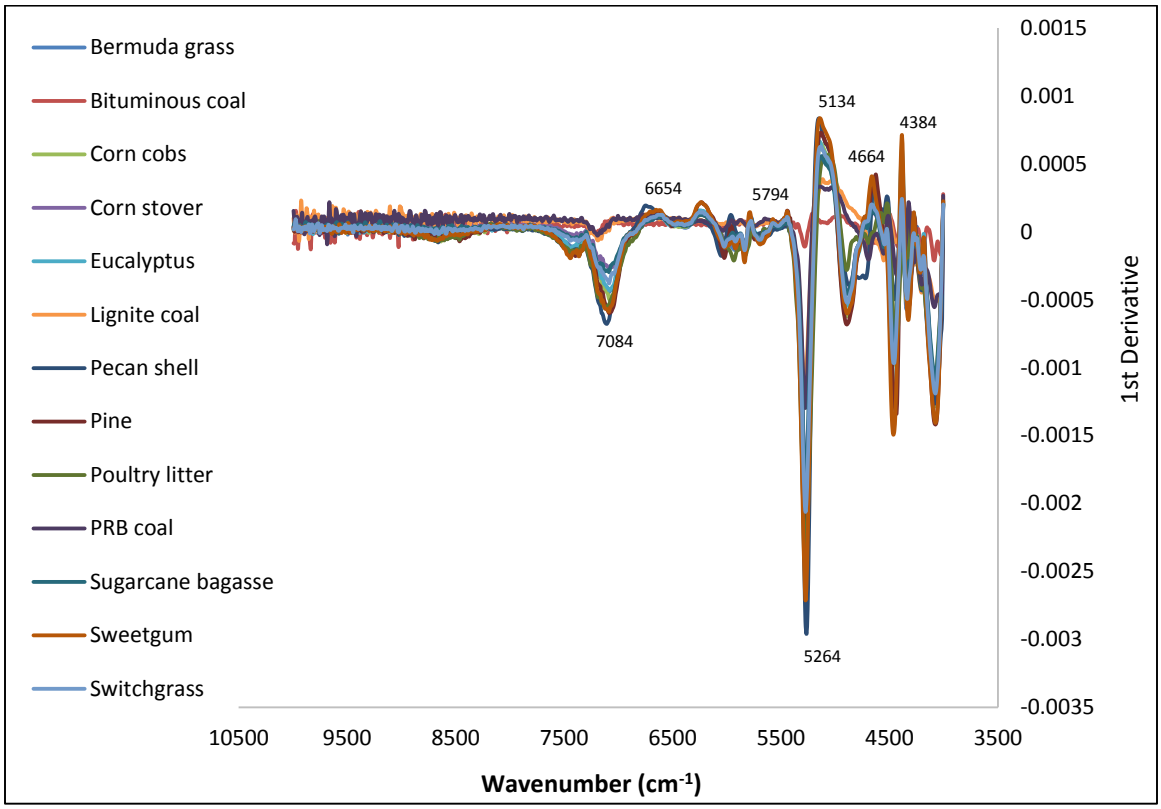

Figure 4.3 First derivative plot of NIR spectra for different dusts showing significant wavenumbers associated with peaks.

Wavenumbers pertaining to different peaks and chemistry associated with them are listed in table 4.2. Hemicellulose (corresponding to wavenumber 5264) (table 4.2) seems to have a greater impact on variation on NIR spectra of dusts since it corresponds to the maximum peak (figure 4.3).

Table 4.2 Chemistry associated with influential wavenumbers derived from first derivative NIR spectra for dust samples (Schwanninger et al., 2011).

Wavenumber (cm^{-1})	Component
4384	Cellulose (4392)
4664	Acetyl groups in Hemicellulose Lignin and extractives (4686)
5134	Water (5220-5150)
5264	Hemicellulose (5245)
5794	Lignin (5795)
6264	Cellulose (6257)
6654	Cellulose (6660)
7084	Phenolic hydroxyl groups Lignin (7092)

4.4.3 PCA Analysis

PC score plots were generated from raw spectral data by comparing various significant (α=0.05) PCs used in models to predict heating and ignition properties of dusts (Figure 4.4). PCs derived from raw spectra were used in this analysis.

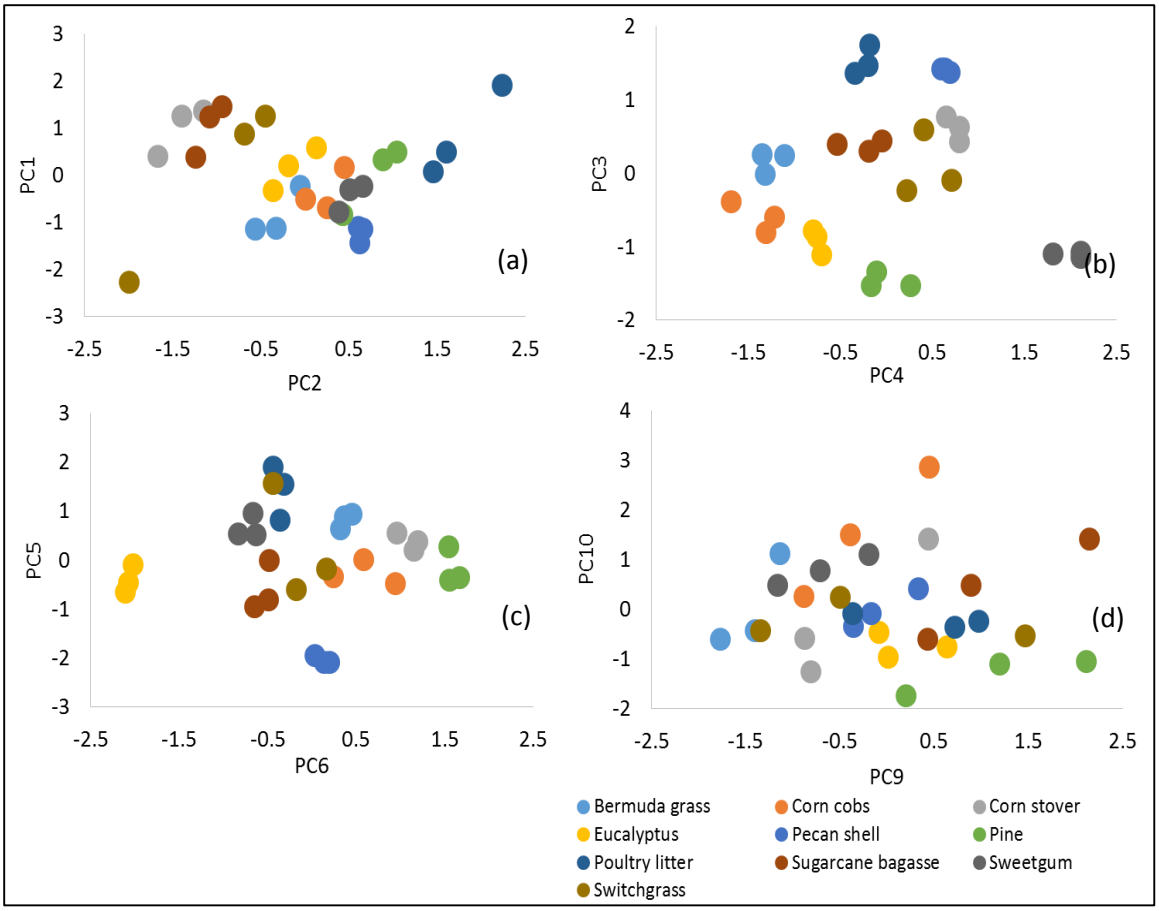

Figure 4.4 Principal component score plots for significant principal components viz. PC1 vs. PC2 (a), PC3 vs. PC4 (b), PC5 vs. PC6 (c) and PC10 vs. PC9 (d) obtained from NIR raw spectral data of biomass dusts.

Generally, PC1 accounts for the baseline shift in the NIR spectra and thus it can be attributed to the difference in densities of the samples in the study. PC1 failed to separate different biomass from each other statistically (α=0.05). PC2, however, was able to statistically separate (α=0.05) corn stover, eucalyptus and poultry litter from each other. This is due to distinct chemical natures of these materials. PC2 was unable to statistically (α=0.05) separate corn stover from sugarcane bagasse and switchgrass which may be due to similarities of chemical or physical nature for these dusts since these biomass are all grassy biomass.

Similarly it was unable to separate pecan shell, sweetgum, corn cobs and eucalyptus from each other.

It can be seen that PC4 was able to statistically (α=0.05) separate corn cobs, eucalyptus, pine, pecan shell and sweetgum from each other (figure 4.4b). Also, it is able to statistically (α=0.05) separate Bermuda grass, poultry litter, pecan shell and sweetgum dusts. Similarly, PC3 statistically (α=0.05) separates poultry litter, sugarcane bagasse, corn cobs and pine. However it fails to separate sugarcane bagasse, switchgrass, corn stover and Bermuda grass from each other. Chemistry associated with the significant PC which was the cause of separation between these biomass dusts will be discussed in a later section.

It is evident from figure 4.4c that PC6 was able to statistically (α=0.05) separate eucalyptus, sweetgum, pecan shell, corn stover and pine from each other. PC5 also statistically (α=0.05) separated eucalyptus, poultry litter and pecan shell. PC6 was however unable to separate switchgrass, poultry litter, sweetgum and sugarcane bagasse from each other. PC5 also was unable to statistically (α=0.05) separate these dusts from each other.

PC9 and PC10 were not able to effectively separate most of the dust samples from each other (figure 4.4d). PC9 only separated pine and sugarcane bagasse from Bermuda grass (α=0.05), whereas PC10 only managed to statistically (α=0.05) separate corn cobs from pine. Thus, dusts showed large variation in the chemistry associated with these PCs which were unable to separate different dusts.

Variation in biomass dusts observed on a particular PC through PC score plots is due to the chemistry associated with that PC. Thus, PC analysis can also be an important analytical tool describing differences in materials/samples under study besides being helpful in prediction model building.

4.4.4 Models for Prediction of Heating and Ignition Properties of Dusts

Models were developed for prediction of heating and ignition properties of biomass dusts using first derivative and raw NIR spectral data (table 4.3). Coefficient of determination (R^2) values obtained for MIT, TORV, TMML, TRE and TME models derived from raw spectra were better than R^2 values for models developed using first derivative data. However, R^2 value for prediction of TOXY was better in case of first derivative model (0.798) than model developed using raw spectra (0.737). Number of PC used for first derivative models were either less than or equal to the number of PC used to develop raw spectral models for respective properties. Lower statistical performance was obtained from first derivative models. Similar conclusion was drawn by Via (2013) in his experiment to develop NIR models for load capacity and deflection of wood composites.

Highest RMSEC, PRESS and RMSEP, and lowest RPD values were obtained from TOXY raw spectra and first derivative spectra models (table 4.3). An effective RPD value should be between 1.5 to 2.5 or greater (Via, 2013). MIT, TORV and TMML models had RPD values greater than 2.5. This means that these models are adequate for internal validation. Except for TOXY, all the models developed using raw spectra had R^2 values of >0.90.

Table 4.3 Calibration and validation statistics for prediction models developed using raw and first derivative NIR spectra.

Model	Type	Number of PCs	C_p	R^2	Adj. R^2	RMSEC	RMSEP	RPD	PRESS
MIT	Raw	10	11.000	0.994	0.991	1.393	1.769	8.333	90.731
	First derivative	8	9.106	0.976	0.966	2.701	3.294	4.475	314.606
TORV	Raw	7	5.418	0.984	0.978	1.612	1.908	5.736	105.536
	First derivative	6	8.015	0.964	0.955	2.319	2.617	4.181	198.611
TMWL	Raw	8	7.885	0.963	0.949	3.381	4.133	3.605	495.444
	First derivative	8	7.690	0.943	0.922	4.171	5.014	2.971	729.167
TOXY	Raw	8	9.824	0.737	0.637	10.213	11.711	1.447	3977.158
	First derivative	8	9.071	0.798	0.721	8.949	10.618	1.596	3269.627
TRE	Raw	8	9.191	0.931	0.904	3.819	4.934	2.500	705.943
	First derivative	8	8.694	0.923	0.894	4.022	4.962	2.486	714.052
TMAX	Raw	7	5.952	0.901	0.869	5.499	6.216	2.444	1120.589
	First derivative	7	6.722	0.895	0.862	5.652	6.631	2.291	1275.262

Figure 4.5 shows actual vs. predicted values for heating and ignition properties of biomass dusts based on raw spectra NIR model. Actual vs. predicted value plots for MIT, TORV and TMML models were found to be linearly related. In case of TOXY model (figure 4.5d), spread of predicted values for given actual values was more as compared to other models. In case of TRE model, it can be seen that pecan shell dust has significantly (α=0.05) lower TRE values as compared to other biomass dusts. Pecan shell dust in this case has high leverage (influence) effecting the mode (figure 4.5e). Similarly, poultry litter was found to have significantly different TME value than the rest of the biomass dusts (figure 4.5f).

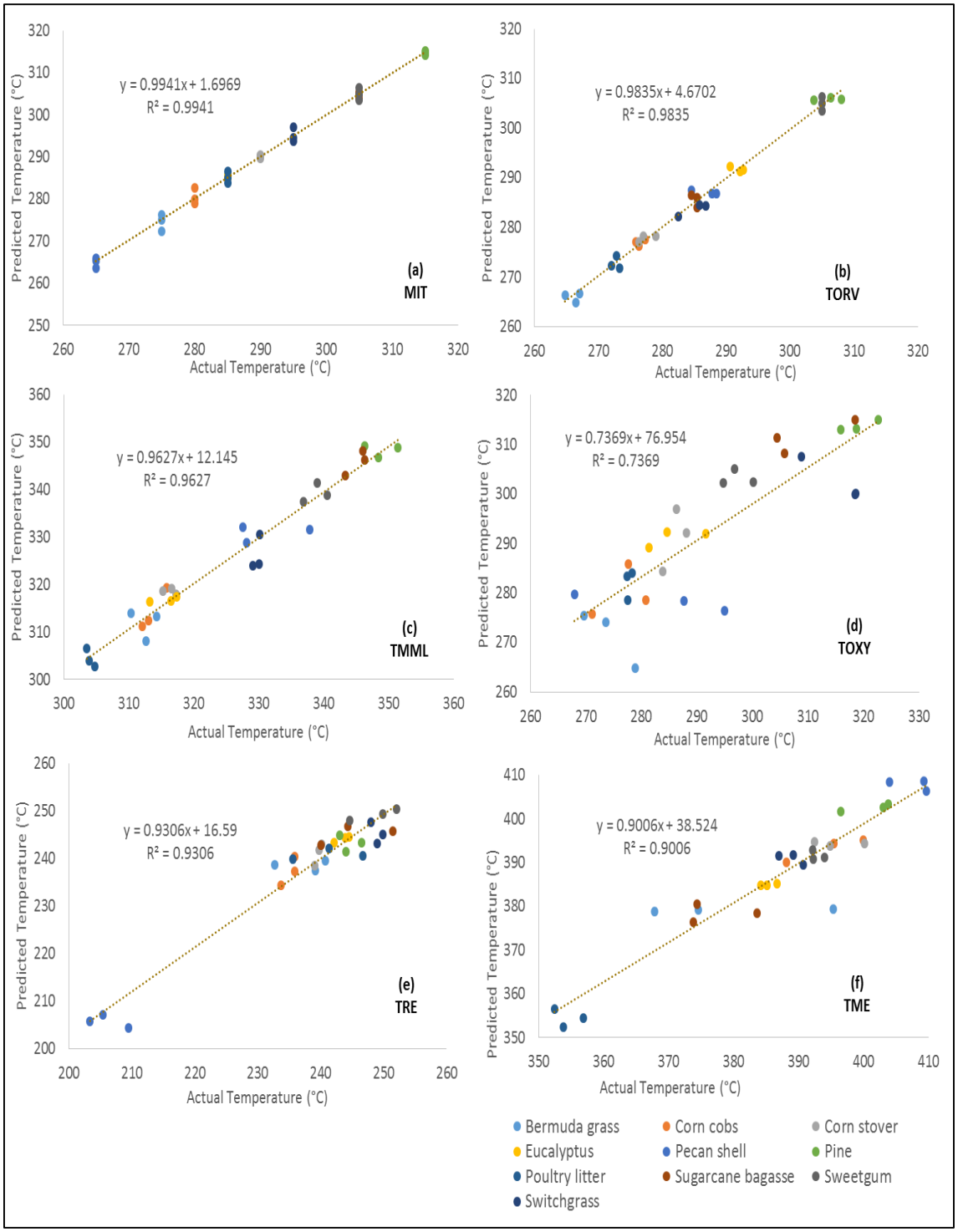

Figure 4.5 Actual vs. predicted values for MIT (a), TORV (b), TMML (c), TOXY (d), TRE (e) and TME (f).

4.4.5 Model Elucidation

Table 4.4 shows all the significant wavelengths affecting heating and ignition properties of biomass dusts corresponding to the statistically significant principal components used for their prediction. The wavelengths were considered significant if the peaks associated with wavenumbers exceeded the 'two standard deviation' mark along the loading distribution for a particular PC (figure 4.6).

It can be seen that all of the significant PC are associated with either lignin, cellulose, hemicellulose or water. Based on PC score plots (figure 4.4) and table 4.4, our summary is that the differences in PC score plots was due to difference in chemical composition of dusts.

4.4.6 External Validation

External validation was performed on the selected models for six heating and ignition properties (TORV, TMML, TOXY, TRE, TME and MIT). Figure 4.7 shows the actual vs. predicted temperature values for four biomass dust samples used for external validation. For prediction of TORV, TMML, TRE, TME and MIT, raw spectra based models were selected for validation purpose. Selection of models was based on their internal cross validation performance discussed in 4.4.4. Although the models suggest a positive correlation between actual and predicted values for the six heating and ignition properties, coefficient of determination (R^2) values obtained were all less than 0.28.

Table 4.4 Chemistry/bond assignment for important wavelengths extracted from statistically significant principal components through regression analysis (Schwanninger et al., 2011).

Significant PCs	Wavenumber	Chemistry/bond assignment
PC2	4534	Lignin (4546)
	4724	Cellulose (4739)
	5634	Cellulose (5618)
	6344	Cellulose (6344)
PC3	4424	Lignin (4411)
	5174	Water (5220-5150)
	5924	Lignin (5935)
	6884	Lignin (6874)
PC4	5024	Water (5051)
	5344	??
	6474	Cellulose (6472)
	8174	Cellulose (8250-8160)
PC5	4414	Lignin (4411)
	4594	cellulose and hemicellulose (4591)
	5734	Cellulose (5776)
	5844	Hemicellulose (5848)
	8164	Cellulose (8250-8160)
PC6	4354	Cellulose (4365)
	4414	Lignin (4411)
	6014	Hemicellulose (6003)
	6554	Cellulose (6520)
	8144	Cellulose (8160)
PC10	8134	Cellulose (8160)
PC9	4344	Cellulose (4365)
	5774	Cellulose (5776)
	8204	Cellulose (8250-8160)
	8354	Lignin (8370)

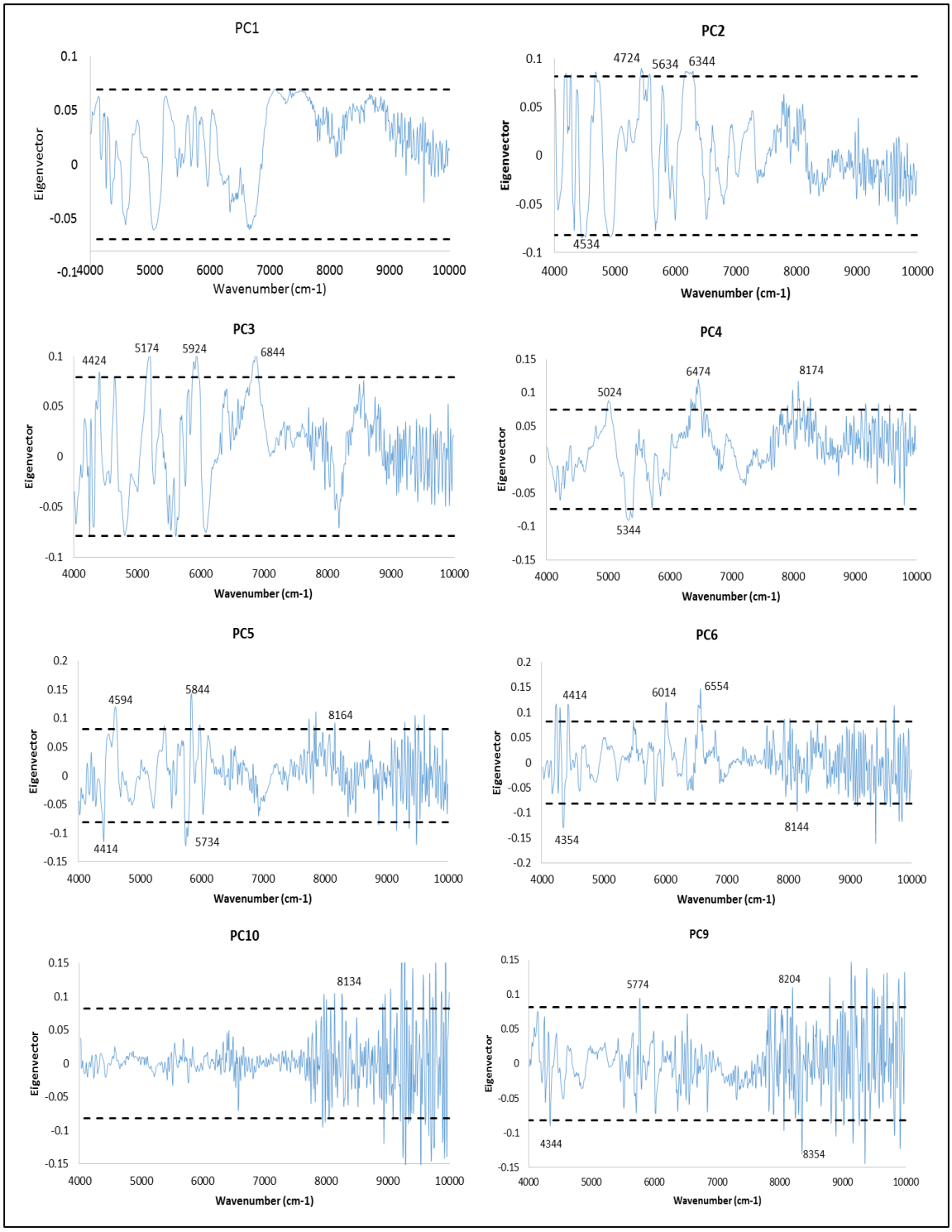

Figure 4.6 Eigenvector loading on NIR spectra showing wavenumber vs. eigenvectors for significant PC. Dashed line represents 95th percentile of eigenvector distribution.

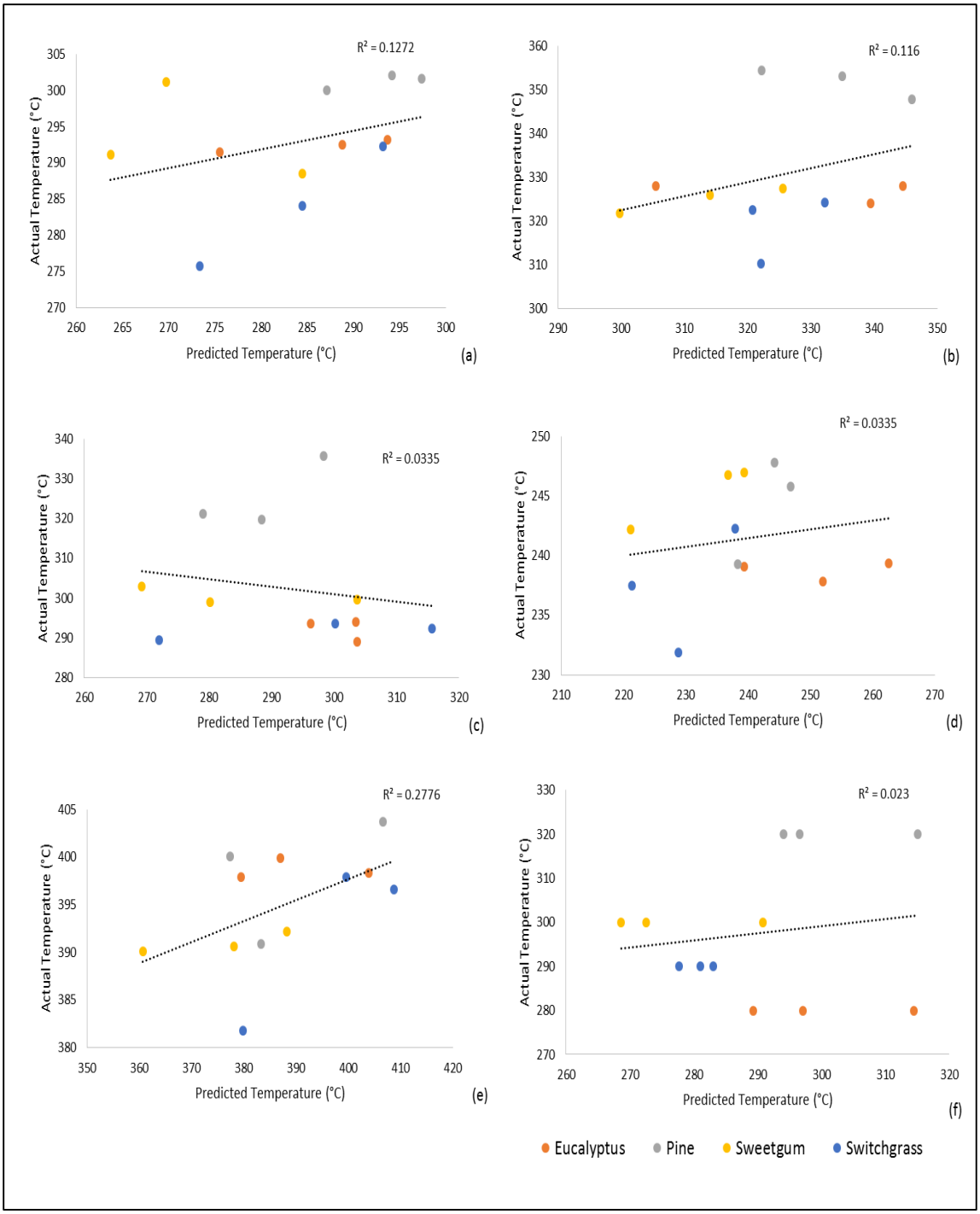

Figure 4.7 External validation results showing actual vs. predicted values for TORV (a), TMML (b), TOXY (c), TRE (d), TME (e) and MIT (f).

Table 4.5 External validation statistics for performance of prediction models developed using raw NIR spectra.

Model	Number of PCs	R^2	Adj. R^2	RMSEP	RPD	PRESS
MIT	10	0.02	-0.07	21.14	0.73	4917.48
TORV	7	0.13	0.04	14.36	0.55	2269.67
TMWL	8	0.12	0.03	17.10	0.80	3217.99
TOXY	8	0.03	-0.06	24.98	0.60	6861.60
TRE	8	0.03	-0.06	12.23	0.39	1646.54
TMAX	7	0.28	0.21	14.50	0.42	2311.26

PRESS and RMSEP values for all the external validation models were high, resulting in low RPD values, ranging from 0.39 to 0.80 (table 4.5). The poor performance of external validation models is due to the variation between biomass of each type (from different sources) which is not accounted for while developing prediction models.

4.5 Conclusion

In case of coal dusts, bituminous coal showed highest absorbance value because of its high bulk density which increases the concentration of material in the path of NIR light beam. Chemistry associated with influential wavenumbers (derived from first derivative spectra) tells us that the difference in chemical constituents of biomass such as lignin, cellulose, hemicellulose, water and other chemical groups are the main reason of variation in NIR spectra obtained.

All the PCs correspond to lignin, cellulose and/or hemicellulose content of the biomass and based on the difference between these constituents of samples, different PCs were able to separate some dusts from others in PC score plots.

R^2 values for internal validation of models were greater than 0.90 for MIT, TORV, TMML, TRE and TME models derived using raw NIR spectra for predicting heating and ignition parameters. For TOXY model, first derivative derived model yielded better R^2 (0.798) than raw derivative based model (R^2=0.737).

R^2 values for external validation of all the models was less than 0.28. The poor performance of models when validated externally with biomass dusts from different sources can be attributed to the variation between biomass of each type (from various sources) which is not accounted for while developing prediction models.

Chapter 5 Summary and Future Recommendation

5.1 Summary

Most of the biomass feedstock showed reduction in moisture content after grinding and sieving. Bituminous coal, sugarcane bagasse and sweetgum however showed an increase in moisture content after grinding operation due to low initial moisture content and hygroscopic nature of the material. Bituminous coal had higher MIT as compared to other biomass dusts because of its low volatile content. TORV and TMML in coal dusts was found to decrease with increase in volatile content. This trend was not observed in biomass due to difference in structure of solid matrices of fuels. Ignition of volatiles corresponded to maximum rate of mass loss in biomass dusts. Based on oxidation temperature and activation energy values, lignite coal was found to have a very high risk of ignition. Bermuda grass, PRB coal, pecan shell, corn cobs, corn stover, eucalyptus and poultry litter were categorized as dusts having high risk of ignition. Switchgrass, pine and sugarcane bagasse were at medium risk of ignition whereas, bituminous coal and sweetgum were at low risk of ignition. High activation energy and TOXY value for bituminous coal can be due to its low volatile content and high carbon content.

Principal component analysis was performed on NIR spectra (raw and first derivative) to obtain models to predict heating and ignition parameters. PC

analysis on raw NIR spectra to build prediction models for MIT, TORV, TMML, TOXY, TRE and TME yielded R2 values in range of 0.737-0.994. Whereas, prediction models based on first derivative NIR spectra for the abovementioned properties yielded R2 values in range of 0.798-0.976. Except for TOXY models, all the prediction models based on raw NIR spectra performed better than models based on first derivative spectra. Significant principal components obtained corresponded mainly to the basic constituents of biomass viz., cellulose, lignin and hemicellulose. Cause of variation in the NIR spectra of biomass dusts was due to variation in these constituents of different biomass dusts.

5.2 Future Recommendation

The study provides an insight into physical, chemical, heating and ignition properties of biomass and coal dusts. The study would be beneficial in setting guidelines for maximum permissible temperatures of process equipment in facilities handling biomass. Findings of this study can be incorporated in a standard against dust fire and explosion hazards. Use of NIR spectroscopy would provide a quick estimation of heating and ignition parameters. However, more robust prediction models can be developed using the procedure given in this study by incorporating samples from a number of sources for each biomass. Developed models can be validated externally to check for robustness.

The fluctuating prices of fossil fuels and its usage's negative impact on environment is drawing a lot of attention on alternative fuels such as biomass. Liu et al. (2002) mentioned that co-combustion of biomass and coal could help in lowering NOx emission. Also, blending of different grades of biomass and/or coal

may help reduce flame stability problems and corrosion problems due to deposited ash (Jiricek et al., 2012). Thus, the study can also be performed on dusts from blends of biomass/coal fuels such as pine – coal blends and other commonly used blends for power generation. Effect of different ratios of blended fuels on heating and ignition properties can be studied.

References

Abbasi T., and S.A. Abbasi. 2007. Dust explosions–Cases, Causes, Consequences, and Control*. J. Hazard. Mat*. 140(1-2): 7-44.

Acheson E.D., R.H. Cowdell, and E.H. Rang. 1981. Nasal cancer in England and Wales: An occupational survey, *Brit. J. Ind. Med*. 38: 218-224.

Amyotte P.R., M.J. Pegg, F. I. Khan, M. Nifuku, and T. Yingxin. 2007. Moderation of dust explosions. *J. Loss Prev. Proc. Ind*. 20(4-6): 675-687.

Amyotte P.R, and R.K. Eckhoff. 2010. Dust Explosion Causation, Prevention and Mitigation: An Overview. *J. Chem. Health Safe*. 17(1): 15-28.

Amyotte P.R., C.T. Cloneya, F.I. Khan, and R.C. Ripley. 2012. Dust explosion risk moderation for flocculent dusts. *J. Loss Prev. Proc. Ind.* 25: 862-869.

An H., and S.W. Searcy. 2012. Economic and energy evaluation of a logistics system based on biomass modules. *Biomass Bioenergy.* 46: 190-202.

ASABE Standard S319.3, 2003. Method of determining and expressing fineness of feed materials by sieving. *American Society of Agricultural and Biological Engineers*. St. Joseph, MI.

ASABE S593.1. 2011. Terminology and Definitions for Biomass Production, Harvesting and Collection, Storage, Processing, Conversion and Utilization. *American Society of Agricultural and Biological Engineers*. St. Joseph, MI.

ASABE S269.5. 2012. Densified Products for Bulk Handling – Definitions and Method. *American Society of Agricultural and Biological Engineers*. St. Joseph, MI.

ASTM E871-82 Reapproved. 2006. Standard Test Method for Moisture Analysis of Particulate Wood Fuels. *American Society for Testing and Materials.* West Conshohocken, PA.

ASTM E2021-09. 2010. Standard Test Method for Hot-Surface Ignition Temperature of Dust Layers. *American Society for Testing and Materials.* West Conshohocken, PA.

ASTM D3174-04. 2004. Standard Test Method for Ash in the Analysis Sample of Coal and Coke from Coal. *American Society for Testing and Materials.* West Conshohocken, PA.

Balat M., and G. Ayar. 2005. Biomass energy in the world, use of biomass and potential trends. *Energy Sources*. 27 (10): 931-940.

Benedetto A., V.D. Sarli, and P. Russo. 2007. On the determination of the minimum ignition temperature for dust/air mixtures. Napoli, Italy. Istituto di Ricerche sulla Combustione, Consiglio Nazionale delle Ricerche (CNR).

Biagini E., A. Fantei, and L. Tognotti. 2008. Effect of the heating rate on the devolatilization of biomass residues. Thermochimica Acta. 472(1-2): 55-63.

Bilbao R., J.F. Mastral, J.A. Lana, J. Ceamanos, M.E. Aldea, and M. Betran. A model for the prediction of the thermal degradation and ignition of wood under constant and variable heat flux. J*. Anal. Appl. Pyrolysis*. 62(1): 63-82.

Biomass Magazine. 2014. Koda energy reopend with new design, Feb 14, 2014. *Biomass Magazine.* Grand Forks, ND.

Blair A.S. 2012. Dust Explosion Primer. *U.S. Chemical Safety and Hazard Investigation Board.* Washington, DC.

BLS. 2013. Bureau of Labor Statistics. United States Department of Labor. Available at http://www.bls.gov/iif/oshwc/cfoi/cftb0266.pdf. Accessed 10 March 2014.

Bobelyn E., A. Serban, M. Nicu, J. Lammertyn, B.M. Nicolai., and W. Saeys. 2010. Postharvest quality of apple predicted by NIR-spectroscopy: Study of the effect of biological variability on spectra and model performance. *Postharv. Biol. Tech*. 55(3): 133-143.

Bowes P.C., and S.E. Townshend. 1962. Ignition of combustible dusts on hot surfaces. Brit. *J. Appl. Phys*. 13: 105-114.

Breitkreitz M.C., I.M. Raimundo, J. R. Rohwedder, C. Pasquini a, H.A. Dantas Filho, G.E. José , and M.C. Araújo. 2003. Determination of total sulfur in diesel fuel employing NIR spectroscopy and multivariate calibration. *Analyst*. 128: 1204-1207.

Brereton R. 2007. *Applied Chemometrics for Scientists*. West Sussex, UK: John Wiley and Sons, Ltd.

Buening-Pfaue H.2003. Analysis of water in food by near infrared spectroscopy. *Food Chem*. 82: 107-115.

Calle´ S., L. Klaba, D. Thomas, L. Perrin, and O. Dufaud. 2005. Influence of the Size Distribution and Concentration on Wood Dust Explosion: Experiments and Reaction Modelling. *Powder Tech*. 157(1-3): 144-148.

Cashdollar K.L. 2000. Overview of dust explosibility characteristics. *J. Loss Prev. Proc. Ind.* 13: 183-199.

Chen Y., S. Mori, and S.P. Pan. 1995. Estimating the combustibility of various coals by TG-DTA. *En. Fuels*. 9: 71-74.

Chen Y., S. Mori, and W.P. Pan. 1996. Studying the mechanisms of ignition of coal particles by TG-DTA. *Thermochimica Acta*. 275: 149-158.

Chiba Lee. 2014. Poultry nutrition and feeding. In *Animal Nutrition Handbook*. 410-425. Auburn, AL.

Collell C., P. Gou, J. Arnau, I. Munoz, and J. Comaposada. 2012. NIR technology for on-line determination of superficial aw and moisture content during the drying process of fermented sausages. *Food Chem*. 135(3): 1750-1755.

Cook J., and J. Beyea. 2000. Bioenergy in the United States: progress and possibilities. *Biom. Bioen*. 18(6): 441-455.

CSB. 2006. Investigation Report – Combustible Dust Hazard Study. Report No. 2006-H-1. Washington, D.C.: U.S. *Chemical Safety and Hazard Investigation Board*.

CSB. 2013. U.S. Chemical safety board. Available at www.csb.gov. Accessed 10 February 2014.

Cuiping L., W. Chuangzhia, Yanyongjieb, and H. Haitaoa. 2004. Chemical elemental characteristics of biomass fuels in China. *Biomass Bioenergy*. 27(2): 119-130.

Demirbas A. 2004. Combustion characteristics of different biomass fuels. Fuel Prog. *En. Combust. Sci*. 30(2): 219–230.

Demirbas A. 2005. Potential applications of renewable energy sources, biomass combustion problems in boiler power systems and combustion related environmental issues. *Prog. Energy. Combust. Sci*. 31 (2): 171-192.

Ebadat V. 2010. Dust explosion hazard assessment. *J. Loss Prev. Proc. Ind.* 23(6): 907-912.

Ebling J.M., and B.M. Jenkins. 1985. Physical and chemical properties of biomass fuels. *Trans. ASAE*. 28(3): 898-902.

Eckhoff R.K. 1991. *Dust Explosions in the Porcess Industry*. 3rd ed. Gulf Professional Publishing. Elsevier Science.

Eckhoff R.K. 2002. Minimum ignition energy (MIE) — a basic ignition sensitivity parameter in design of intrinsically safe electrical apparatus for explosive dust clouds. *J. Loss Prev. Proc. Ind.* 15(4).: 305-310.

Eckhoff R. K. 2003. Dust explosions in the process industries. 3rd ed. Boston, Mass.: Gulf Professional Publishing/Elsevier.

EIA. 2013. United States Energy Information Administration. Available at http://www.eia.gov. Accessed 28 Dec, 2013.

Esteban L.S., and J.E. Carrasco. 2006. Evaluation of different strategies for pulverization of forest biomasses. *Powder Tech*. 166 (3): 139-151.

Fasina O. O. 2008. Physical properties of peanut hull pellets. *Biores. Tech*. 99 (5): 1259-1266.

Field P. 1982. *Handbook of Powder Technology*. Vol. 4. Dust Explosions. Elsevier Science.

Foley W.J., A. McIlwee, I. Lawler, L. Aragones, A. P. Woolnough, and N. Berdig. 1998. Ecological applications of near infrared reflectance spectroscopy: A tool for rapid, cost-effective prediction of the composition of plant and animal tissues and aspects of animal performance. *Oecologia*. 116:293–305.

Friedman H.L. 1963. Kinetics of thermal degradation of char-foaming plactics from thermo-gravimetry—application to a phenolic resin. *Polym. Sci*. 6: 183-195.

Gan J., and C.T. Smith. 2007. Co-benefits of utilizing logging residues for bioenergy production: the case for East Texas, USA. *Biom. Bioen*. 31(9): 623-630.

Gani, A., I. Naruse. 2007. Effect of cellulose and lignin content on pyrolysis and combustion characteristics for several types of biomass. *Renewable Energy*. 32(4): 649–661.

Garcia-Torrent J., E. Conde-Lazaro, C. Wilen, and A. Rautalin. 1998. Biomass dust explosibility at elevated initial pressures. *Fuel*. 77 (9/10): 1093-1097.

Gil M.V., D. Cascal, C. Pevida, J.J. Pis and F. Rubiera. 2010. Thermal behaviour and kinetics of coal/biomass blends during co-combustion. *Biores. Tech*. 101: 5601-5608.

Gronli M., M.J. Antal Jr., G. Varhegyi. 1999. A round-robin study of cellulose pyrolysis kinetics by thermogravimetry. *Ind. Eng. Chem. Res*. 38(6): 2238-2244.

Grotkjaer T., K.D. Johansen, A.D. Jensen, and P. Glarborg. 2003. An experimental study of biomass ignition. *Fuel*. 82(7): 825-833.

Hausen B. 1981. Woods injurious to human health- A manual. *Walter De Gruyter Inc.* Berlin, German Federal Republic.

Haykiri-Acma H. 2003. Combustion characteristics of different biomass materials. *En. Cons. Mgmt*. 44(1): 155-162.

Hehar G.S. 2013. Physicochemical and Ignition Properties of Dust from Loblolly Pine Wood. MS Thesis. Auburn Ala.: Auburn University, Department of Biosystems Engineering.

ISO 562. 2010. Hard coal and coke. Determination of volatile matter. *International Organization for Standardization.* Geneva, Switzerland.

Jamshidi B., S. Minaei, E. Mohajerani, and H. Ghassemian. 2012. Reflectance Vis/NIR spectroscopy for nondestructive taste characterization of Valencia oranges. *Comp. Elec. Agri*. 85: 64-69.

Janes A., D. Carson, A. Accorsi, J. Chaineaux, B. Tribouilloy, and D. Morainvillers. 2008. Correlation between self-ignition of a dust layer on a hot surface and in baskets in an oven. *J. Haz. Mat*. 159 (2-3): 528-535.

Jenkins B.M. 1989. Biomass handbook. In *Physical properties of biomass*, Ch 5.2. New York, NY.: Gordon & Breach,

Jenkins B.M., L.L Baxter, T.R Miles Jr., and T.R Miles. 1998. Combustion properties of biomass. *Fuel Proc. Tech*. 54(1-3): 17-46.

Jeske, A., and H. Beck. 1989. Evaluation of dust explosions in the Federal Republic of Germany. *EUROPEX Newsletter.* No 9: 2.

Jiricek I., P. Rudasov, and T. Zemlov. 2012. A thermogravimetric study of the behaviour of biomass blends during combustion. *Acta Polytechnica*. 52(3): 39-42.

Joshi K.A., V. Raghavan, and A.S. Rangwala. 2012. An experimental study of coal dust ignition in wedge shaped hot plate configurations. *Combust. Flame*. 159(1): 376-384.

Kauffman C.W. 1982. *Agricultural dust explosions in grain handling facilities.* J.H.S. Lee, C.M. Guirao (Eds.). Fuel-air Explosions. University of Waterloo Press. Waterloo, Ontario, Canada: 305–347.

Kettaneh N., A. Berglund, and S. Wold. 2005. PCA and PLS with very large data sets. *Comp. Stat. Data An*. 56: 101-8.

Kheshgi H.S., R.C. Prince, and G. Marland. 2000. The potential of biomass fuels in the context of global climate change: focus on transportation fuels. *Annual Rev. Energy Environ*. 25: 199-244.

Khan, N., M. Bradley, and R. Berry. 2008. Best Practice Guide for Handling of Biomass Fuels and Coal-Biomass Mixes. *The Wolfson Centre for Bulk Solids Handling Technology*.

Liang Y.L., and O.M. Kvalheim. 1996. Robust methods for multivariate analysis – a tutorial view. *Chemometr. Intell. Lab*. 32:1-10.

Liodakis S., and A. Dimitrakopoulos. 2002. Ignition characteristics of forest species in relation to thermal analysis data. *Thermochimica Acta*. 390 (1-2): 83-91.

Littlefield B., O.O. Fasina, J. Shaw, S. Adhikari, and B. Via. 2011. Physical and flow properties of pecan shells—Particle size and moisture effects. *Powder Tech*. 212 (1): 173-180.

Liu D.C., C.L. Zhang, T. Mi, B.X. Shen, and B. Feng. 2002. Reduction of N_2O and NO emissions by co-combustion of coal and biomass. *J. Inst. Energy*. 75: 81-85.

Liu X., and X.T. Bi. 2011. Removal of inorganic constituents from pine barks and switchgrass. *Fuel Proc. Tech*. 92(7): 1273-1279.

Louw E.D., and K.I. Theron. 2010. Robust prediction models for quality parameters in Japanese plums. *Postharvest Biol. Tech*. 58: 176–184.

Lu R., and B.B. Bailey. 2005. NIR measurement of apple fruit soluble solids content and firmness as affected by postharvest storage. *ASAE Annual International Meeting, Tampa, Fla*. Paper No. 056070.

Lunn G.A. 1992. Dust explosions in the process industries : by R. K. Eckhoff, published by Butterworth Heinemann, Oxford, 1991, 599 pp.; ISBN: 0-7506-1109-x; £80.00. *Powder Tech*. 73 (1): 97.

Mafakheri F., and F. Nasiri. 2014. Modeling of biomass-to-energy supply chain operations: Applications, challenges and research directions. *Energy Pol*. 67: 116-126.

Mani S., L.G Tabil, and S. Sokhansanj. 2003. An overview of compaction of biomass grinds. *Powder Handling Proc*. 15 (3): 160–168.

Mani S., L. G. Tabil, and S. Sokhansanj. 2004. Grinding performance and physical properties of wheat and barley straws, corn stover and switchgrass. *Biomass Bioenergy*. 27(4): 339-352.

Martens H. 1979. Factor analysis of chemical mixtures. *Anal. Chim. Acta*. 112: 423-42.

Mayfield C.A., D. Foster, T. Smith, J. Gan, and S. Fox. 2007. Opportunities, barriers, and strategies for forest bioenergy and bio-based product development in the Southern United States. *Biom. Bioen.* 31(9): 631-637.

McKendry P. 2002. Energy production from biomass (part 1): overview of biomass. *Biores. Tech*. 83(1): 37-46.

McNew K., and D. Griffith. 2005. Measuring the impact of ethanol plants on local grain prices. *Review. Agri. Eco*. 27: 164-180.

Michaels L. 1967. Lung changes in woodworkers. *Can. Med. Assoc. J*. 96: 1150.

Miron Y., and C. P. Lazzara. 1988. Hot-surface ignition temperatures of dust layers. *Fire Matls*. 12: 115-126.

Moes J.J., M.M. Ruijken, E. Gouta, H.W. Frijlink, and M.I. Ugwokea. 2008. Application of process analytical technology in tablet process development using NIR spectroscopy: Blend uniformity, content uniformity and coating thickness measurements. Int.J. Pharma. 357(1-2): 108-118.

Moqbel S., D. Reinhart, and R.H. Chen. 2010. Factors influencing spontaneous combustion of solid waste. *Waste Mgmt*. 30 (8–9): 1600-1607.

Muthuraman M., T. Namiokaa, K. Yoshikawab. 2010. A comparison of co-combustion characteristics of coal with wood and hydrothermally treated municipal solid waste. *Biores. Tech*. 101(7): 2477-2482.

NCDOL. 2012. A guide to combustible dusts. N.C. department of labor - Occupational Safety and Health Division. Available at http://www.nclabor.com/osha/etta/indguide/ig43.pdf. Accessed 11 February 2014.

Neter J., M. Kunter, C. Nachtsheim, and W. Wasserman. 1996. Applied Linear Statistical Models. *4th Ed*. Irwin, Boston, MA, USA.

NFPA. 2013. Standard for Prevention of Dust Explosions from the Manufacturing, Processing and Handling of Combustible Particulate Solids. NFPA 654. Quincy, Mass.: *National Fire Protection Association*.

NFPA. 2013. Recommended practice for the classification of combustible dusts and of hazardous locations for electrical installations in chemical process areas online. NFPA 499. Quincy, Mass.: *National Fire Protection Association*.

Nicolai B.M., B.E. Verlinden, M. Desmet, S. Saevels, W. Sayes, K. Theron, R. Cubeddu, A. Pifferi, and A. Torricelli. 2008. Time-resolved and continuous wave NIR reflectance spectroscopy to predict soluble solids content and firmness of pear*. Postharvest Biol. Tech*. 47(1): 68-74.

Nifuku M., H. Tsujita, K. Fujino, K. Takaichi, C. Barre, M. Hattori, S. Fujiwara, S. Horiguchi, and E. Paya. 2005. A study on ignition characteristics for dust explosion of industrial wastes. *J. Electrostatics.* 6(6-10): 455-462.

Norris K. H. 1964. Reports on design and development of a new moisture meter. *Agric. Eng*. 45(7): 370-372.

NREL. 2005. Determination of Ash in Biomass by Laboratory Analytical Procedure. *National Renewable Energy Laboratory.* NREL/TP-510-42622.

Orfao J.J.M., F.J.A. Antunes, and J.L. Figueiredo. Pyrolysis kinetics of lignocellulosic materials: three independent reactions model. *Fuel*. 78: 349-358.

Osborne B.G., T. Fearn, and P.H. Hindle. 1993. Practical NIR spectroscopy with applications in food and beverage analysis. *Longman Group United Kingdom. 2nd sub Ed*. ISBN: 0-582-09946-3.

OSHA. 2014. OSHA Regional News Release. *Occupational Safety and Health Administration*. Available at: https://www.osha.gov/pls/oshaweb/owadisp.show_document?p_table=NEWS_RELEASES&p_id=25695. Accessed Jul 7, 2014.

Park H. 2006. Hot surface ignition temperature of dust layers With and without Combustible additives. Master's Thesis. Worcester Polytechnic Institute, Mass., USA.

Park H., A.S. Rangwala, and N.A. Dembsey. 2009. A means to estimate thermal and kinetic parameters of coal dust layer from hot surface ignition tests. *J. Hazard. Mat*. 168 (1): 145-155.

Park Y.H., J. Kim, S.S. Kim, and Y.K. Park. 2009. Pyrolysis characteristics and kinetics of oak trees using thermogravimetric analyzer and micro-tubing reactor. *Biores. Tech*. 100(1): 400-405.

Parikka, M. 2004. Global biomass fuel resources. *Biomass and Bioenergy*. 27: 613-620.

Perlack, R. D., L. L. Wright, A. F. Turhollow, R. L. Graham, B. J. Stokes, and D. C. Erbach. 2005. Biomass as feedstock for a bioenergy and bioproducts industrythe technical feasibility of a billion-ton annual supply. *United States Department of Energy*. Oak Ridge, TN.

Pinho R., F. Bonatto, M. Andrades, M. Frota, C.Ritter, F. Klamt, F. Dal-Pizzol, J.M. Uldrich-Kulczynski, and J.F. Moreiraa.2004. Lung oxidative response after acute coal dust exposure. *Environ. Res*. 96: 290-297.

Polka M., Z. Salamonowicz, M. Wolinski, and B. Kukfisz. 2012. Experimental analysis of minimal ignition temperatures of a dust layer and clouds on a heated surface of selected flammable dusts. *Procedia Engineering.* Vol. 45: 414-423.

Porteir J., D. Patino, J. Collazo, E. Granada, J. Moran, and J.L. Miguez. 2010. Experimental analysis of the ignition front propagation of several biomass fuels in a fixed-bed combustor. *Fuel*. 89 (1): 26-35.

Probst K.V., R. P. Kingsly Ambrose, R. L. Pinto, R. Bali, P. Krishnakumar, and K. E. Ileleji. 2013. The effect of moisture content on the grinding performance of corn and corncobs by hammermilling .*Trans. ASABE*. 56(3): 1025-1033.

Rajagopal D., S. Sexton, G. Hochman, D. Roland-Holst, and D. Zilberman. 2009. Model estimates food-versus-biofuel trade-off. *Cali. Agri*. 63(4): 199-201.

Rambla F.J., S. Garriguea, and M. de la Guardia. 1997. PLS-NIR determination of total sugar, glucose, fructose and sucrose in aqueous solutions of fruit juices. *Analytica Chimica Acta*. 344: 41-53.

Ramirez A. 2009. Determination of parameters used to prevent ignition of stored materials and to protect against explosions in food industries. *Pedro J. Aguadoc*. 168(1): 115-120.

Ramírez A., J. García-Torrent, and A. Tascón. 2010. Experimental determination of self-heating and self-ignition risks associated with the dusts of agricultural materials commonly stored in silos. *J. Hazard. Mat.* 175: 920-927.

Reddy P. D., P. R. Amyotte, and M. J. Pegg. 1998. Effect of inerts on layer ignition temperatures of coal dust. *combustion flame.* 114(1–2):41-53.

Renewables International Magazine. 2011. Following explosion, world's largest pellet plant resumes operation. Available at http://www.renewablesinternational.net/following-explosion-worlds-largest-pellet-plant-resumes-operation/150/515/31440/. Accessed 12 March 2014.

Rhodes M. 1998. Introduction to Particle Technology. John Wiley and Sons. New York.

Ryu C., Y.B. Yang, A. Khor, N.E. Yates, V.N. Sharifi, and J. Swithenbank. 2006. Effect of fuel properties on biomass combustion: Part I. Experiments—fuel type, equivalence ratio and particle size. *Fuel*. 85: 1039-1046.

Sahu S.G., P. Sarkar, N. Chakraborty, and A.K. Adak. 2010. Thermogravimetric assessment of combustion characteristics of blends of a coal with different biomass chars. *Fuel Proc. Tech*. 91(3): 369-378.

Samaras P., E. Diamadopoulos, and G.P. Sakellaropoulosa. 1996. The effect of mineral matter and pyrolysis conditions on the gasification of Greek lignite by carbon dioxide. *Fuel*. 75(9): 1108-1114.

Sapko M.J., E.S. Weiss, K.L. Cashdollar, and I.A. Zlochower. 2000. Experimental mine and laboratory dust explosion research at NIOSH. *J. of Loss Prev. in Proc. Ind.* 13 (3-5): 229-242.

SAS. 2009. SAS User's Guide: Statistics. Ver. 6a. Cary, N.C.: *SAS Institute, Inc*.

Schoeff R.W. 2006. Agricultural Dust Explosions in 2005. Available at krex.kstate.edu/dspace/bitstream/handle/2097/4305/2005Dust_Explosions.pdf?sequence=1. Accessed on 2 february 2014.

Schwanninger M., J.C. Rodrigues, K. Fackler. 2011. A review of band assignments in near infrared spectra of wood and wood components. *J. Near Infrared Spectroscopy.* 19: 287-308.

Shi l., and M. Chew. 2011. Influence of moisture on autoignition of woods in conecalorimeter. *J. Fire Sc*. 30(2): 158-169.

Shiroma C., and L. Rodriguez-Saona. 2009. Application of NIR and MIR spectroscopy in quality control of potato chips. *J. Food Comp. Anal*. 22(6): 596-605.

Sorum L., M.G. Gronli, and J.E. Hustad. 2001. Pyrolysis characteristics and Kinetics of municipal solid wastes. *Fuel*. 80 (9): 1217-1227.

SSCHE. 2009. Proceedings: 36th International Conference of Slovak Society of Chemical Engineering. ISBN 978-80-227-3072-3. Slovak Society of Chemical Engineering.

Stephenson A.H., T.A. McCaskey, and B.G. Ruffin. 1990. A survey of broiler litter composition and value as a nutrient resource potential. *Biol. Wastes*. 34(1): 1-9.

Sweis F.K. 1998. The effect of admixed material on the ignition temperature of dust layers in hot environments. *J. Hazard. Mat.* 63(1): 25-35.

Swinehart D.F. 1962. The Beer-Lambert law. *J. Chem. Educ*. 39 (7): 333.

Tabil L.G. Pelleting and binding characteristics of alfalfa. 1996. Ph.D thesis, *Department of Agricultural and Bioresource Engineering, Saskatoon, SK Canada. University of Saskatchewan.*

Tembo G., F.M. Epplin, and R.L. Huhnke. 2003. Integrative investment appraisal of a lignocellulosic biomass-to-ethanol industry. *J. Agr. Res. Econ*. 28 (3): 611–633.

Theimer O.P.1973. Cause and prevention of dust explosions in grain elevators and flour mills. *Powder tech*. 8: 137-147.

Tiqui S.M., and N.F.Y Tam. 2000. Fate of nitrogen during composting of chicken litter. *Environ. Poll*. 110(3): 535-541.

Tognotti L., A. Malotti, I. Petarca, and S. Zanelli. 1985. Measurement of ignition temperature of coal particles using a thermogravimetric technique. *Combust. Sci. Technol*. 44: 15-28.

United Nations. 2014. UN News Center. Available at http://www.un.org/apps/news/story.asp?NewsID=45165#.U0IGEUco4eg. Accessed 13 march 2014.

U.S. Department of Energy. 2010. Biomass multi-year program plan. Available at http://www1.eere.energy.gov/biomass/pdfs/biomass_mypp_november2010.pdf; 2010. Accessed 30 November 2013.

USCB. 2014. United States Census Bureau. Available at http://www.census.gov/population/international/data/worldpop/table_population.php. Accessed 2 February 2014.

USDA. 2010. Agricultural Research Service. Chicken litter has advantages over conventional fertilizers. Available at www.sciencedaily.com/releases/2010/06/100623124254.htm. Accesed 10 March, 2014.

Vamvuka D., E. Kakaras, E. Kastanaki, and P. Grammelis. 2003. Pyrolysis characteristics and kinetics of biomass residuals mixtures with lignite. *Fuel*. 82(15-17): 1949-1960.

Vamvuka D., and S. Sfakiotakis. 2011. Combustion behaviour of biomass fuels and their blends with lignite. *Thermochimica Acta*. 526 (1-2): 192-199.

Vergnoux A., M. Guiliano, Y.L. Dréau, J. Kister, N. Dupuy, and P. Doumenq. 2009. Monitoring of the evolution of an industrial compost and prediction of some compost properties by NIR spectroscopy. *Sci. Total Environ*. 407(7): 2390-2403.

Via B.K., T.F. Shupe, L.H. Groom, M. Stine, and C. So. 2003. Multivariate modelling of density, strength and stiffness from near infrared spectra for mature, juvenile and pith wood of longleaf pine (pinus palustris). *J Near Infrared Spectrosc*. 11 (5):365–378

Via B.K. 2010. Prediction of oriented strand board wood strand density by near infrared and Fourier transform infrared refplectance spectroscopy. *J Near Infrared Spectrosc*. 27: 491-498.

Via B.K., O.O. Fasina, and H. Pan. 2011. Assessment of pine biomass density through midinfrared spectroscopy and multivariate modeling. *Biores*. 6 (1): 807–822.

Via B. 2013. Characterization and evaluation of wood strand composite load capacity with near infrared spectroscopy. *Mat. Struct*. 46: 1801-1810.

Via B.K., S. Adhikari, and S. Taylor. 2013. Modeling for proximate analysis and heating value of torrefied biomass with vibration spectroscopy. *Biores. Tech*. 133: 1-8.

Vijayraghavan G. 2004. Impact assessment, modeling and control of dust explosions in chemical process industries. MTech Thesis. Department of Chemical Engineering, Coimbatore Institute of Technology.

Vijayraghavan G. 2011. Emerging emergency due to dust explosions in process industry. *J. Engg. Res. Stud.* 2 (4): 193-198.

Virk S.S., J.P. Fulton, O.O. Fasina, and T.P. McDonald. 2013. Capacitance and near-infrared techniques for the real-time moisture measurement of broiler litter. *Biosys. Eng*. 116: 357-367.

Vuthaluru H.B. 2004. Investigations into the pyrolytic behaviour of coal/biomass blends using thermogravimetric analysis. *Biores. Tech*. 92(2): 187-195.

Wang. C., Y. Wu, Q. Liu, and H. Yang. 2011. Study of the characteristics of the ashing process of straw/coal combustion. *Fuel*. 90: 2939-2944.

White J.E., W.J. Catallo, and B.L. Legendre. 2011. Biomass pyrolysis kinetics: A comparitive critical review with relevant agricultural residue case studies. J. Anal. App. Pyrolysis. 91 (1): 1-33.

Wiedenhofer D., M. Lenzen, and J.K. Steinberger. 2013. Energy requirements of consumption: Urban form, climatic and socio-economic factors, rebounds and their policy implications. *Energy Pol*. 63: 696-707.

Windham W.R., F.E. Barton II, and J.A. Robertson. 1988. Moisture analysis of forage by near infrared reflectance spectroscopy: Preliminary collaborative study and comparison between Karl Fischer and oven drying reference methods. *J. Assoc. Off. Anal. Chem*. 71: 256-262.

Wypych P., D. Cook, and P. Cooper. 2005. Controlling dust emissions and explosion hazards in powder handling plants. *Chem. Eng. Proc.: Proc. Intes*. 44 (2): 323-326.

Yang H., R. Yan, H. Chen, C. Zheng, D.H. Lee, and D.T. Liang. 2006. In-depth investigation of biomass pyrolysis based on three major components: hemicellulose, cellulose and lignin. *Energy Fuels*. 20: 388-393.

Yang H., R. Yan, H. Chen, D.H. Lee, and C. Zheng. 2007. Characteristics of hemicellulose, cellulose and lignin pyrolysis. *Fuel*. 86(12-13): 1781-1788.

Zalosh R. 2008. Dust Explosion Fundamentals: Ignition Criteria and Pressure Development. Wellesley, Mass.: National Fire Protection Association. Available at http://www.nfpa.org/assets/files/pdf/foundation%20proceedings/dust_explosion_fundamentals_ignition_criteria_and_pressure_d.pdf. Accessed on 25 November 2012.

Zhang D.K., and T.F. Wall. 1994. Ignition of coal particles—the influence of experimental technique. *Fuel*. 73: 1114-1119.

Appendix A – Initial Moisture Content and Physiochemical Properties of Dusts and Ground Material.

Table A.1 Initial moisture content of feedstock.

Biomass	Moisture content (% w.b.)	Mean Moisture Content (% w.b.)	Standard Deviation (% w.b.)
Bermuda grass	11.28 10.71 10.74	10.91	0.32
Bituminous coal	2.52 2.35 2.39	2.42	0.09
Corn cobs	9.62 9.24 9.49	9.45	0.19
Corn stover	9.28 9.27 10.23	9.59	0.55
Eucalyptus	7.11 6.86 6.91	6.96	0.13
Lignite coal	29.36 29.44 29.41	29.40	0.04
Pecan shell	12.70 12.98 12.45	12.71	0.27
Pine	11.53 11.70 11.99	11.74	0.23
Poultry Litter	14.82 14.79 14.82	14.81	0.02
PRB coal	15.26 15.23 15.26	15.25	0.02
Sugarcane Bagasse (after drying)	5.71 5.62 5.71	5.68	0.05
Sugarcane Bagasse (before drying)	25.64 23.05 25.62	24.77	1.49
Sweetgum (After drying)	5.50 5.36 5.50	5.45	0.08
Sweetgum (before drying)	51.97 50.79 51.97	51.58	0.68
Switchgrass	12.08 11.85 13.32	12.42	0.79

Table A.2 Moisture content of dust samples.

Sample	Moisture Content (w.b.%)	Mean Moisture Content (W.b.%)	Standard Deviation (w.b.%)
Bermuda grass	8.35	8.06	0.27
	8.02		
	7.82		
Bituminous coal	2.98	2.96	0.02
	2.96		
	2.95		
Corn cobs	6.88	7.40	0.65
	8.13		
	7.18		
Corn stover	7.08	6.99	0.10
	6.89		
	7.01		
Eucalyptus	7.18	6.80	0.33
	6.63		
	6.57		
Lignite coal	29.36	29.40	0.04
	29.44		
	29.41		
Pecan shell	12.70	12.71	0.27
	12.98		
	12.45		
Pine	7.17	7.20	0.10
	7.11		
	7.30		
Poultry litter	11.91	11.89	0.07
	11.81		
	11.94		
PRB coal	13.79	13.79	0.02
	13.77		
	13.81		
Sugarcane bagasse	6.11	6.06	0.05
	6.06		
	6.01		
sweetgum	8.05	8.23	0.21
	8.17		
	8.46		
Switchgrass	8.00	8.27	0.63
	8.98		
	7.82		

Table A.3 Bulk densities of dust samples.

Sample	Bulk Density (kg/m^3)	Mean Bulk Density (kg/m^3)	Standard Deviation (kg/m^3)
Bermuda grass	157.65	159.28	1.43
	159.06		
	161.13		
Bituminous coal	648.09	651.75	3.88
	657.12		
	650.04		
Corn cobs	164.64	164.86	2.00
	167.41		
	162.53		
Corn stover	124.36	126.52	1.76
	128.67		
	126.52		
Eucalyptus	215.08	217.60	2.08
	220.18		
	217.55		
Lignite coal	499.02	503.40	3.34
	507.12		
	504.05		
Pecan shell	401.50	403.95	2.61
	402.80		
	407.56		
Pine	173.61	173.06	3.43
	176.96		
	168.60		
Poultry litter	356.98	360.74	3.71
	359.45		
	365.79		
PRB coal	655.32	655.66	3.19
	659.72		
	651.93		
Sugarcane bagasse	111.65	112.34	1.74
	114.73		
	110.64		
sweetgum	182.19	183.57	1.37
	185.44		
	183.09		
Switchgrass	140.92	141.01	0.63
	141.82		
	140.28		

Table A.4 Particle densities for dust samples.

Sample	Particle Density ($kg/m^{3)}$	Mean Particle Density (kg/m3)	Standard Deviation (kg/m3)
Bermuda grass	1169.50	1167.33	1.65
	1165.50		
	1167.00		
Bituminous coal	1392.50	1406.20	13.98
	1425.40		
	1400.70		
Corn cobs	1481.20	1481.43	0.17
	1481.60		
	1481.50		
Corn stover	1506.80	1500.90	4.56
	1495.70		
	1500.20		
Eucalyptus	1493.20	1490.30	2.19
	1487.90		
	1489.80		
Lignite coal	1674.40	1672.20	2.38
	1673.30		
	1668.90		
Pecan shell	1520.70	1521.93	0.95
	1523.00		
	1522.10		
Pine	1477.10	1471.87	3.80
	1468.20		
	1470.30		
Poultry litter	1537.20	1539.23	1.51
	1540.80		
	1539.70		
PRB coal	1505.70	1505.13	0.66
	1504.20		
	1505.50		
Sugarcane bagasse	1582.00	1585.27	2.42
	1587.80		
	1586.00		
sweetgum	1484.50	1480.47	2.85
	1478.30		
	1478.60		
Switchgrass	1373.10	1366.17	5.59
	1359.40		
	1366.00		

Table A.5 Ash content values for dust samples.

Sample	Ash Content (% d.b.)	Mean Ash Content (% d.b.)	Standard deviation (% d.b.)
Bermuda grass	4.80	4.68	0.16
	4.46		
	4.79		
Bituminous coal	9.16	10.27	1.81
	12.83		
	8.83		
Corn cobs	2.67	2.62	0.08
	2.51		
	2.68		
Corn stover	13.97	14.33	0.26
	14.45		
	14.58		
Eucalyptus	1.25	1.40	0.12
	1.55		
	1.40		
Lignite coal	20.70	20.84	0.16
	20.75		
	21.05		
Pecan shell	2.66	2.68	0.04
	2.74		
	2.65		
Pine	1.11	1.10	0.14
	1.27		
	0.93		
Poultry litter	13.71	13.74	0.07
	13.67		
	13.84		
PRB coal	8.22	8.14	0.07
	8.05		
	8.16		
Sugarcane bagasse	15.66	15.52	0.27
	15.77		
	15.15		
sweetgum	1.62	1.41	0.22
	1.11		
	1.49		
Switchgrass	8.06	7.57	0.35
	7.26		
	7.40		

Table A.6 Volatile content values for dust samples.

Sample	Volatile Matter (% d.b.)	Mean Volatile Matter (% d.b.)	Standard deviation (% d.b.)
Bermuda grass	78.70	78.61	0.85
	79.61		
	77.52		
Bituminous coal	33.07	33.00	0.05
	32.94		
	32.99		
Corn cobs	80.52	81.51	1.51
	83.65		
	80.36		
Corn stover	73.69	72.97	0.58
	72.95		
	72.26		
Eucalyptus	81.13	81.27	0.14
	81.46		
	81.21		
Lignite coal	55.35	53.69	7.14
	61.49		
	44.23		
Pecan shell	65.20	64.93	0.19
	64.76		
	64.83		
Pine	84.21	84.97	0.82
	84.59		
	86.10		
Poultry litter	71.24	71.43	0.21
	71.31		
	71.73		
PRB coal	47.54	47.06	0.53
	46.32		
	47.31		
Sugarcane bagasse	72.88	72.41	1.18
	73.56		
	70.79		
sweetgum	87.50	86.82	0.55
	86.81		
	86.15		
Switchgrass	78.86	77.86	0.73
	77.54		
	77.17		

Table A.7 Energy content values for dust samples.

Sample	Energy Content (MJ/kg)	Mean Energy Content (MJ/kg)	Standard deviation (MJ/kg)
Bermuda grass	19.07	19.14	0.06
	19.14		
	19.21		
Bituminous coal	32.26	32.26	0.02
	32.23		
	32.29		
Corn cobs	19.05	19.08	0.05
	19.04		
	19.15		
Corn stover	17.10	17.17	0.07
	17.15		
	17.26		
Eucalyptus	19.57	19.51	0.06
	19.43		
	19.53		
Lignite coal	25.99	26.78	0.57
	27.32		
	27.02		
Pecan shell	20.07	20.31	0.17
	20.40		
	20.47		
Pine	20.63	20.55	0.07
	20.56		
	20.46		
Poultry litter	17.51	17.43	0.06
	17.36		
	17.43		
PRB coal	27.34	27.41	0.16
	27.63		
	27.25		
Sugarcane bagasse	16.65	16.69	0.07
	16.79		
	16.64		
sweetgum	19.69	19.71	0.07
	19.63		
	19.80		
Switchgrass	18.60	18.77	0.12
	18.89		
	18.81		

Table A.8 Moisture content values for ground samples.

Sample	Moisture content (% w.b.)	Mean moisture content (% w.b.)	Standard deviation (% w.b.)
Bermuda grass	8.05	8.07	0.02
	8.09		
	8.06		
Bituminous coal	2.90	2.90	0.02
	2.91		
	2.88		
Corn cobs	8.86	8.85	0.02
	8.82		
	8.86		
Corn stover	9.14	9.13	0.02
	9.14		
	9.11		
Eucalyptus	6.44	6.45	0.01
	6.44		
	6.46		
Pine	8.36	8.37	0.08
	8.45		
	8.30		
Poultry litter	13.71	13.45	0.35
	13.05		
	13.60		
PRB coal	15.05	15.01	0.04
	15.00		
	14.98		
Sugarcane bagasse	5.94	6.10	0.15
	6.13		
	6.23		
Sweetgum	8.37	8.58	0.21
	8.78		
	8.60		
Switchgrass	8.00	8.01	0.02
	8.01		
	8.03		

Table A.9 Bulk density values for ground samples.

Sample	Bulk density (kg/m^3)	Mean bulk density (kg/m^3)	Stdev (kg/m^3)
Bermuda grass	128.66	127.01	1.65
	125.36		
Bituminous coal	650.07	651.74	1.67
	653.40		
Corn cobs	161.30	160.24	1.06
	159.18		
Corn stover	92.26	93.61	1.35
	94.97		
Eucalyptus	195.43	196.34	0.91
	197.25		
Pine	183.07	184.44	1.37
	185.80		
Poultry litter	268.40	271.09	2.70
	273.79		
PRB coal	617.01	615.41	1.60
	613.81		
Sugarcane bagasse	93.64	92.20	1.44
	90.76		
Sweetgum	167.12	166.42	0.71
	165.71		
Switchgrass	143.54	142.13	1.41
	140.72		

Table A.10 Particle density values for ground samples.

Sample	Particle density (kg/m^3)	Mean particle density (kg/m^3)	Stdev (kg/m^3)
Bermuda grass	1103.10	1106.60	3.10
	1109.00		
	1107.70		
Bituminous coal	1384.10	1385.03	1.88
	1387.20		
	1383.80		
Corn cobs	1357.00	1359.03	1.77
	1360.20		
	1359.90		
Corn stover	1264.40	1267.00	2.51
	1267.20		
	1269.40		
Eucalyptus	1426.30	1427.47	2.84
	1430.70		
	1425.40		
Pine	1465.90	1465.47	2.08
	1463.20		
	1467.30		
Poultry litter	1503.00	1501.27	1.86
	1499.30		
	1501.50		
PRB coal	1493.50	1490.57	3.00
	1487.50		
	1490.70		
Sugarcane bagasse	1539.30	1535.27	5.12
	1529.50		
	1537.00		
Sweetgum	1462.20	1461.40	0.75
	1460.70		
	1461.30		
Switchgrass	1322.20	1319.43	3.57
	1315.40		
	1320.70		

Table A.11 Ash content values for ground samples.

Sample	Ash content (% d.b.)	Mean Ash content (% d.b.)	Standard deviation (% d.b.)
Bermuda grass	4.16	4.02	0.15
	3.85		
	4.05		
Bituminous coal	10.42	10.47	0.95
	9.56		
	11.45		
Corn cobs	1.08	1.06	0.01
	1.05		
	1.05		
Corn stover	8.95	7.58	1.59
	7.95		
	5.84		
Eucalyptus	1.00	0.66	0.52
	0.93		
	0.06		
Pine	0.43	0.48	0.04
	0.52		
	0.48		
Poultry litter	9.41	9.43	0.15
	9.28		
	9.58		
PRB coal	7.57	7.82	0.24
	7.85		
	8.04		
Sugarcane bagasse	5.49	5.84	0.52
	6.43		
	5.58		
Sweetgum	0.73	0.66	0.06
	0.60		
	0.66		
Switchgrass	5.30	4.94	0.31
	4.73		
	4.79		

Table A.12 Volatile matter values for ground samples.

Sample	Volatile matter (% d.b.)	Mean volatile matter (% d.b.)	Standard deviation (% d.b.)
Bermuda grass	84.42	84.51	0.48
	85.03		
	84.08		
Bituminous coal	39.12	38.87	0.24
	38.64		
	38.84		
Corn cobs	88.21	88.57	0.85
	89.54		
	87.97		
Corn stover	78.99	81.24	2.02
	81.86		
	82.87		
Eucalyptus	87.47	88.36	1.36
	87.69		
	89.92		
Pine	85.84	85.44	1.02
	86.20		
	84.28		
Poultry litter	85.63	84.83	0.76
	84.12		
	84.76		
PRB coal	53.58	53.71	0.54
	53.24		
	54.30		
Sugarcane bagasse	83.85	83.81	0.22
	83.57		
	84.01		
Sweetgum	91.86	89.86	1.75
	89.10		
	88.61		
Switchgrass	84.52	84.16	0.74
	84.66		
	83.31		

Table A.13 Energy content values for ground samples.

Sample	Energy content (MJ/kg)	Mean energy content (MJ/kg)	Standard deviation (MJ/kg)
Bermuda grass	19.42	19.42	0.06
	19.35		
	19.48		
Bituminous coal	31.93	31.75	0.58
	31.10		
	32.21		
Corn cobs	19.22	19.25	0.05
	19.22		
	19.31		
Corn stover	18.16	18.16	0.01
	18.17		
	18.14		
Eucalyptus	19.87	19.80	0.06
	19.74		
	19.78		
Pine	20.63	20.68	0.04
	20.69		
	20.71		
Poultry litter	18.60	18.35	0.33
	17.97		
	18.47		
PRB coal	27.08	27.11	0.07
	27.05		
	27.19		
Sugarcane bagasse	19.05	19.01	0.08
	18.92		
	19.06		
Sweetgum	20.15	19.88	0.24
	19.69		
	19.81		
Switchgrass	19.10	19.13	0.14
	19.29		
	19.01		

Table A.14 Moisture content values for feedstock, ground material and dust samples (biomass and coal)

Moisture Content (% w.b.)			
Sample	**Feedstock**	**Ground material**	**Dust**
Biomass Samples			
Bermuda grass	10.91±0.32^{c}	8.07±0.02^{e}	8.06±0.27^{b,c}
Corn cobs	9.45±0.19^{d}	8.85±0.02^{b,c}	7.40±0.65^{b,c,d}
Corn stover	9.59±0.55^{d}	9.13±0.02^{b}	6.99±0.10^{d,e}
Eucalyptus	6.96±0.13^{e}	6.45±0.01^{f}	6.80±0.33^{d,e}
Pecan shell	12.71±0.27^{b}	___	12.71±0.27^{a}
Pine	11.74±0.23^{b,c}	8.37±0.08^{d,e}	7.20±0.10^{c,d}
Poultry litter	14.81±0.02^{a}	13.45±0.35^{a}	11.89±0.07^{a}
Sugarcane bagasse	5.68±0.05^{f}	6.10±0.15^{f}	6.06±0.05^{e}
Sweetgum	5.45±0.08^{f}	8.58±0.21^{c,d}	8.23±0.21^{b}
Switchgrass	12.42±0.79^{b}	8.01±0.02^{e}	8.27±0.63^{b}
Coal Samples			
Bituminous coal	2.42±0.09^{c}	2.90±0.02^{b}	2.96±0.02^{c}
Lignite coal	29.40±0.04^{a}	___	29.40±0.04^{a}
PRB coal	15.25±0.02^{b}	15.01±0.04^{a}	13.79±0.02^{b}

Superscripts with same letters in a column are not significantly different from each other (α=0.05).

Pecan shell and lignite coal samples were obtained in dust form.

Sweetgum and sugarcane bagasse samples were dried prior to measuring initial moisture content of the feedstock.

Appendix B – Hot Plate Ignition Test, Thermogravimetric Analysis (TGA) and Differential Scanning Calorimetry (DSC) Results.

Table B.1 Temperature of rapid volatilization (TORV) for dust samples.

Sample	TORV (˚C)	Mean TORV (˚C)	Standard deviation (˚C)
Bermuda grass	267.06	266.12	0.97
	266.51		
	264.78		
Bituminous coal	444.53	447.60	2.18
	448.91		
	449.35		
Corn cobs	276.38	276.52	0.62
	277.34		
	275.83		
Corn stover	279.03	277.47	1.14
	276.36		
	277.01		
Eucalyptus	290.66	291.88	0.88
	292.25		
	292.72		
Lignite coal	314.17	311.64	4.52
	305.29		
	315.46		
Pecan shell	287.85	286.96	1.73
	284.54		
	288.49		
Pine	308.07	306.08	1.78
	306.43		
	303.74		
Poultry litter	272.88	272.79	0.52
	272.11		
	273.37		
PRB coal	315.18	317.34	1.57
	318.86		
	317.98		
Sugarcane bagasse	285.48	285.17	0.40
	284.61		
	285.43		
sweetgum	289.77	290.23	0.75
	291.28		
	289.63		
Switchgrass	285.82	285.05	1.82
	282.54		
	286.79		

Table B.2 Temperature of maximum rate of mass loss (TMML) values for dust samples.

Sample	TMML (˚C)	Mean TMML (˚C)	Standard deviation (˚C)
Bermuda grass	310.34	312.42	1.61
	312.67		
	314.25		
Bituminous coal	482.56	485.12	4.36
	481.54		
	491.26		
Corn cobs	312.12	313.67	1.60
	315.88		
	313.02		
Corn stover	316.63	316.41	0.83
	317.29		
	315.30		
Eucalyptus	313.25	315.69	1.76
	317.33		
	316.48		
Lignite coal	353.71	349.77	6.17
	341.06		
	354.55		
Pecan shell	327.57	331.21	4.74
	337.90		
	328.15		
Pine	348.43	348.75	2.09
	351.45		
	346.36		
Poultry litter	303.55	304.07	0.49
	304.73		
	303.94		
PRB coal	380.91	379.39	1.62
	377.15		
	380.10		
Sugarcane bagasse	343.33	345.21	1.33
	346.00		
	346.30		
sweetgum	336.89	338.80	1.49
	339.00		
	340.52		
Switchgrass	330.10	329.76	0.49
	329.07		
	330.12		

Table B.3 Oxidation temperature (TOXY) values for dust samples.

Sample	TOXY (˚C)	Mean TOXY (˚C)	Standard deviation (˚C)
Bermuda grass	269.61	274.02	3.80
	278.88		
	273.58		
Bituminous coal	399.62	423.10	16.72
	437.31		
	432.37		
Corn cobs	280.77	276.51	4.02
	271.12		
	277.63		
Corn stover	288.13	286.12	1.74
	283.88		
	286.36		
Eucalyptus	281.41	285.87	4.23
	284.64		
	291.56		
Lignite coal	246.22	241.80	3.33
	238.18		
	241.00		
Pecan shell	267.92	283.52	11.42
	287.69		
	294.94		
Pine	315.87	319.08	2.79
	318.70		
	322.68		
Poultry litter	278.36	277.77	0.42
	277.53		
	277.43		
PRB coal	280.44	258.68	18.42
	260.19		
	235.40		
Sugarcane bagasse	305.74	309.57	6.34
	318.51		
	304.46		
sweetgum	300.11	297.22	2.20
	296.78		
	294.77		
Switchgrass	318.44	315.28	4.61
	308.77		
	318.64		

Table B.4 Activation energy values for dust samples.

Sample	Activation Energy (kJ/mol)	Mean Activation Energy (kJ/mol)	Standard deviation (kJ/mol)
Bermuda grass	47.77	48.25	0.60
	49.09		
	47.88		
Bituminous coal	98.90	91.56	6.29
	92.24		
	83.54		
Corn cobs	64.75	63.15	2.45
	65.02		
	59.69		
Corn stover	70.67	71.26	0.52
	71.16		
	71.95		
Eucalyptus	74.45	72.35	1.55
	71.84		
	70.75		
Lignite coal	57.24	56.82	0.48
	56.16		
	57.07		
Pecan shell	55.86	55.55	0.31
	55.67		
	55.13		
Pine	64.28	64.43	0.11
	64.53		
	64.49		
Poultry litter	69.50	71.06	1.11
	72.02		
	71.65		
PRB coal	48.87	49.77	0.79
	49.66		
	50.80		
Sugarcane bagasse	77.51	77.08	0.54
	76.32		
	77.42		
sweetgum	97.81	95.16	1.88
	94.02		
	93.65		
Switchgrass	60.69	61.64	1.27
	60.79		
	63.42		

Table B.5 Temperature of rapid exothermic reaction (TRE) values for dust samples.

Sample	TRE (˚C)	Mean TRE (˚C)	Standard deviation (˚C)
Bermuda grass	240.73	237.53	3.47
	239.16		
	232.71		
Bituminous coal	222.44	223.43	1.50
	225.56		
	222.30		
Corn cobs	235.87	235.16	1.04
	233.68		
	235.92		
Corn stover	239.79	239.67	0.43
	239.09		
	240.13		
Eucalyptus	244.54	243.54	1.00
	242.17		
	243.90		
Lignite coal	221.74	221.20	2.42
	223.86		
	218.00		
Pecan shell	205.37	206.05	2.52
	203.36		
	209.43		
Pine	243.06	244.53	1.44
	246.48		
	244.06		
Poultry litter	246.71	241.21	4.56
	241.38		
	235.55		
PRB coal	245.03	244.90	2.41
	241.89		
	247.78		
Sugarcane bagasse	240.04	245.29	4.73
	244.32		
	251.51		
sweetgum	249.88	248.86	3.10
	252.05		
	244.66		
Switchgrass	248.00	248.96	0.77
	249.00		
	249.89		

Table B.6 Maximum temperature reached during exothermic reaction (TME) values for dust samples.

Sample	TME (˚C)	Mean TME (˚C)	Standard deviation (˚C)
Bermuda grass	374.61	379.27	11.73
	367.81		
	395.39		
Bituminous coal	392.59	395.60	2.17
	396.64		
	397.58		
Corn cobs	395.50	394.56	4.88
	400.00		
	388.17		
Corn stover	400.17	395.83	3.21
	392.50		
	394.83		
Eucalyptus	386.66	385.37	0.99
	385.19		
	384.25		
Lignite coal	428.38	428.00	1.29
	429.36		
	426.27		
Pecan shell	409.67	407.65	2.59
	404.00		
	409.28		
Pine	403.06	401.12	3.29
	396.49		
	403.82		
Poultry litter	352.44	354.38	1.87
	353.81		
	356.90		
PRB coal	430.92	429.11	3.04
	431.57		
	424.83		
Sugarcane bagasse	374.40	377.25	4.48
	373.78		
	383.58		
sweetgum	392.30	392.82	0.83
	394.00		
	392.17		
Switchgrass	390.77	388.98	1.55
	389.18		
	386.98		

Table B.7 Exothermic energy values for dust samples.

Sample	Exothermic energy (MJ/kg)	Mean Exothermic energy (MJ/kg)	Stdev (MJ/kg)
Bermuda grass	7.96	7.95	0.01
	7.94		
	7.94		
Bituminous coal	3.63	3.51	0.10
	3.39		
	3.51		
Corn cobs	8.07	8.15	0.11
	8.30		
	8.08		
Corn stover	7.83	7.78	0.24
	7.46		
	8.04		
Eucalyptus	7.21	7.52	0.22
	7.69		
	7.67		
Lignite coal	4.09	5.16	0.87
	6.22		
	5.17		
Pecan shell	5.47	5.61	0.15
	5.81		
	5.55		
Pine	6.75	6.14	0.46
	5.64		
	6.02		
Poultry litter	4.48	4.48	0.26
	4.80		
	4.17		
PRB coal	4.48	4.64	0.86
	3.68		
	5.77		
Sugarcane bagasse	8.35	7.55	0.73
	6.59		
	7.71		
sweetgum	6.63	6.57	0.05
	6.53		
	6.54		
Switchgrass	7.46	7.69	0.16
	7.85		
	7.75		

Table B.8 Minimum hot surface ignition temperature (MIT) for dust samples.

Sample	MIT (˚C)	Mean MIT (˚C)	Standard deviation (˚C)
Bermuda grass	275.00	275.00	0.00
	275.00		
	275.00		
Bituminous coal	335.00	335.00	0.00
	335.00		
	335.00		
Corn cobs	280.00	280.00	0.00
	280.00		
	280.00		
Corn stover	290.00	290.00	0.00
	290.00		
	290.00		
Eucalyptus	285.00	285.00	0.00
	285.00		
	285.00		
Lignite coal	240.00	240.00	0.00
	240.00		
	240.00		
Pecan shell	265.00	265.00	0.00
	265.00		
	265.00		
Pine	315.00	315.00	0.00
	315.00		
	315.00		
Poultry litter	285.00	285.00	0.00
	285.00		
	285.00		
PRB coal	240.00	240.00	0.00
	240.00		
	240.00		
Sugarcane bagasse	305.00	305.00	0.00
	305.00		
	305.00		
sweetgum	305.00	305.00	0.00
	305.00		
	305.00		
Switchgrass	295.00	295.00	0.00
	295.00		
	295.00		

Table B.9 Particle density of ash derived from sugarcane bagasse dust.

Sample	Particle Density (kg/m^3)	Mean particle density (kg/m^3)	Stdev (kg/m^3)
Sugarcane bagasse ash	2785.40	2781.50	3.46
	2778.80		
	2780.30		

Appendix C – SAS Codes for Tukey tests, correlation matrices and ANOVA results (first objective)

SAS code for Tukey test on physical, chemical, heating and ignition properties.

```
/*******************************
 * Author: Jaskaran Dhiman      *
 * Research work                *
 * Date: 01/30/2014             *
 *******************************/

/*ANOVA analysis*/

%MACRO anova;
ods listing close;
proc import datafile=&inputfile
out=&dataset
replace;
range="&range";
run;
proc sort data=&dataset
out=&dataset;
by Biomass;
run;
ods html file=&outfile;
title &titleanova;
proc anova data=&dataset;
class Biomass;
model &prop=Biomass;
means Biomass/tukey;
run;
title;
title &title2;
proc univariate data=&dataset;
var &prop;
run;
title;
ods html close;
ods listing;
%MEND anova;

%LET title2='Descriptive Statistics: UNIVARIATE - Moisture
Content(MC)';
%LET titleanova='MC';
%LET inputfile='I:\Desktop\MCbiomass.xls';
```

```
%LET dataset=work.MCanova;
%LET range=A1:B31;
%LET prop=MC;
%LET outfile='I:\Desktop\MCbiomass.htm';
%anova

%LET title2='Descriptive Statistics: UNIVARIATE - Ash Content(AC)';
%LET titleanova='AC';
%LET inputfile='I:\Desktop\ACbiomass.xls';
%LET dataset=work.ACanova;
%LET range=A1:B31;
%LET prop=AC;
%LET outfile='I:\Desktop\ACbiomass.htm';
%anova

%LET title2='Descriptive Statistics: UNIVARIATE - Bulk Density(BD)';
%LET titleanova='BD';
%LET inputfile='I:\Desktop\BDbiomass.xls';
%LET dataset=work.BDanova;
%LET range=A1:B31;
%LET prop=BD;
%LET outfile='I:\Desktop\BDbiomass.htm';
%anova

%LET title2='Descriptive Statistics: UNIVARIATE - Temperature of
Maximum Mass Loss(TMML)';
%LET titleanova='TMML';
%LET inputfile='I:\Desktop\TMMLbiomass.xls';
%LET dataset=work.TMMLanova;
%LET range=A1:B31;
%LET prop=TMML;
%LET outfile='I:\Desktop\TMMLbiomass.htm';
%anova

%LET title2='Descriptive Statistics: UNIVARIATE - Temperature of Rapid
Exothermic Reaction(TRE)';
%LET titleanova='TRE';
%LET inputfile='I:\Desktop\TREbiomass.xls';
%LET dataset=work.TREanova;
%LET range=A1:B31;
%LET prop=TRE;
%LET outfile='I:\Desktop\TREbiomass.htm';
%anova

%LET title2='Descriptive Statistics: UNIVARIATE - Volatile Matter
(VM)';
%LET titleanova='VM';
%LET inputfile='I:\Desktop\VMbiomass.xls';
%LET dataset=work.VManova;
%LET range=A1:B31;
%LET prop=VM;
%LET outfile='I:\Desktop\VMbiomass.htm';
%anova

%LET title2='Descriptive Statistics: UNIVARIATE - Oxidation
Temperature(TOXY)';
%LET titleanova='TOXY';
```

```
%LET inputfile='I:\Desktop\TOXYbiomass.xls';
%LET dataset=work.TOXYanova;
%LET range=A1:B31;
%LET prop=TOXY;
%LET outfile='I:\Desktop\TOXYbiomass.htm';
%anova

%LET title2='Descriptive Statistics: UNIVARIATE - Temperature of Onset
of Rapid Volatalization (TORV)';
%LET titleanova='TORV';
%LET inputfile='I:\Desktop\TORVbiomass.xls';
%LET dataset=work.TORVanova;
%LET range=A1:B40;
%LET prop=TORV;
%LET outfile='I:\Desktop\TORVbiomass.htm';
%anova

%LET title2='Descriptive Statistics: UNIVARIATE - Maximum Temperature
reached during exothermic reaction (TME)';
%LET titleanova='TME';
%LET inputfile='I:\Desktop\TMEbiomass.xls';
%LET dataset=work.TMEanova;
%LET range=A1:B40;
%LET prop=TME;
%LET outfile='I:\Desktop\TMEbiomass.htm';
%anova

%LET title2='Descriptive Statistics: UNIVARIATE – Exothermic Energy
(Q)';
%LET titleanova='Q';
%LET inputfile='I:\Desktop\Qbiomass.xls';
%LET dataset=work.Qanova;
%LET range=A1:B31;
%LET prop=Q;
%LET outfile='I:\Desktop\Qbiomass.htm';
%anova

%LET title2='Descriptive Statistics: UNIVARIATE - Particle Density
(PD)';
%LET titleanova='PD';
%LET inputfile='I:\Desktop\PDbiomass.xls';
%LET dataset=work.PDanova;
%LET range=A1:B31;
%LET prop=PD;
%LET outfile='I:\Desktop\PDbiomass.htm';
%anova

%LET title2='Descriptive Statistics: UNIVARIATE - Energy Content
(EC)';
%LET titleanova='EC';
%LET inputfile='I:\Desktop\ECbiomass.xls';
%LET dataset=work.ECanova;
%LET range=A1:B31;
%LET prop=EC;
%LET outfile='I:\Desktop\ECbiomass.htm';
%anova
```

```
%LET title2='Descriptive Statistics: UNIVARIATE - Geometric Mean
Diameter (dgw)';
%LET titleanova='dgw';
%LET inputfile='I:\Desktop\dgwbiomass.xls';
%LET dataset=work.dgwanova;
%LET range=A1:B31;
%LET prop=dgw;
%LET outfile='I:\Desktop\dgwbiomass.htm';
%anova

%LET title2='Descriptive Statistics: UNIVARIATE - Activation Energy
(AE)';
%LET titleanova='AE';
%LET inputfile='I:\Desktop\AEbiomass.xls';
%LET dataset=work.AEanova;
%LET range=A1:B31;
%LET prop=AE;
%LET outfile='I:\Desktop\AEbiomass.htm';
%anova

%LET title2='Descriptive Statistics: UNIVARIATE – Minimum Ignition
Temperature of dust layer (MIT)';
%LET titleanova='MIT';
%LET inputfile='I:\Desktop\MITbiomass.xls';
%LET dataset=work.MITanova;
%LET range=A1:B31;
%LET prop=MIT;
%LET outfile='I:\Desktop\MITbiomass.htm';
%anova

%LET title2='Descriptive Statistics: UNIVARIATE - Moisture
Content(MC)';
%LET titleanova='MC';
%LET inputfile='I:\Desktop\MCcoal.xls';
%LET dataset=work.MCanova;
%LET range=A1:B10;
%LET prop=MC;
%LET outfile='I:\Desktop\MCcoal.htm';
%anova

%LET title2='Descriptive Statistics: UNIVARIATE - Ash Content(AC)';
%LET titleanova='AC';
%LET inputfile='I:\Desktop\ACcoal.xls';
%LET dataset=work.ACanova;
%LET range=A1:B10;
%LET prop=AC;
%LET outfile='I:\Desktop\ACcoal.htm';
%anova

%LET title2='Descriptive Statistics: UNIVARIATE - Bulk Density(BD)';
%LET titleanova='BD';
%LET inputfile='I:\Desktop\BDcoal.xls';
%LET dataset=work.BDanova;
%LET range=A1:B10;
%LET prop=BD;
%LET outfile='I:\Desktop\BDcoal.htm';
%anova
```

```
%LET title2='Descriptive Statistics: UNIVARIATE - Temperature of
Maximum Mass Loss(TMML)';
%LET titleanova='TMML';
%LET inputfile='I:\Desktop\TMMLcoal.xls';
%LET dataset=work.TMMLanova;
%LET range=A1:B10;
%LET prop=TMML;
%LET outfile='I:\Desktop\TMMLcoal.htm';
%anova

%LET title2='Descriptive Statistics: UNIVARIATE - Temperature of Rapid
Exothermic Reaction(TRE)';
%LET titleanova='TRE';
%LET inputfile='I:\Desktop\TREcoal.xls';
%LET dataset=work.TREanova;
%LET range=A1:B10;
%LET prop=TRE;
%LET outfile='I:\Desktop\TREcoal.htm';
%anova

%LET title2='Descriptive Statistics: UNIVARIATE - Volatile Matter
(VM)';
%LET titleanova='VM';
%LET inputfile='I:\Desktop\VMcoal.xls';
%LET dataset=work.VManova;
%LET range=A1:B10;
%LET prop=VM;
%LET outfile='I:\Desktop\VMcoal.htm';
%anova

%LET title2='Descriptive Statistics: UNIVARIATE - Oxidation
Temperature(TOXY)';
%LET titleanova='TOXY';
%LET inputfile='I:\Desktop\TOXYcoal.xls';
%LET dataset=work.TOXYanova;
%LET range=A1:B10;
%LET prop=TOXY;
%LET outfile='I:\Desktop\TOXYcoal.htm';
%anova

%LET title2='Descriptive Statistics: UNIVARIATE - Temperature of Onset
of Rapid Volatalization (TORV)';
%LET titleanova='TORV';
%LET inputfile='I:\Desktop\TORVcoal.xls';
%LET dataset=work.TORVanova;
%LET range=A1:B40;
%LET prop=TORV;
%LET outfile='I:\Desktop\TORVcoal.htm';
%anova

%LET title2='Descriptive Statistics: UNIVARIATE - Maximum Temperature
reached during exothermic reaction (TME)';
%LET titleanova='TME';
%LET inputfile='I:\Desktop\TMEcoal.xls';
%LET dataset=work.TMEanova;
%LET range=A1:B40;
```

```
%LET prop=TME;
%LET outfile='I:\Desktop\TMEcoal.htm';
%anova

%LET title2='Descriptive Statistics: UNIVARIATE – Exothermic Energy
(Q)';
%LET titleanova='Q';
%LET inputfile='I:\Desktop\Qcoal.xls';
%LET dataset=work.Qanova;
%LET range=A1:B10;
%LET prop=Q;
%LET outfile='I:\Desktop\Qcoal.htm';
%anova

%LET title2='Descriptive Statistics: UNIVARIATE - Particle Density
(PD)';
%LET titleanova='PD';
%LET inputfile='I:\Desktop\PDcoal.xls';
%LET dataset=work.PDanova;
%LET range=A1:B10;
%LET prop=PD;
%LET outfile='I:\Desktop\PDcoal.htm';
%anova

%LET title2='Descriptive Statistics: UNIVARIATE - Energy Content
(EC)';
%LET titleanova='EC';
%LET inputfile='I:\Desktop\ECcoal.xls';
%LET dataset=work.ECanova;
%LET range=A1:B10;
%LET prop=EC;
%LET outfile='I:\Desktop\ECcoal.htm';
%anova

%LET title2='Descriptive Statistics: UNIVARIATE - Geometric Mean
Diameter (dgw)';
%LET titleanova='dgw';
%LET inputfile='I:\Desktop\dgwcoal.xls';
%LET dataset=work.dgwanova;
%LET range=A1:B10;
%LET prop=dgw;
%LET outfile='I:\Desktop\dgwcoal.htm';
%anova

%LET title2='Descriptive Statistics: UNIVARIATE - Activation Energy
(AE)';
%LET titleanova='AE';
%LET inputfile='I:\Desktop\AEcoal.xls';
%LET dataset=work.AEanova;
%LET range=A1:B10;
%LET prop=AE;
%LET outfile='I:\Desktop\AEcoal.htm';
%anova

%LET title2='Descriptive Statistics: UNIVARIATE – Minimum Ignition
Temperature of dust layer (MIT)';
%LET titleanova='MIT';
```

```
%LET inputfile='I:\Desktop\MITcoal.xls';
%LET dataset=work.MITanova;
%LET range=A1:B10;
%LET prop=MIT;
%LET outfile='I:\Desktop\MITcoal.htm';
%anova



proc import datafile='C:\Users\jzd0028\Desktop\Combined_woody.xls'
out=work.corr1
replace;
range="A1:P10";
run;
ods html file='C:\Users\jzd0028\Desktop\woody_ corr.htm';
proc corr data=worK.corr1;
var AC AE BD dgw EC MC PD Q TME TMML TORV TOXY TRE VM MIT;
RUN;

proc import datafile='C:\Users\jzd0028\Desktop\Combined_grassy.xls'
out=work.corr2
replace;
range="A1:P13";
run;
ods html file='C:\Users\jzd0028\Desktop\grassy_corr.htm';
proc corr data=worK.corr2;
var AC AE BD dgw EC MC PD Q TME TMML TORV TOXY TRE VM MIT;
RUN;

proc import datafile='C:\Users\jzd0028\Desktop\Combined_biomass.xls'
out=work.corr3
replace;
range="A1:P31";
run;
ods html file='C:\Users\jzd0028\Desktop\biomass_corr.htm';
proc corr data=worK.corr3;
var AC AE BD dgw EC MC PD Q TME TMML TORV TOXY TRE VM MIT;
RUN;

proc import datafile='C:\Users\jzd0028\Desktop\Combined_all.xls'
out=work.corr4
replace;
range="A1:P40";
run;
ods html file='C:\Users\jzd0028\Desktop\all_corr.htm';
proc corr data=worK.corr4;
var AC AE BD dgw EC MC PD Q TME TMML TORV TOXY TRE VM MIT;
RUN;
```

Table C.1 ANOVA results for Tukey test on moisture content (MC) for biomass dust.

Source	DF	Sum of Squares	Mean Square	F Value	Pr > F
Model	9	130.0453486	14.4494832	126.77	<.0001
Error	20	2.2795512	0.1139776		
Corrected Total	29	132.3248998			

R-Square	Coeff Var	Root MSE	MC Mean
0.982773	4.038353	0.337606	8.359982

Source	DF	Anova SS	Mean Square	F Value	Pr > F
Sample	9	130.0453486	14.4494832	126.77	<.0001

Table C.2 ANOVA results for Tukey test on ash content (AC) for biomass dust.

Source	DF	Sum of Squares	Mean Square	F Value	Pr > F
Model	9	931.0711157	103.4523462	1804.35	<.0001
Error	20	1.1467003	0.0573350		
Corrected Total	29	932.2178159			

R-Square	Coeff Var	Root MSE	AC Mean
0.998770	3.680139	0.239447	6.506475

Source	DF	Anova SS	Mean Square	F Value	Pr > F
Biomass	9	931.0711157	103.4523462	1804.35	<.0001

Table C.3 ANOVA results for Tukey test on activation energy (AE) for biomass dust.

Source	DF	Sum of Squares	Mean Square	F Value	Pr > F
Model	9	4442.711331	493.634592	208.25	<.0001
Error	20	47.407565	2.370378		
Corrected Total	29	4490.118896			

R-Square	Coeff Var	Root MSE	AE Mean
0.989442	2.264383	1.539603	67.99217

Source	DF	Anova SS	Mean Square	F Value	Pr > F
Biomass	9	4442.711331	493.634592	208.25	<.0001

Table C.4 ANOVA results for Tukey test on bulk density (BD) for biomass dust.

Source	DF	Sum of Squares	Mean Square	F Value	Pr > F
Model	9	264035.6623	29337.2958	3826.42	<.0001
Error	20	153.3405	7.6670		
Corrected Total	29	264189.0028			

R-Square	Coeff Var	Root MSE	BD Mean
0.999420	1.355370	2.768939	204.2940

Source	DF	Anova SS	Mean Square	F Value	Pr > F
Biomass	9	264035.6623	29337.2958	3826.42	<.0001

Table C.5 ANOVA results for Tukey test on geometric mean diameter (dgw) for biomass dust.

Source	DF	Sum of Squares	Mean Square	F Value	Pr > F
Model	9	0.64206673	0.07134075	Infty	<.0001
Error	20	0.00000000	0.00000000		
Corrected Total	29	0.64206673			

R-Square	Coeff Var	Root MSE	dgw Mean
1.000000	0	0	0.377688

Source	DF	Anova SS	Mean Square	F Value	Pr > F
Biomass	9	0.64206673	0.07134075	Infty	<.0001

Table C.6 ANOVA results for Tukey test on energy content (EC) for biomass dust.

Source	DF	Sum of Squares	Mean Square	F Value	Pr > F
Model	9	47454058.42	5272673.16	451.31	<.0001
Error	20	233658.47	11682.92		
Corrected Total	29	47687716.89			

R-Square	Coeff Var	Root MSE	EC Mean
0.995100	0.573826	108.0876	18836.30

Source	DF	Anova SS	Mean Square	F Value	Pr > F
Biomass	9	47454058.42	5272673.16	451.31	<.0001

Table C.7 ANOVA results for Tukey test on particle density (PD) for biomass dust.

Source	DF	Sum of Squares	Mean Square	F Value	Pr > F
Model	9	371614.3737	41290.4860	3016.62	<.0001
Error	20	273.7533	13.6877		
Corrected Total	29	371888.1270			

R-Square	Coeff Var	Root MSE	PD Mean
0.999264	0.253318	3.699685	1460.490

Source	DF	Anova SS	Mean Square	F Value	Pr > F
Biomass	9	371614.3737	41290.4860	3016.62	<.0001

Table C.8 ANOVA results for Tukey test exothermic energy (Q) for biomass dust.

Source	DF	Sum of Squares	Mean Square	F Value	Pr > F
Model	9	39.06237438	4.34026382	29.64	<.0001
Error	20	2.92818643	0.14640932		
Corrected Total	29	41.99056081			

R-Square	Coeff Var	Root MSE	Q Mean
0.930266	5.511725	0.382635	6.942195

Source	DF	Anova SS	Mean Square	F Value	Pr > F
Biomass	9	39.06237438	4.34026382	29.64	<.0001

Table C.9 ANOVA results for Tukey test on maximum temperature reached during exothermic reaction (TME) for biomass dust.

Source	DF	Sum of Squares	Mean Square	F Value	Pr > F
Model	9	6044.605963	671.622885	20.65	<.0001
Error	20	650.636933	32.531847		
Corrected Total	29	6695.242897			

R-Square	Coeff Var	Root MSE	TME Mean
0.902821	1.471066	5.703670	387.7237

Source	DF	Anova SS	Mean Square	F Value	Pr > F
Biomass	9	6044.605963	671.622885	20.65	<.0001

Table C.10 ANOVA results for Tukey test on temperature of maximum rate of mass loss (TMML) for biomass dust.

Source	DF	Sum of Squares	Mean Square	F Value	Pr > F
Model	9	6316.689137	701.854349	116.32	<.0001
Error	20	120.679933	6.033997		
Corrected Total	29	6437.369070			

R-Square	Coeff Var	Root MSE	TMML Mean
0.981253	0.754431	2.456419	325.5990

Source	DF	Anova SS	Mean Square	F Value	Pr > F
Biomass	9	6316.689137	701.854349	116.32	<.0001

Table C.11 ANOVA results for Tukey test on temperature of onset of rapid volatilization (TORV) for biomass dust.

Source	DF	Sum of Squares	Mean Square	F Value	Pr > F
Model	9	3430.537680	381.170853	183.11	<.0001
Error	20	41.633867	2.081693		
Corrected Total	29	3472.171547			

R-Square	Coeff Var	Root MSE	TORV Mean
0.988009	0.508343	1.442807	283.8253

Source	DF	Anova SS	Mean Square	F Value	Pr > F
Biomass	9	3430.537680	381.170853	183.11	<.0001

Table C.12 ANOVA results for Tukey test on oxidation temperature (TOXY) for biomass dust.

Source	DF	Sum of Squares	Mean Square	F Value	Pr > F
Model	9	7556.354363	839.594929	21.85	<.0001
Error	20	768.614267	38.430713		
Corrected Total	29	8324.968630			

R-Square	Coeff Var	Root MSE	TOXY Mean
0.907674	2.119424	6.199251	292.4970

Source	DF	Anova SS	Mean Square	F Value	Pr > F
Biomass	9	7556.354363	839.594929	21.85	<.0001

Table C.13 ANOVA results for Tukey test on temperature of rapid exothermic reaction (TRE) for biomass dust.

Source	DF	Sum of Squares	Mean Square	F Value	Pr > F
Model	9	4185.010013	465.001113	40.71	<.0001
Error	20	228.428133	11.421407		
Corrected Total	29	4413.438147			

R-Square	Coeff Var	Root MSE	TRE Mean
0.948243	1.413560	3.379557	239.0813

Source	DF	Anova SS	Mean Square	F Value	Pr > F
Biomass	9	4185.010013	465.001113	40.71	<.0001

Table C.14 ANOVA results for Tukey test on volatile matter (VM) for biomass dust.

Source	DF	Sum of Squares	Mean Square	F Value	Pr > F
Model	9	1245.119098	138.346566	145.28	<.0001
Error	20	19.045808	0.952290		
Corrected Total	29	1264.164907			

R-Square	Coeff Var	Root MSE	VM Mean
0.984934	1.262799	0.975854	77.27705

Source	DF	Anova SS	Mean Square	F Value	Pr > F
Biomass	9	1245.119098	138.346566	145.28	<.0001

Table C.15 ANOVA results for Tukey test on minimum hot surface ignition temperature (MIT) for biomass dust.

Source	DF	Sum of Squares	Mean Square	F Value	Pr > F
Model	9	6300.000000	700.000000	Infty	<.0001
Error	20	0.000000	0.000000		
Corrected Total	29	6300.000000			

R-Square	Coeff Var	Root MSE	MIT Mean
1.000000	0	0	290.0000

Source	DF	Anova SS	Mean Square	F Value	Pr > F
Biomass	9	6300.000000	700.000000	Infty	<.0001

Table C.16 ANOVA results for Tukey test on ash content (AC) for coal dust.

Source	DF	Sum of Squares	Mean Square	F Value	Pr > F
Model	2	277.3325531	138.6662766	83.86	<.0001
Error	6	9.9211421	1.6535237		
Corrected Total	8	287.2536952			

R-Square	Coeff Var	Root MSE	AC Mean
0.965462	9.829077	1.285894	13.08255

Source	DF	Anova SS	Mean Square	F Value	Pr > F
Biomass	2	277.3325531	138.6662766	83.86	<.0001

Table C.17 ANOVA results for Tukey test on activation energy (AE) for coal dust.

Source	DF	Sum of Squares	Mean Square	F Value	Pr > F
Model	2	3002.795344	1501.397672	74.27	<.0001
Error	6	121.293156	20.215526		
Corrected Total	8	3124.088500			

R-Square	Coeff Var	Root MSE	AE Mean
0.961175	6.806950	4.496168	66.05261

Source	DF	Anova SS	Mean Square	F Value	Pr > F
Biomass	2	3002.795344	1501.397672	74.27	<.0001

Table C.18 ANOVA results for Tukey test on bulk density (BD) for coal dust.

Source	DF	Sum of Squares	Mean Square	F Value	Pr > F
Model	2	45207.75978	22603.87989	1243.39	<.0001
Error	6	109.07517	18.17920		
Corrected Total	8	45316.83495			

R-Square	Coeff Var	Root MSE	BD Mean
0.997593	0.706376	4.263707	603.6030

Source	DF	Anova SS	Mean Square	F Value	Pr > F
Biomass	2	45207.75978	22603.87989	1243.39	<.0001

Table C.19 ANOVA results for Tukey test on geometric mean diameter (dgw) for coal dust.

Source	DF	Sum of Squares	Mean Square	F Value	Pr > F
Model	2	0.37376761	0.18688380	5.05E15	<.0001
Error	6	0.00000000	0.00000000		
Corrected Total	8	0.37376761			

R-Square	Coeff Var	Root MSE	dgw Mean
1.000000	1.61018E-6	6.08337E-9	0.377808

Source	DF	Anova SS	Mean Square	F Value	Pr > F
Biomass	2	0.37376761	0.18688380	5.05E15	<.0001

Table C.20 ANOVA results for Tukey test on energy content (EC) for coal dust.

Source	DF	Sum of Squares	Mean Square	F Value	Pr > F
Model	2	53987555.20	26993777.60	154.00	<.0001
Error	6	1051700.64	175283.44		
Corrected Total	8	55039255.84			

R-Square	Coeff Var	Root MSE	EC Mean
0.980892	1.453015	418.6687	28813.79

Source	DF	Anova SS	Mean Square	F Value	Pr > F
Biomass	2	53987555.20	26993777.60	154.00	<.0001

Table C.21 ANOVA results for Tukey test on moisture content (MC) for coal dust.

Source	DF	Sum of Squares	Mean Square	F Value	Pr > F
Model	2	1060.026849	530.013424	659672	<.0001
Error	6	0.004821	0.000803		
Corrected Total	8	1060.031669			

R-Square	Coeff Var	Root MSE	MC Mean
0.999995	0.184235	0.028345	15.38536

Source	DF	Anova SS	Mean Square	F Value	Pr > F
Biomass	2	1060.026849	530.013424	659672	<.0001

Table C.22 ANOVA results for Tukey test on particle density (PD) for coal dust.

Source	DF	Sum of Squares	Mean Square	F Value	Pr > F
Model	2	108455.0756	54227.5378	537.93	<.0001
Error	6	604.8467	100.8078		
Corrected Total	8	109059.9222			

R-Square	Coeff Var	Root MSE	PD Mean
0.994454	0.657155	10.04031	1527.844

Source	DF	Anova SS	Mean Square	F Value	Pr > F
Biomass	2	108455.0756	54227.5378	537.93	<.0001

Table C.23 ANOVA results for Tukey test on exothermic energy (Q) for coal dust.

Source	DF	Sum of Squares	Mean Square	F Value	Pr > F
Model	2	4.26432203	2.13216101	2.84	0.1355
Error	6	4.50297828	0.75049638		
Corrected Total	8	8.76730030			

R-Square	Coeff Var	Root MSE	Q Mean
0.486389	19.51531	0.866312	4.439140

Source	DF	Anova SS	Mean Square	F Value	Pr > F
Biomass	2	4.26432203	2.13216101	2.84	0.1355

Table C.24 ANOVA results for Tukey test on maximum temperature reached during an exothermic energy (TME) for coal dust.

Source	DF	Sum of Squares	Mean Square	F Value	Pr > F
Model	2	2173.450689	1086.725344	139.64	<.0001
Error	6	46.695000	7.782500		
Corrected Total	8	2220.145689			

R-Square	Coeff Var	Root MSE	TME Mean
0.978968	0.668081	2.789713	417.5711

Source	DF	Anova SS	Mean Square	F Value	Pr > F
Biomass	2	2173.450689	1086.725344	139.64	<.0001

Table C.25 ANOVA results for Tukey test on temperature of maximum rate of mass loss(TMML) for coal dust.

Source	DF	Sum of Squares	Mean Square	F Value	Pr > F
Model	2	30375.20747	15187.60373	508.69	<.0001
Error	6	179.13773	29.85629		
Corrected Total	8	30554.34520			

R-Square	Coeff Var	Root MSE	TMML Mean
0.994137	1.349958	5.464091	404.7600

Source	DF	Anova SS	Mean Square	F Value	Pr > F
Biomass	2	30375.20747	15187.60373	508.69	<.0001

Table C.26 ANOVA results for Tukey test on temperature of onset of rapid volatilization(TORV) for coal dust.

Source	DF	Sum of Squares	Mean Square	F Value	Pr > F
Model	2	35483.50442	17741.75221	1284.01	<.0001
Error	6	82.90487	13.81748		
Corrected Total	8	35566.40929			

R-Square	Coeff Var	Root MSE	TORV Mean
0.997669	1.035835	3.717187	358.8589

Source	DF	Anova SS	Mean Square	F Value	Pr > F
Biomass	2	35483.50442	17741.75221	1284.01	<.0001

Table C.27 ANOVA results for Tukey test on oxidation temperature (TOXY) for coal dust.

Source	DF	Sum of Squares	Mean Square	F Value	Pr > F
Model	2	60189.54442	30094.77221	95.53	<.0001
Error	6	1890.18427	315.03071		
Corrected Total	8	62079.72869			

R-Square	Coeff Var	Root MSE	TOXY Mean
0.969552	5.765338	17.74910	307.8589

Source	DF	Anova SS	Mean Square	F Value	Pr > F
Biomass	2	60189.54442	30094.77221	95.53	<.0001

Table C.28 ANOVA results for Tukey test on temperature of rapid exothermic energy (TRE) for coal dust.

Source	DF	Sum of Squares	Mean Square	F Value	Pr > F
Model	2	1027.495556	513.747778	73.79	<.0001
Error	6	41.772467	6.962078		
Corrected Total	8	1069.268022			

R-Square	Coeff Var	Root MSE	TRE Mean
0.960934	1.147983	2.638575	229.8444

Source	DF	Anova SS	Mean Square	F Value	Pr > F
Biomass	2	1027.495556	513.747778	73.79	<.0001

Table C.29 ANOVA results for Tukey test on volatile matter (VM) for coal dust.

Source	DF	Sum of Squares	Mean Square	F Value	Pr > F
Model	2	669.6700713	334.8350356	13.06	0.0065
Error	6	153.8719318	25.6453220		
Corrected Total	8	823.5420031			

R-Square	Coeff Var	Root MSE	VM Mean
0.813158	11.35916	5.064121	44.58184

Source	DF	Anova SS	Mean Square	F Value	Pr > F
Biomass	2	669.6700713	334.8350356	13.06	0.0065

Table C.30 ANOVA results for Tukey test on minimum ignition temperature (MIT) for coal dust.

Source	DF	Sum of Squares	Mean Square	F Value	Pr > F
Model	2	18050.00000	9025.00000	Infty	<.0001
Error	6	0.00000	0.00000		
Corrected Total	8	18050.00000			

R-Square	Coeff Var	Root MSE	MIT Mean
1.000000	0	0	271.6667

Source	DF	Anova SS	Mean Square	F Value	Pr > F
Biomass	2	18050.00000	9025.00000	Infty	<.0001

Table C.31 ANOVA results for Tukey test on moisture content (MC) for ground biomass.

Source	DF	Sum of Squares	Mean Square	F Value	Pr > F
Model	8	106.3450000	13.2931250	609.47	<.0001
Error	18	0.3926000	0.0218111		
Corrected Total	26	106.7376000			

R-Square	Coeff Var	Root MSE	MC Mean
0.996322	1.725974	0.147686	8.556667

Source	DF	Anova SS	Mean Square	F Value	Pr > F
Sample	8	106.3450000	13.2931250	609.47	<.0001

Table C.32 ANOVA results for Tukey test on bulk density (BD) for ground biomass.

Source	DF	Sum of Squares	Mean Square	F Value	Pr > F
Model	2	4.26432203	2.13216101	2.84	0.1355
Error	6	4.50297828	0.75049638		
Corrected Total	8	8.76730030			

R-Square	Coeff Var	Root MSE	Q Mean
0.486389	19.51531	0.866312	4.439140

Source	DF	Anova SS	Mean Square	F Value	Pr > F
Biomass	2	4.26432203	2.13216101	2.84	0.1355

Table C.33 ANOVA results for Tukey test on particle density (PD) for ground biomass.

Source	DF	Sum of Squares	Mean Square	F Value	Pr > F
Model	8	439688.9474	54961.1184	6643.16	<.0001
Error	18	148.9200	8.2733		
Corrected Total	26	439837.8674			

R-Square	Coeff Var	Root MSE	PD Mean
0.999661	0.208046	2.876340	1382.548

Source	DF	Anova SS	Mean Square	F Value	Pr > F
Biomass	8	439688.9474	54961.1184	6643.16	<.0001

Table C.34 ANOVA results for Tukey test on volatile matter (VM) for ground biomass.

Source	DF	Sum of Squares	Mean Square	F Value	Pr > F
Model	8	182.0291098	22.7536387	16.89	<.0001
Error	18	24.2525601	1.3473644		
Corrected Total	26	206.2816699			

R-Square	Coeff Var	Root MSE	VM Mean
0.882430	1.355351	1.160760	85.64276

Source	DF	Anova SS	Mean Square	F Value	Pr > F
Sample	8	182.0291098	22.7536387	16.89	<.0001

Table C.35 ANOVA results for Tukey test on ash content (AC) for ground biomass

Source	DF	Sum of Squares	Mean Square	F Value	Pr > F
Model	8	268.8139148	33.6017394	94.20	<.0001
Error	18	6.4204212	0.3566901		
Corrected Total	26	275.2343360			

R-Square	Coeff Var	Root MSE	AC Mean
0.976673	15.50393	0.597235	3.852156

Source	DF	Anova SS	Mean Square	F Value	Pr > F
Sample	8	268.8139148	33.6017394	94.20	<.0001

Table C.36 ANOVA results for Tukey test on energy content (EC) for ground biomass.

Source	DF	Sum of Squares	Mean Square	F Value	Pr > F
Model	8	14.45738444	1.80717306	78.39	<.0001
Error	18	0.41498679	0.02305482		
Corrected Total	26	14.87237123			

R-Square	Coeff Var	Root MSE	EC Mean
0.972097	0.786828	0.151838	19.29751

Source	DF	Anova SS	Mean Square	F Value	Pr > F
Sample	8	14.45738444	1.80717306	78.39	<.0001

Table C.37 ANOVA results for Tukey test on moisture content (MC) for ground coal.

Source	DF	Sum of Squares	Mean Square	F Value	Pr > F
Model	1	220.0992667	220.0992667	287086	<.0001
Error	4	0.0030667	0.0007667		
Corrected Total	5	220.1023333			

R-Square	Coeff Var	Root MSE	MC Mean
0.999986	0.309256	0.027689	8.953333

Source	DF	Anova SS	Mean Square	F Value	Pr > F
Sample	1	220.0992667	220.0992667	287086	<.0001

Table C.38 ANOVA results for Tukey test on bulk density (BD) for ground coal.

Source	DF	Sum of Squares	Mean Square	F Value	Pr > F
Model	1	1319.727674	1319.727674	247.14	0.0040
Error	2	10.680060	5.340030		
Corrected Total	3	1330.407733			

R-Square	Coeff Var	Root MSE	BD Mean
0.991972	0.364733	2.310850	633.5730

Source	DF	Anova SS	Mean Square	F Value	Pr > F
Biomass	1	1319.727674	1319.727674	247.14	0.0040

Table C.39 ANOVA results for Tukey test on particle density (PD) for ground coal.

Source	DF	Sum of Squares	Mean Square	F Value	Pr > F
Model	1	16705.92667	16705.92667	2660.89	<.0001
Error	4	25.11333	6.27833		
Corrected Total	5	16731.04000			

R-Square	Coeff Var	Root MSE	PD Mean
0.998499	0.174270	2.505660	1437.800

Source	DF	Anova SS	Mean Square	F Value	Pr > F
Biomass	1	16705.92667	16705.92667	2660.89	<.0001

Table C.40 ANOVA results for Tukey test on volatile matter (VM) for ground coal.

Source	DF	Sum of Squares	Mean Square	F Value	Pr > F
Model	1	59.5350000	59.5350000	2.32	0.2023
Error	4	102.5933333	25.6483333		
Corrected Total	5	162.1283333			

R-Square	Coeff Var	Root MSE	PD Mean
0.367209	0.364403	5.064418	1389.783

Source	DF	Anova SS	Mean Square	F Value	Pr > F
Sample	1	59.53500000	59.53500000	2.32	0.2023

Table C.41 ANOVA results for Tukey test on ash content (AC) for ground coal.

Source	DF	Sum of Squares	Mean Square	F Value	Pr > F
Model	1	1.39011120	1.39011120	2.98	0.1595
Error	4	1.86763650	0.46690913		
Corrected Total	5	3.25774770			

R-Square	Coeff Var	Root MSE	AC Mean
0.426709	6.837435	0.683307	9.993623

Source	DF	Anova SS	Mean Square	F Value	Pr > F
Sample	1	1.39011120	1.39011120	2.98	0.1595

Table C.42 ANOVA results for Tukey test on energy content (EC) for ground coal.

Source	DF	Sum of Squares	Mean Square	F Value	Pr > F
Model	1	32.30221089	32.30221089	190.84	0.0002
Error	4	0.67705021	0.16926255		
Corrected Total	5	32.97926110			

R-Square	Coeff Var	Root MSE	EC Mean
0.979470	1.398088	0.411415	29.42700

Source	DF	Anova SS	Mean Square	F Value	Pr > F
Sample	1	32.30221089	32.30221089	190.84	0.0002

Table C.43 Correlation matrix showing Pearson's correlation coefficient and respective p-value for relation between all measured properties for all biomass dusts.

Pearson Correlation Coefficients, N = 30 Prob > |r| under H0: Rho=0															
	AC	**AE**	**BD**	**dgw**	**EC**	**MC**	**PD**	**EXO**	**TME**	**TMML**	**TORV**	**TOXY**	**TRE**	**VM**	**MIT**
AC	1	0.12266	-0.13268	-0.36749	-0.95166	-0.03054	0.29242	-0.04946	-0.53532	-0.17014	-0.43601	0.0215	0.18754	-0.55663	0.09934
AC		0.5185	0.4846	0.0457	<.0001	0.8727	0.1169	0.7952	0.0023	0.3687	0.016	0.9102	0.321	0.0014	0.6015
AE	0.12266	1	-0.17463	-0.28046	-0.2204	-0.24789	0.56296	-0.12172	-0.11226	0.29796	0.3236	0.24372	0.48965	0.35046	0.58746
AE	0.5185		0.356	0.1333	0.2419	0.1866	0.0012	0.5217	0.5548	0.1098	0.0811	0.1943	0.006	0.0576	0.0006
BD	-0.13268	-0.17463	1	-0.56656	0.27145	0.91985	0.26726	-0.78542	-0.10118	-0.26564	-0.04332	-0.39324	-0.66861	-0.53264	-0.55579
BD	0.4846	0.356		0.0011	0.1468	<.0001	0.1534	<.0001	0.5947	0.156	0.8202	0.0316	<.0001	0.0024	0.0014
dgw	-0.36749	-0.28046	-0.56656	1	0.37129	-0.35769	-0.71011	0.43487	0.30007	0.27588	0.1281	0.41901	0.35999	0.56439	0.31001
dgw	0.0457	0.1333	0.0011		0.0434	0.0523	<.0001	0.0163	0.1072	0.14	0.4999	0.0212	0.0507	0.0012	0.0955
EC	-0.95166	-0.2204	0.27145	0.37129	1	0.19766	-0.26747	-0.13219	0.5812	0.26696	0.51112	0.0819	-0.30977	0.402	-0.09295
EC	<.0001	0.2419	0.1468	0.0434		0.2951	0.153	0.4862	0.0008	0.1538	0.0039	0.667	0.0957	0.0277	0.6252
MC	-0.03054	-0.24789	0.91985	-0.35769	0.19766	1	0.09156	-0.73898	-0.10948	-0.26553	-0.21253	-0.37311	-0.64196	-0.56803	-0.56044
MC	0.8727	0.1866	<.0001	0.0523	0.2951		0.6304	<.0001	0.5647	0.1561	0.2595	0.0423	0.0001	0.0011	0.0013
PD	0.29242	0.56296	0.26726	-0.71011	-0.26747	0.09156	1	-0.38356	0.02026	0.25597	0.39999	0.17944	-0.09125	-0.27073	0.25369
PD	0.1169	0.0012	0.1534	<.0001	0.153	0.6304		0.0364	0.9154	0.1722	0.0285	0.3427	0.6315	0.1479	0.1761
EXO	-0.04946	-0.12172	-0.78542	0.43487	-0.13219	-0.73898	-0.38356	1	0.2483	-0.02485	-0.1753	0.00633	0.26154	0.30233	0.01518
EXO	0.7952	0.5217	<.0001	0.0163	0.4862	<.0001	0.0364		0.1858	0.8963	0.3542	0.9735	0.1627	0.1044	0.9365
TME	-0.53532	-0.11226	-0.10118	0.30007	0.5812	-0.10948	0.02026	0.2483	1	0.45024	0.48393	0.202	-0.38992	0.12467	-0.00023
TME	0.0023	0.5548	0.5947	0.1072	0.0008	0.5647	0.9154	0.1858		0.0125	0.0067	0.2844	0.0332	0.5116	0.999
TMML	-0.17014	0.29796	-0.26564	0.27588	0.26696	-0.26553	0.25597	-0.02485	0.45024	1	0.74923	0.79854	0.10795	0.20921	0.67161
TMML	0.3687	0.1098	0.156	0.14	0.1538	0.1561	0.1722	0.8963	0.0125		<.0001	<.0001	0.5702	0.2672	<.0001
TORV	-0.43601	0.3236	-0.04332	0.1281	0.51112	-0.21253	0.39999	-0.1753	0.48393	0.74923	1	0.6916	0.13231	0.36941	0.61194
TORV	0.016	0.0811	0.8202	0.4999	0.0039	0.2595	0.0285	0.3542	0.0067	<.0001		<.0001	0.4858	0.0445	0.0003
TOXY	0.0215	0.24372	-0.39324	0.41901	0.0819	-0.37311	0.17944	0.00633	0.202	0.79854	0.6916	1	0.42601	0.26795	0.77622
TOXY	0.9102	0.1943	0.0316	0.0212	0.667	0.0423	0.3427	0.9735	0.2844	<.0001	<.0001		0.0189	0.1523	<.0001
TRE	0.18754	0.48965	-0.66861	0.35999	-0.30977	-0.64196	-0.09125	0.26154	-0.38992	0.10795	0.13231	0.42601	1	0.6329	0.72869
TRE	0.321	0.006	<.0001	0.0507	0.0957	0.0001	0.6315	0.1627	0.0332	0.5702	0.4858	0.0189		0.0002	<.0001
VM	-0.55663	0.35046	-0.53264	0.56439	0.402	-0.56803	-0.27073	0.30233	0.12467	0.20921	0.36941	0.26795	0.6329	1	0.55377
VM	0.0014	0.0576	0.0024	0.0012	0.0277	0.0011	0.1479	0.1044	0.5116	0.2672	0.0445	0.1523	0.0002		0.0015
MIT	0.09934	0.58746	-0.55579	0.31001	-0.09295	-0.56044	0.25369	0.01518	-0.00023	0.67161	0.61194	0.77622	0.72869	0.55377	1
MIT	0.6015	0.0006	0.0014	0.0955	0.6252	0.0013	0.1761	0.9365	0.999	<.0001	0.0003	<.0001	<.0001	0.0015	

Table C.44 Correlation matrix showing Pearson's correlation coefficient and respective p-value for relation between all measured properties for grassy biomass (Bermuda grass, corn stover, sugarcane bagasse and switchgrass) dusts.

Pearson Correlation Coefficients, N = 12 Prob > |r| under H0: Rho=0															
	AC	**AE**	**BD**	**dgw**	**EC**	**MC**	**PD**	**EXO**	**TME**	**TMML**	**TORV**	**TOXY**	**TRE**	**VM**	**MIT**
AC	1	0.96439	-0.95927	-0.90833	-0.98865	-0.87393	0.96507	-0.26175	0.13222	0.54427	0.57588	0.32522	0.11841	-0.93959	0.75127
AC		<.0001	<.0001	<.0001	<.0001	0.0002	<.0001	0.4112	0.6821	0.0673	0.0501	0.3023	0.714	<.0001	0.0049
AE	0.96439	1	-0.98858	-0.79526	-0.94187	-0.8181	0.99648	-0.2676	0.11806	0.68513	0.75795	0.53377	0.33712	-0.89303	0.88209
AE	<.0001		<.0001	0.002	<.0001	0.0011	<.0001	0.4004	0.7148	0.0139	0.0043	0.0739	0.2839	<.0001	0.0001
BD	-0.95927	-0.98858	1	0.82313	0.95529	0.8468	-0.98934	0.25625	-0.04136	-0.73095	-0.74419	-0.52105	-0.34232	0.88964	-0.89013
BD	<.0001	<.0001		0.001	<.0001	0.0005	<.0001	0.4214	0.8984	0.0069	0.0055	0.0824	0.2761	0.0001	0.0001
dgw	-0.90833	-0.79526	0.82313	1	0.94439	0.92204	-0.78927	0.16521	0.0481	-0.39022	-0.23882	0.00377	0.16008	0.91166	-0.5051
dgw	<.0001	0.002	0.001		<.0001	<.0001	0.0023	0.6079	0.882	0.2098	0.4547	0.9907	0.6192	<.0001	0.0939
EC	-0.98865	-0.94187	0.95529	0.94439	1	0.9137	-0.94192	0.23063	-0.05325	-0.55581	-0.52828	-0.27242	-0.09399	0.94045	-0.72605
EC	<.0001	<.0001	<.0001	<.0001		<.0001	<.0001	0.4708	0.8694	0.0606	0.0775	0.3917	0.7714	<.0001	0.0075
MC	-0.87393	-0.8181	0.8468	0.92204	0.9137	1	-0.80645	0.26283	0.1196	-0.5902	-0.4012	-0.22589	0.01245	0.85895	-0.63245
MC	0.0002	0.0011	0.0005	<.0001	<.0001		0.0015	0.4092	0.7112	0.0434	0.1961	0.4802	0.9694	0.0003	0.0273
PD	0.96507	0.99648	-0.98934	-0.78927	-0.94192	-0.80645	1	-0.30407	0.13872	0.69093	0.76572	0.54565	0.34204	-0.88093	0.88847
PD	<.0001	<.0001	<.0001	0.0023	<.0001	0.0015		0.3366	0.6672	0.0128	0.0037	0.0665	0.2765	0.0002	0.0001
EXO	-0.26175	-0.2676	0.25625	0.16521	0.23063	0.26283	-0.30407	1	0.08093	-0.37218	-0.30521	-0.44612	-0.28288	0.10953	-0.34604
EXO	0.4112	0.4004	0.4214	0.6079	0.4708	0.4092	0.3366		0.8026	0.2335	0.3347	0.146	0.373	0.7347	0.2705
TME	0.13222	0.11806	-0.04136	0.0481	-0.05325	0.1196	0.13872	0.08093	1	-0.28255	0.08848	-0.05317	-0.07893	-0.21158	-0.02793
TME	0.6821	0.7148	0.8984	0.882	0.8694	0.7112	0.6672	0.8026		0.3736	0.7845	0.8697	0.8074	0.5092	0.9313
TMML	0.54427	0.68513	-0.73095	-0.39022	-0.55581	-0.5902	0.69093	-0.37218	-0.28255	1	0.81356	0.81684	0.61873	-0.45915	0.91516
TMML	0.0673	0.0139	0.0069	0.2098	0.0606	0.0434	0.0128	0.2335	0.3736		0.0013	0.0012	0.032	0.1332	<.0001
TORV	0.57588	0.75795	-0.74419	-0.23882	-0.52828	-0.4012	0.76572	-0.30521	0.08848	0.81356	1	0.92303	0.76096	-0.43636	0.93601
TORV	0.0501	0.0043	0.0055	0.4547	0.0775	0.1961	0.0037	0.3347	0.7845	0.0013		<.0001	0.004	0.1561	<.0001
TOXY	0.32522	0.53377	-0.52105	0.00377	-0.27242	-0.22589	0.54565	-0.44612	-0.05317	0.81684	0.92303	1	0.77355	-0.15272	0.83257
TOXY	0.3023	0.0739	0.0824	0.9907	0.3917	0.4802	0.0665	0.146	0.8697	0.0012	<.0001		0.0032	0.6356	0.0008
TRE	0.11841	0.33712	-0.34232	0.16008	-0.09399	0.01245	0.34204	-0.28288	-0.07893	0.61873	0.76096	0.77355	1	-0.0694	0.62723
TRE	0.714	0.2839	0.2761	0.6192	0.7714	0.9694	0.2765	0.373	0.8074	0.032	0.004	0.0032		0.8303	0.029
VM	-0.93959	-0.89303	0.88964	0.91166	0.94045	0.85895	-0.88093	0.10953	-0.21158	-0.45915	-0.43636	-0.15272	-0.0694	1	-0.6401
VM	<.0001	<.0001	0.0001	<.0001	<.0001	0.0003	0.0002	0.7347	0.5092	0.1332	0.1561	0.6356	0.8303		0.025
MIT	0.75127	0.88209	-0.89013	-0.5051	-0.72605	-0.63245	0.88847	-0.34604	-0.02793	0.91516	0.93601	0.83257	0.62723	-0.6401	1
MIT	0.0049	0.0001	0.0001	0.0939	0.0075	0.0273	0.0001	0.2705	0.9313	<.0001	<.0001	0.0008	0.029	0.025	

Table C.45 Correlation matrix showing Pearson's correlation coefficient and respective p-value for relation between all measured properties for woody biomass (eucalyptus, pine and sweetgum) dusts.

	Prob > |r| under H0: Rho=0														
	AC	**AE**	**BD**	**dgw**	**EC**	**MC**	**PD**	**EXO**	**TME**	**TMML**	**TORV**	**TOXY**	**TRE**	**VM**	**MIT**
AC	1	0.47651	0.46759	-0.51748	-0.60407	0.06685	0.52025	0.44833	-0.69158	-0.42273	-0.62187	-0.58117	0.00746	-0.13301	-0.48468
AC		0.1947	0.2044	0.1536	0.0849	0.8643	0.1511	0.2261	0.039	0.257	0.0738	0.1008	0.9848	0.733	0.1861
AE	0.47651	1	-0.04958	-0.13831	-0.54803	0.82583	0.21809	0.01799	-0.26049	-0.03329	-0.75531	-0.40825	0.69806	0.56008	-0.06018
AE	0.1947		0.8992	0.7227	0.1266	0.0061	0.5729	0.9634	0.4984	0.9322	0.0186	0.2753	0.0365	0.1168	0.8778
BD	0.46759	-0.04958	1	-0.97493	-0.7893	-0.52998	0.8712	0.87995	-0.92059	-0.96726	-0.58072	-0.86478	-0.31984	-0.83075	-0.98626
BD	0.2044	0.8992		<.0001	0.0114	0.1422	0.0022	0.0018	0.0004	<.0001	0.1011	0.0026	0.4014	0.0055	<.0001
dgw	-0.51748	-0.13831	-0.97493	1	0.88979	0.35838	-0.92566	-0.88472	0.94358	0.98515	0.73464	0.933	0.21227	0.71211	0.99688
dgw	0.1536	0.7227	<.0001		0.0013	0.3436	0.0003	0.0015	0.0001	<.0001	0.0242	0.0002	0.5835	0.0314	<.0001
EC	-0.60407	-0.54803	-0.7893	0.88979	1	-0.04415	-0.82848	-0.73697	0.88995	0.82984	0.94279	0.93634	-0.16345	0.32167	0.85292
EC	0.0849	0.1266	0.0114	0.0013		0.9102	0.0058	0.0235	0.0013	0.0056	0.0001	0.0002	0.6743	0.3986	0.0035
MC	0.06685	0.82583	-0.52998	0.35838	-0.04415	1	-0.25971	-0.44979	0.2526	0.4394	-0.34466	0.04522	0.65172	0.82402	0.42692
MC	0.8643	0.0061	0.1422	0.3436	0.9102		0.4998	0.2245	0.512	0.2367	0.3637	0.908	0.0572	0.0063	0.2518
PD	0.52025	0.21809	0.8712	-0.92566	-0.82848	-0.25971	1	0.90117	-0.83344	-0.93425	-0.71483	-0.89865	-0.16184	-0.62162	-0.91747
PD	0.1511	0.5729	0.0022	0.0003	0.0058	0.4998		0.0009	0.0053	0.0002	0.0304	0.001	0.6774	0.0739	0.0005
EXO	0.44833	0.01799	0.87995	-0.88472	-0.73697	-0.44979	0.90117	1	-0.75894	-0.88544	-0.5443	-0.79788	-0.37989	-0.71256	-0.8894
EXO	0.2261	0.9634	0.0018	0.0015	0.0235	0.2245	0.0009		0.0177	0.0015	0.1298	0.01	0.3132	0.0312	0.0013
TME	-0.69158	-0.26049	-0.92059	0.94358	0.88995	0.2526	-0.83344	-0.75894	1	0.88618	0.77089	0.90994	0.07144	0.6056	0.92999
TME	0.039	0.4984	0.0004	0.0001	0.0013	0.512	0.0053	0.0177		0.0015	0.015	0.0007	0.8551	0.0839	0.0003
TMML	-0.42273	-0.03329	-0.96726	0.98515	0.82984	0.4394	-0.93425	-0.88544	0.88618	1	0.66024	0.8844	0.27502	0.75872	0.99106
TMML	0.257	0.9322	<.0001	<.0001	0.0056	0.2367	0.0002	0.0015	0.0015		0.0529	0.0015	0.4739	0.0178	<.0001
TORV	-0.62187	-0.75531	-0.58072	0.73464	0.94279	-0.34466	-0.71483	-0.5443	0.77089	0.66024	1	0.86357	-0.30058	0.06411	0.68052
TORV	0.0738	0.0186	0.1011	0.0242	0.0001	0.3637	0.0304	0.1298	0.015	0.0529		0.0027	0.4319	0.8698	0.0436
TOXY	-0.58117	-0.40825	-0.86478	0.933	0.93634	0.04522	-0.89865	-0.79788	0.90994	0.8844	0.86357	1	0.03118	0.5136	0.90797
TOXY	0.1008	0.2753	0.0026	0.0002	0.0002	0.908	0.001	0.01	0.0007	0.0015	0.0027		0.9365	0.1573	0.0007
TRE	0.00746	0.69806	-0.31984	0.21227	-0.16345	0.65172	-0.16184	-0.37989	0.07144	0.27502	-0.30058	0.03118	1	0.66718	0.26815
TRE	0.9848	0.0365	0.4014	0.5835	0.6743	0.0572	0.6774	0.3132	0.8551	0.4739	0.4319	0.9365		0.0496	0.4854
VM	-0.13301	0.56008	-0.83075	0.71211	0.32167	0.82402	-0.62162	-0.71256	0.6056	0.75872	0.06411	0.5136	0.66718	1	0.76192
VM	0.733	0.1168	0.0055	0.0314	0.3986	0.0063	0.0739	0.0312	0.0839	0.0178	0.8698	0.1573	0.0496		0.017
MIT	-0.48468	-0.06018	-0.98626	0.99688	0.85292	0.42692	-0.91747	-0.8894	0.92999	0.99106	0.68052	0.90797	0.26815	0.76192	1
MIT	0.1861	0.8778	<.0001	<.0001	0.0035	0.2518	0.0005	0.0013	0.0003	<.0001	0.0436	0.0007	0.4854	0.017	

Appendix – D SAS Codes and Results for Principal Component Analysis (PCA) on NIR Data for Internal Validation of Models

SAS code for PCA on raw NIR spectral data for biomass dusts used for internal validation

```
/*******************************
 * Author: Jaskaran Dhiman      *
 * Research work                *
 * Date: 01/31/2014             *
 *******************************/

ods html file='C:\Users\jzd0028\Desktop\Research\NIR new
analysis\output_raw.html';
options nodate pageno=1;
data work.jasnir;
infile 'C:\Users\jzd0028\Desktop\Research\NIR new
analysis\raw_data_SAS.csv' delimiter = ',' MISSOVER DSD lrecl=32767
firstobs=1 n=1500;
input Number$ Biomass$ MIT TORV TMML TOXY TRE TME
w9994 w9984 w9974 w9964 w9954 w9944 w9934 w9924 w9914 w9904 w9894
      w9884 w9874
w9864 w9854 w9844 w9834 w9824 w9814 w9804 w9794 w9784 w9774 w9764
      w9754 w9744
w9734 w9724 w9714 w9704 w9694 w9684 w9674 w9664 w9654 w9644 w9634
      w9624 w9614
w9604 w9594 w9584 w9574 w9564 w9554 w9544 w9534 w9524 w9514 w9504
      w9494 w9484
w9474 w9464 w9454 w9444 w9434 w9424 w9414 w9404 w9394 w9384 w9374
      w9364 w9354
w9344 w9334 w9324 w9314 w9304 w9294 w9284 w9274 w9264 w9254 w9244
      w9234 w9224
w9214 w9204 w9194 w9184 w9174 w9164 w9154 w9144 w9134 w9124 w9114
      w9104 w9094
w9084 w9074 w9064 w9054 w9044 w9034 w9024 w9014 w9004 w8994 w8984
      w8974 w8964
w8954 w8944 w8934 w8924 w8914 w8904 w8894 w8884 w8874 w8864 w8854
      w8844 w8834
w8824 w8814 w8804 w8794 w8784 w8774 w8764 w8754 w8744 w8734 w8724
      w8714 w8704
w8694 w8684 w8674 w8664 w8654 w8644 w8634 w8624 w8614 w8604 w8594
      w8584 w8574
w8564 w8554 w8544 w8534 w8524 w8514 w8504 w8494 w8484 w8474 w8464
      w8454 w8444
w8434 w8424 w8414 w8404 w8394 w8384 w8374 w8364 w8354 w8344 w8334
      w8324 w8314
```

w8304 w8294 w8284 w8274 w8264 w8254 w8244 w8234 w8224 w8214 w8204
w8194 w8184
w8174 w8164 w8154 w8144 w8134 w8124 w8114 w8104 w8094 w8084 w8074
w8064 w8054
w8044 w8034 w8024 w8014 w8004 w7994 w7984 w7974 w7964 w7954 w7944
w7934 w7924
w7914 w7904 w7894 w7884 w7874 w7864 w7854 w7844 w7834 w7824 w7814
w7804 w7794
w7784 w7774 w7764 w7754 w7744 w7734 w7724 w7714 w7704 w7694 w7684
w7674 w7664
w7654 w7644 w7634 w7624 w7614 w7604 w7594 w7584 w7574 w7564 w7554
w7544 w7534
w7524 w7514 w7504 w7494 w7484 w7474 w7464 w7454 w7444 w7434 w7424
w7414 w7404
w7394 w7384 w7374 w7364 w7354 w7344 w7334 w7324 w7314 w7304 w7294
w7284 w7274
w7264 w7254 w7244 w7234 w7224 w7214 w7204 w7194 w7184 w7174 w7164
w7154 w7144
w7134 w7124 w7114 w7104 w7094 w7084 w7074 w7064 w7054 w7044 w7034
w7024 w7014
w7004 w6994 w6984 w6974 w6964 w6954 w6944 w6934 w6924 w6914 w6904
w6894 w6884
w6874 w6864 w6854 w6844 w6834 w6824 w6814 w6804 w6794 w6784 w6774
w6764 w6754
w6744 w6734 w6724 w6714 w6704 w6694 w6684 w6674 w6664 w6654 w6644
w6634 w6624
w6614 w6604 w6594 w6584 w6574 w6564 w6554 w6544 w6534 w6524 w6514
w6504 w6494
w6484 w6474 w6464 w6454 w6444 w6434 w6424 w6414 w6404 w6394 w6384
w6374 w6364
w6354 w6344 w6334 w6324 w6314 w6304 w6294 w6284 w6274 w6264 w6254
w6244 w6234
w6224 w6214 w6204 w6194 w6184 w6174 w6164 w6154 w6144 w6134 w6124
w6114 w6104
w6094 w6084 w6074 w6064 w6054 w6044 w6034 w6024 w6014 w6004 w5994
w5984 w5974
w5964 w5954 w5944 w5934 w5924 w5914 w5904 w5894 w5884 w5874 w5864
w5854 w5844
w5834 w5824 w5814 w5804 w5794 w5784 w5774 w5764 w5754 w5744 w5734
w5724 w5714
w5704 w5694 w5684 w5674 w5664 w5654 w5644 w5634 w5624 w5614 w5604
w5594 w5584
w5574 w5564 w5554 w5544 w5534 w5524 w5514 w5504 w5494 w5484 w5474
w5464 w5454
w5444 w5434 w5424 w5414 w5404 w5394 w5384 w5374 w5364 w5354 w5344
w5334 w5324
w5314 w5304 w5294 w5284 w5274 w5264 w5254 w5244 w5234 w5224 w5214
w5204 w5194
w5184 w5174 w5164 w5154 w5144 w5134 w5124 w5114 w5104 w5094 w5084
w5074 w5064
w5054 w5044 w5034 w5024 w5014 w5004 w4994 w4984 w4974 w4964 w4954
w4944 w4934
w4924 w4914 w4904 w4894 w4884 w4874 w4864 w4854 w4844 w4834 w4824
w4814 w4804
w4794 w4784 w4774 w4764 w4754 w4744 w4734 w4724 w4714 w4704 w4694
w4684 w4674

```
w4664 w4654 w4644 w4634 w4624 w4614 w4604 w4594 w4584 w4574 w4564
      w4554 w4544
w4534 w4524 w4514 w4504 w4494 w4484 w4474 w4464 w4454 w4444 w4434
      w4424 w4414
w4404 w4394 w4384 w4374 w4364 w4354 w4344 w4334 w4324 w4314 w4304
      w4294 w4284
w4274 w4264 w4254 w4244 w4234 w4224 w4214 w4204 w4194 w4184 w4174
      w4164 w4154
w4144 w4134 w4124 w4114 w4104 w4094 w4084 w4074 w4064 w4054 w4044
      w4034 w4024
w4014 w4004;
datalines;
;
run;

proc princomp data=work.jasnir out=prinvars std;
var w9994   w9984 w9974 w9964 w9954 w9944 w9934 w9924 w9914 w9904
      w9894 w9884 w9874
w9864 w9854 w9844 w9834 w9824 w9814 w9804 w9794 w9784 w9774 w9764
      w9754 w9744
w9734 w9724 w9714 w9704 w9694 w9684 w9674 w9664 w9654 w9644 w9634
      w9624 w9614
w9604 w9594 w9584 w9574 w9564 w9554 w9544 w9534 w9524 w9514 w9504
      w9494 w9484
w9474 w9464 w9454 w9444 w9434 w9424 w9414 w9404 w9394 w9384 w9374
      w9364 w9354
w9344 w9334 w9324 w9314 w9304 w9294 w9284 w9274 w9264 w9254 w9244
      w9234 w9224
w9214 w9204 w9194 w9184 w9174 w9164 w9154 w9144 w9134 w9124 w9114
      w9104 w9094
w9084 w9074 w9064 w9054 w9044 w9034 w9024 w9014 w9004 w8994 w8984
      w8974 w8964
w8954 w8944 w8934 w8924 w8914 w8904 w8894 w8884 w8874 w8864 w8854
      w8844 w8834
w8824 w8814 w8804 w8794 w8784 w8774 w8764 w8754 w8744 w8734 w8724
      w8714 w8704
w8694 w8684 w8674 w8664 w8654 w8644 w8634 w8624 w8614 w8604 w8594
      w8584 w8574
w8564 w8554 w8544 w8534 w8524 w8514 w8504 w8494 w8484 w8474 w8464
      w8454 w8444
w8434 w8424 w8414 w8404 w8394 w8384 w8374 w8364 w8354 w8344 w8334
      w8324 w8314
w8304 w8294 w8284 w8274 w8264 w8254 w8244 w8234 w8224 w8214 w8204
      w8194 w8184
w8174 w8164 w8154 w8144 w8134 w8124 w8114 w8104 w8094 w8084 w8074
      w8064 w8054
w8044 w8034 w8024 w8014 w8004 w7994 w7984 w7974 w7964 w7954 w7944
      w7934 w7924
w7914 w7904 w7894 w7884 w7874 w7864 w7854 w7844 w7834 w7824 w7814
      w7804 w7794
w7784 w7774 w7764 w7754 w7744 w7734 w7724 w7714 w7704 w7694 w7684
      w7674 w7664
w7654 w7644 w7634 w7624 w7614 w7604 w7594 w7584 w7574 w7564 w7554
      w7544 w7534
w7524 w7514 w7504 w7494 w7484 w7474 w7464 w7454 w7444 w7434 w7424
      w7414 w7404
```

```
w7394 w7384 w7374 w7364 w7354 w7344 w7334 w7324 w7314 w7304 w7294
      w7284 w7274
w7264 w7254 w7244 w7234 w7224 w7214 w7204 w7194 w7184 w7174 w7164
      w7154 w7144
w7134 w7124 w7114 w7104 w7094 w7084 w7074 w7064 w7054 w7044 w7034
      w7024 w7014
w7004 w6994 w6984 w6974 w6964 w6954 w6944 w6934 w6924 w6914 w6904
      w6894 w6884
w6874 w6864 w6854 w6844 w6834 w6824 w6814 w6804 w6794 w6784 w6774
      w6764 w6754
w6744 w6734 w6724 w6714 w6704 w6694 w6684 w6674 w6664 w6654 w6644
      w6634 w6624
w6614 w6604 w6594 w6584 w6574 w6564 w6554 w6544 w6534 w6524 w6514
      w6504 w6494
w6484 w6474 w6464 w6454 w6444 w6434 w6424 w6414 w6404 w6394 w6384
      w6374 w6364
w6354 w6344 w6334 w6324 w6314 w6304 w6294 w6284 w6274 w6264 w6254
      w6244 w6234
w6224 w6214 w6204 w6194 w6184 w6174 w6164 w6154 w6144 w6134 w6124
      w6114 w6104
w6094 w6084 w6074 w6064 w6054 w6044 w6034 w6024 w6014 w6004 w5994
      w5984 w5974
w5964 w5954 w5944 w5934 w5924 w5914 w5904 w5894 w5884 w5874 w5864
      w5854 w5844
w5834 w5824 w5814 w5804 w5794 w5784 w5774 w5764 w5754 w5744 w5734
      w5724 w5714
w5704 w5694 w5684 w5674 w5664 w5654 w5644 w5634 w5624 w5614 w5604
      w5594 w5584
w5574 w5564 w5554 w5544 w5534 w5524 w5514 w5504 w5494 w5484 w5474
      w5464 w5454
w5444 w5434 w5424 w5414 w5404 w5394 w5384 w5374 w5364 w5354 w5344
      w5334 w5324
w5314 w5304 w5294 w5284 w5274 w5264 w5254 w5244 w5234 w5224 w5214
      w5204 w5194
w5184 w5174 w5164 w5154 w5144 w5134 w5124 w5114 w5104 w5094 w5084
      w5074 w5064
w5054 w5044 w5034 w5024 w5014 w5004 w4994 w4984 w4974 w4964 w4954
      w4944 w4934
w4924 w4914 w4904 w4894 w4884 w4874 w4864 w4854 w4844 w4834 w4824
      w4814 w4804
w4794 w4784 w4774 w4764 w4754 w4744 w4734 w4724 w4714 w4704 w4694
      w4684 w4674
w4664 w4654 w4644 w4634 w4624 w4614 w4604 w4594 w4584 w4574 w4564
      w4554 w4544
w4534 w4524 w4514 w4504 w4494 w4484 w4474 w4464 w4454 w4444 w4434
      w4424 w4414
w4404 w4394 w4384 w4374 w4364 w4354 w4344 w4334 w4324 w4314 w4304
      w4294 w4284
w4274 w4264 w4254 w4244 w4234 w4224 w4214 w4204 w4194 w4184 w4174
      w4164 w4154
w4144 w4134 w4124 w4114 w4104 w4094 w4084 w4074 w4064 w4054 w4044
      w4034 w4024
w4014 w4004;
run;


proc reg data=prinvars outest=est press;
```

```
model MIT = prin1-prin10 / selection=stepwise vif p;
model TORV= prin1-prin10 / selection=stepwise vif p;
model TMML= prin1-prin10 / selection=stepwise vif p;
model TOXY= prin1-prin10 / selection=stepwise vif p;
model TRE= prin1-prin10 / selection=stepwise vif p;
model TME= prin1-prin10 / selection=stepwise vif p;
run;

proc print data=prinvars;
var prin1-prin10;
run;
ods html close;
```

Table D.1 ANOVA results and model parameter estimates for MIT (raw data model).

Analysis of Variance					
Source	**DF**	**Sum of Squares**	**Mean Square**	**F Value**	**Pr > F**
Model	10	6263.135	626.3135	322.8	<.0001
Error	19	36.86515	1.94027		
Corrected Total	29	6300			
Root MSE	1.39294	**R-Square**	0.9941		
Dependent Mean	290	**Adj R-Sq**	0.9911		
Coeff Var	0.48032				

Parameter Estimates						
Variable	**DF**	**Parameter Estimate**	**Standard Error**	**t Value**	**Pr > |t|**	**Variance Inflation**
Intercept	**1**	290	0.25431	1140.32	<.0001	0
Prin1	**1**	5.19486	0.25866	20.08	<.0001	1
Prin2	**1**	-1.61427	0.25866	-6.24	<.0001	1
Prin3	**1**	-8.44735	0.25866	-32.66	<.0001	1
Prin4	**1**	5.2108	0.25866	20.15	<.0001	1
Prin5	**1**	3.58786	0.25866	13.87	<.0001	1
Prin6	**1**	1.8311	0.25866	7.08	<.0001	1
Prin7	**1**	-4.84083	0.25866	-18.71	<.0001	1
Prin8	**1**	-2.07599	0.25866	-8.03	<.0001	1
Prin9	**1**	6.04782	0.25866	23.38	<.0001	1
Prin10	**1**	-2.706	0.25866	-10.46	<.0001	1

Table D.2 ANOVA results and model parameter estimates for TORV (raw data model).

Analysis of Variance					
Source	**DF**	**Sum of Squares**	**Mean Square**	**F Value**	**Pr > F**
Model	7	3415.039	487.8627	187.86	<.0001
Error	22	57.13287	2.59695		
Corrected Total	29	3472.172			
Root MSE	1.61151	**R-Square**	0.9835		
Dependent Mean	283.8253	**Adj R-Sq**	0.9783		
Coeff Var	0.56778				

Parameter Estimates						
Variable	**DF**	**Parameter Estimate**	**Standard Error**	**t Value**	**Pr > |t|**	**Variance Inflation**
Intercept	**1**	283.8253	0.29422	964.67	<.0001	0
Prin2	**1**	1.42119	0.29925	4.75	<.0001	1
Prin3	**1**	-6.39864	0.29925	-21.38	<.0001	1
Prin4	**1**	4.151	0.29925	13.87	<.0001	1
Prin5	**1**	-4.34895	0.29925	-14.53	<.0001	1
Prin8	**1**	-0.51608	0.29925	-1.72	0.0986	1
Prin9	**1**	4.8256	0.29925	16.13	<.0001	1
Prin10	**1**	-3.88595	0.29925	-12.99	<.0001	1

Table D.3 ANOVA results and model parameter estimates for TMML (raw data model).

Analysis of Variance					
Source	**DF**	**Sum of Squares**	**Mean Square**	**F Value**	**Pr > F**
Model	8	6197.26	774.6576	67.75	<.0001
Error	21	240.1086	11.43374		
Corrected Total	29	6437.369			
Root MSE	3.38138	**R-Square**	0.9627		
Dependent Mean	325.599	**Adj R-Sq**	0.9485		
Coeff Var	1.03851				

Parameter Estimates						
Variable	**DF**	**Parameter Estimate**	**Standard Error**	**t Value**	**Pr > |t|**	**Variance Inflation**
Intercept	**1**	325.599	0.61735	527.41	<.0001	0
Prin2	**1**	-1.92959	0.62791	-3.07	0.0058	1
Prin3	**1**	-5.95946	0.62791	-9.49	<.0001	1
Prin4	**1**	6.82824	0.62791	10.87	<.0001	1
Prin5	**1**	-5.83541	0.62791	-9.29	<.0001	1
Prin6	**1**	2.47788	0.62791	3.95	0.0007	1
Prin7	**1**	-7.32868	0.62791	-11.67	<.0001	1
Prin9	**1**	5.5779	0.62791	8.88	<.0001	1
Prin10	**1**	-1.67951	0.62791	-2.67	0.0142	1

Table D.4 ANOVA results and model parameter estimates for TOXY (raw data model).

Analysis of Variance					
Source	**DF**	**Sum of Squares**	**Mean Square**	**F Value**	**Pr > F**
Model	8	6134.713	766.8392	7.35	0.0001
Error	21	2190.255	104.2979		
Corrected Total	29	8324.969			
Root MSE	10.21263	**R-Square**	0.7369		
Dependent Mean	292.497	**Adj R-Sq**	0.6367		
Coeff Var	3.49153				

Parameter Estimates						
Variable	**DF**	**Parameter Estimate**	**Standard Error**	**t Value**	**Pr > |t|**	**Variance Inflation**
Intercept	**1**	292.497	1.86456	156.87	<.0001	0
Prin1	**1**	3.27558	1.89644	1.73	0.0988	1
Prin2	**1**	-3.8124	1.89644	-2.01	0.0574	1
Prin3	**1**	-6.48977	1.89644	-3.42	0.0026	1
Prin4	**1**	5.90992	1.89644	3.12	0.0052	1
Prin7	**1**	-4.884	1.89644	-2.58	0.0176	1
Prin8	**1**	-3.86455	1.89644	-2.04	0.0544	1
Prin9	**1**	6.83182	1.89644	3.6	0.0017	1
Prin10	**1**	-4.87563	1.89644	-2.57	0.0178	1

Table D.5 ANOVA results and model parameter estimates for TRE (raw data model).

Analysis of Variance					
Source	**DF**	**Sum of Squares**	**Mean Square**	**F Value**	**Pr > F**
Model	8	4107.185	513.3981	35.2	<.0001
Error	21	306.2536	14.58351		
Corrected Total	29	4413.438			
Root MSE	3.81884	**R-Square**	0.9306		
Dependent Mean	239.0813	**Adj R-Sq**	0.9042		
Coeff Var	1.5973				

Parameter Estimates						
Variable	**DF**	**Parameter Estimate**	**Standard Error**	**t Value**	**Pr > |t|**	**Variance Inflation**
Intercept	**1**	239.0813	0.69722	342.91	<.0001	0
Prin1	**1**	5.30679	0.70914	7.48	<.0001	1
Prin2	**1**	-2.58712	0.70914	-3.65	0.0015	1
Prin3	**1**	-6.34311	0.70914	-8.94	<.0001	1
Prin5	**1**	7.30407	0.70914	10.3	<.0001	1
Prin6	**1**	-2.03127	0.70914	-2.86	0.0093	1
Prin7	**1**	-2.03972	0.70914	-2.88	0.009	1
Prin8	**1**	-1.93073	0.70914	-2.72	0.0128	1
Prin10	**1**	-1.08312	0.70914	-1.53	0.1416	1

Table D.6 ANOVA results and model parameter estimates for TME (raw data model).

Analysis of Variance					
Source	**DF**	**Sum of Squares**	**Mean Square**	**F Value**	**Pr > F**
Model	7	6030.005	861.4292	28.49	<.0001
Error	22	665.2383	30.2381		
Corrected Total	29	6695.243			
Root MSE	5.49892	**R-Square**	0.9006		
Dependent Mean	387.7237	**Adj R-Sq**	0.869		
Coeff Var	1.41826				

Parameter Estimates						
Variable	**DF**	**Parameter Estimate**	**Standard Error**	**t Value**	**Pr > |t|**	**Variance Inflation**
Intercept	**1**	387.7237	1.00396	386.19	<.0001	0
Prin1	**1**	-5.66085	1.02112	-5.54	<.0001	1
Prin2	**1**	-3.26223	1.02112	-3.19	0.0042	1
Prin3	**1**	-5.15126	1.02112	-5.04	<.0001	1
Prin4	**1**	4.5388	1.02112	4.44	0.0002	1
Prin5	**1**	-8.74419	1.02112	-8.56	<.0001	1
Prin6	**1**	5.56589	1.02112	5.45	<.0001	1
Prin7	**1**	3.26613	1.02112	3.2	0.0041	1

Table D.7 Principal components (PC) obtained from raw NIR spectral data of biomass dusts used for PCA and internal validation of prediction models.

Biomass	Prin1	Prin2	Prin3	Prin4	Prin5	Prin6	Prin7	Prin8	Prin9	Prin10
Bermuda grass	-1.1351	-0.32287	0.23064	-1.10264	0.92603	0.45807	-1.31803	1.03633	-1.76528	-0.61445
	-0.25238	-0.05082	-0.02108	-1.30793	0.62838	0.3299	-0.29684	2.01612	-1.12981	1.10698
	-1.15384	-0.55506	0.24567	-1.34312	0.88007	0.37118	-1.14435	1.39141	-1.39295	-0.44614
Corn Cobs	-0.70121	0.2608	-0.60282	-1.20992	0.00345	0.59135	0.81393	-1.70254	-0.38918	1.49325
	0.14763	0.44831	-0.80973	-1.30511	-0.48265	0.94892	0.57285	-0.13284	0.45194	2.84933
	-0.51796	0.01126	-0.39748	-1.68119	-0.34742	0.24598	0.18217	-2.70359	-0.87651	0.24709
Corn stover	1.24493	-1.39243	0.6204	0.80381	0.19613	1.16057	1.20157	0.42113	-0.86688	-0.59185
	1.34682	-1.14546	0.41903	0.80172	0.37403	1.19784	1.86822	1.54371	0.44003	1.39488
	0.39264	-1.6682	0.75538	0.65258	0.55052	0.96428	0.95999	-0.46623	-0.8018	-1.27211
Eucalyptus	0.57291	0.13772	-1.12152	-0.69313	-0.66353	-2.10345	1.35774	0.78325	-0.07767	-0.47519
	-0.33907	-0.35192	-0.79305	-0.7898	-0.10687	-2.01643	1.18441	0.85046	0.63667	-0.7791
	0.18702	-0.17752	-0.87142	-0.7471	-0.46554	-2.06823	1.1946	0.52999	0.01603	-0.98021
Pecan shell	-1.12387	0.61508	1.41127	0.60446	-2.09772	0.14601	-0.09211	0.26204	-0.35425	-0.36449
	-1.15177	0.65958	1.36627	0.70197	-2.10299	0.20543	0.19522	0.41186	-0.16408	-0.10525
	-1.4345	0.62567	1.4183	0.63814	-1.95337	0.03564	0.58171	0.27887	0.33572	0.39232
Pine	0.48014	1.05127	-1.53225	0.27349	-0.37381	1.67629	-0.22252	-0.06733	0.20915	-1.75086
	0.31817	0.88863	-1.53914	-0.15847	-0.41169	1.5587	-0.25987	0.25759	1.20038	-1.11813
	-0.83409	0.43132	-1.34793	-0.09802	0.26407	1.55085	-0.15746	0.46496	2.12016	-1.06663
Poultry Litter	0.49017	1.61278	1.45754	-0.19658	1.53553	-0.30998	0.1279	-0.1442	0.72193	-0.3744
	1.89974	2.24891	1.35431	-0.33459	0.81344	-0.35211	0.08603	-0.42111	-0.36378	-0.0952
	0.05656	1.4613	1.73581	-0.17307	1.89418	-0.43134	0.14331	-0.34858	0.97929	-0.26116
Sugarcane bagasse	0.36963	-1.23359	0.43652	-0.04143	-0.00852	-0.47572	-1.26553	0.28632	2.15221	1.40104
	1.22078	-1.07428	0.39362	-0.52875	-0.96103	-0.6447	-2.56862	-0.39001	0.43911	-0.62015
	1.44235	-0.93345	0.29276	-0.18301	-0.82626	-0.48695	-1.91633	-0.10856	0.89421	0.46685
Sweetgum	-0.32227	0.51231	-1.10513	1.81865	0.53331	-0.82633	-0.56853	-0.198	-0.70702	0.76562
	-0.24292	0.66241	-1.14979	2.12033	0.50466	-0.62678	-1.01991	-0.28249	-1.15765	0.4614
	-0.79177	0.39501	-1.08469	2.11827	0.93987	-0.66229	-0.42148	0.29863	-0.18795	1.09435
Switchgrass	1.24927	-0.44321	-0.23768	0.22908	-0.60985	-0.17137	0.2095	-1.75171	-1.33557	-0.44829
	-2.28191	-1.98996	0.58133	0.41442	1.55231	-0.43245	0.53188	-1.61503	1.46875	-0.54262
	0.8639	-0.68356	-0.10511	0.71696	-0.18474	0.16711	0.04056	-0.50046	-0.49522	0.2331

Table D.8 Result of Tukey test on principal component values of different biomass dust samples for PC1.

Means with the same letter are not significantly different.			
Tukey Grouping	**Mean**	**N**	**Biomass**
A	1.0109	3	Sugarcane bagasse
A			
A	0.9948	3	Corn stover
A			
A	0.8155	3	Poultry Litter
A			
A	0.1403	3	Eucalyptus
A			
A	-0.0119	3	Pine
A			
A	-0.0562	3	Switchgrass
A			
A	-0.3572	3	Corn Cobs
A			
A	-0.4523	3	Sweetgum
A			
A	-0.8471	3	Bermuda grass
A			
A	-1.2367	3	Pecan shell

Table D.9 Result of Tukey test on principal component values of different biomass dust samples for PC2.

Means with the same letter are not significantly different.					
Tukey Grouping			**Mean**	**N**	**Biomass**
	A		1.7743	3	Poultry Litter
	A				
B	A		0.7904	3	Pine
B					
B	C		0.6334	3	Pecan shell
B	C				
B	C		0.5232	3	Sweetgum
B	C				
B	C		0.2401	3	Corn Cobs
B	C				
B	C	D	-0.1306	3	Eucalyptus
	C	D			
	C	D	-0.3096	3	Bermuda grass
		D			
	E	D	-1.0389	3	Switchgrass
	E	D			
	E	D	-1.0804	3	Sugarcane bagasse
	E				
	E		-1.4020	3	Corn stover

Table D.10 Result of Tukey test on principal component values of different biomass dust samples for PC3.

Means with the same letter are not significantly different.				
Tukey	**Grouping**	**Mean**	**N**	**Biomass**
	A	1.5159	3	Poultry Litter
	A			
	A	1.3986	3	Pecan shell
	B	0.5983	3	Corn stover
	B			
	B	0.3743	3	Sugarcane bagasse
	B			
	B	0.1517	3	Bermuda grass
	B			
	B	0.0795	3	Switchgrass
	C	-0.6033	3	Corn Cobs
	C			
D	C	-0.9287	3	Eucalyptus
D	C			
D	C	-1.1132	3	Sweetgum
D				
D		-1.4731	3	Pine

Table D.11 Result of Tukey test on principal component values of different biomass dust samples for PC4.

Means with the same letter are not significantly different.				
Tukey Grouping		**Mean**	**N**	**Biomass**
	A	2.0191	3	Sweetgum
	B	0.7527	3	Corn stover
	B			
	B	0.6482	3	Pecan shell
	B			
C	B	0.4535	3	Switchgrass
C				
C	D	0.0057	3	Pine
	D			
	D	-0.2347	3	Poultry Litter
	D			
E	D	-0.2511	3	Sugarcane bagasse
E				
E		-0.7433	3	Eucalyptus
	F	-1.2512	3	Bermuda grass
	F			
	F	-1.3987	3	Corn Cobs

Table D.12 Result of Tukey test on principal component values of different biomass dust samples for PC5.

Means with the same letter are not significantly different.					
Tukey Grouping			**Mean**	**N**	**Biomass**
	A		1.4144	3	Poultry Litter
	A				
B	A		0.8115	3	Bermuda grass
B	A				
B	A	C	0.6593	3	Sweetgum
B	A	C			
B	A	C	0.3736	3	Corn stover
B	A	C			
B	A	C	0.2526	3	Switchgrass
B		C			
B		C	-0.1738	3	Pine
B		C			
B		C	-0.2755	3	Corn Cobs
B		C			
B		C	-0.4120	3	Eucalyptus
		C			
		C	-0.5986	3	Sugarcane bagasse
	D		-2.0514	3	Pecan shell

Table D.13 Result of Tukey test on principal component values of different biomass dust samples for PC6.

Means with the same letter are not significantly different.				
Tukey Grouping		**Mean**	**N**	**Biomass**
	A	1.5953	3	Pine
	B	1.1076	3	Corn stover
	C	0.5954	3	Corn Cobs
	C			
	C	0.3864	3	Bermuda grass
	C			
D	C	0.1290	3	Pecan shell
D				
D	E	-0.1456	3	Switchgrass
	E			
F	E	-0.3645	3	Poultry Litter
F	E			
F	E	-0.5358	3	Sugarcane bagasse
F				
F		-0.7051	3	Sweetgum
	G	-2.0627	3	Eucalyptus

Table D.14 Result of Tukey test on principal component values of different biomass dust samples for PC9.

Means with the same letter are not significantly different.				
Tukey Grouping		**Mean**	**N**	**Biomass**
	A	1.1766	3	Pine
	A			
	A	1.1618	3	Sugarcane bagasse
	A			
B	A	0.4458	3	Poultry Litter
B	A			
B	A	0.1917	3	Eucalyptus
B	A			
B	A	-0.0609	3	Pecan shell
B	A			
B	A	-0.1207	3	Switchgrass
B	A			
B	A	-0.2713	3	Corn Cobs
B	A			
B	A	-0.4096	3	Corn stover
B	A			
B	A	-0.6842	3	Sweetgum
B				
B		-1.4293	3	Bermuda grass

Table D.15 Result of Tukey test on principal component values of different biomass dust samples for PC10.

Means with the same letter are not significantly different.				
Tukey Grouping		**Mean**	**N**	**Biomass**
	A	1.5299	3	Corn Cobs
	A			
B	A	0.7738	3	Sweetgum
B	A			
B	A	0.4159	3	Sugarcane bagasse
B	A			
B	A	0.0155	3	Bermuda grass
B	A			
B	A	-0.0258	3	Pecan shell
B	A			
B	A	-0.1564	3	Corn stover
B	A			
B	A	-0.2436	3	Poultry Litter
B	A			
B	A	-0.2526	3	Switchgrass
B	A			
B	A	-0.7448	3	Eucalyptus
B				
B		-1.3119	3	Pine

SAS code for PCA on first derivative NIR spectral data and internal validation of prediction models

```
/*******************************
 * Author: Jaskaran Dhiman      *
 * Research work                *
 * Date: 01/31/2014             *
 *******************************/

ods html file='C:\Users\jzd0028\Desktop\Research\NIR new
analysis\output_firstderivative.html';
options nodate pageno=1;
data work.jasnir;
infile 'C:\Users\jzd0028\Desktop\Research\NIR new
analysis\firstderivative_data_SAS.csv' delimiter = ',' MISSOVER DSD
lrecl=32767 firstobs=1 n=1500;
input Number$ Biomass$ MIT TORV TMML TOXY TRE TME
w9994 w9984 w9974 w9964 w9954 w9944 w9934 w9924 w9914 w9904 w9894
      w9884 w9874
w9864 w9854 w9844 w9834 w9824 w9814 w9804 w9794 w9784 w9774 w9764
      w9754 w9744
w9734 w9724 w9714 w9704 w9694 w9684 w9674 w9664 w9654 w9644 w9634
      w9624 w9614
w9604 w9594 w9584 w9574 w9564 w9554 w9544 w9534 w9524 w9514 w9504
      w9494 w9484
w9474 w9464 w9454 w9444 w9434 w9424 w9414 w9404 w9394 w9384 w9374
      w9364 w9354
w9344 w9334 w9324 w9314 w9304 w9294 w9284 w9274 w9264 w9254 w9244
      w9234 w9224
w9214 w9204 w9194 w9184 w9174 w9164 w9154 w9144 w9134 w9124 w9114
      w9104 w9094
w9084 w9074 w9064 w9054 w9044 w9034 w9024 w9014 w9004 w8994 w8984
      w8974 w8964
w8954 w8944 w8934 w8924 w8914 w8904 w8894 w8884 w8874 w8864 w8854
      w8844 w8834
w8824 w8814 w8804 w8794 w8784 w8774 w8764 w8754 w8744 w8734 w8724
      w8714 w8704
w8694 w8684 w8674 w8664 w8654 w8644 w8634 w8624 w8614 w8604 w8594
      w8584 w8574
w8564 w8554 w8544 w8534 w8524 w8514 w8504 w8494 w8484 w8474 w8464
      w8454 w8444
w8434 w8424 w8414 w8404 w8394 w8384 w8374 w8364 w8354 w8344 w8334
      w8324 w8314
w8304 w8294 w8284 w8274 w8264 w8254 w8244 w8234 w8224 w8214 w8204
      w8194 w8184
w8174 w8164 w8154 w8144 w8134 w8124 w8114 w8104 w8094 w8084 w8074
      w8064 w8054
w8044 w8034 w8024 w8014 w8004 w7994 w7984 w7974 w7964 w7954 w7944
      w7934 w7924
w7914 w7904 w7894 w7884 w7874 w7864 w7854 w7844 w7834 w7824 w7814
      w7804 w7794
w7784 w7774 w7764 w7754 w7744 w7734 w7724 w7714 w7704 w7694 w7684
      w7674 w7664
```

```
w7654 w7644 w7634 w7624 w7614 w7604 w7594 w7584 w7574 w7564 w7554
      w7544 w7534
w7524 w7514 w7504 w7494 w7484 w7474 w7464 w7454 w7444 w7434 w7424
      w7414 w7404
w7394 w7384 w7374 w7364 w7354 w7344 w7334 w7324 w7314 w7304 w7294
      w7284 w7274
w7264 w7254 w7244 w7234 w7224 w7214 w7204 w7194 w7184 w7174 w7164
      w7154 w7144
w7134 w7124 w7114 w7104 w7094 w7084 w7074 w7064 w7054 w7044 w7034
      w7024 w7014
w7004 w6994 w6984 w6974 w6964 w6954 w6944 w6934 w6924 w6914 w6904
      w6894 w6884
w6874 w6864 w6854 w6844 w6834 w6824 w6814 w6804 w6794 w6784 w6774
      w6764 w6754
w6744 w6734 w6724 w6714 w6704 w6694 w6684 w6674 w6664 w6654 w6644
      w6634 w6624
w6614 w6604 w6594 w6584 w6574 w6564 w6554 w6544 w6534 w6524 w6514
      w6504 w6494
w6484 w6474 w6464 w6454 w6444 w6434 w6424 w6414 w6404 w6394 w6384
      w6374 w6364
w6354 w6344 w6334 w6324 w6314 w6304 w6294 w6284 w6274 w6264 w6254
      w6244 w6234
w6224 w6214 w6204 w6194 w6184 w6174 w6164 w6154 w6144 w6134 w6124
      w6114 w6104
w6094 w6084 w6074 w6064 w6054 w6044 w6034 w6024 w6014 w6004 w5994
      w5984 w5974
w5964 w5954 w5944 w5934 w5924 w5914 w5904 w5894 w5884 w5874 w5864
      w5854 w5844
w5834 w5824 w5814 w5804 w5794 w5784 w5774 w5764 w5754 w5744 w5734
      w5724 w5714
w5704 w5694 w5684 w5674 w5664 w5654 w5644 w5634 w5624 w5614 w5604
      w5594 w5584
w5574 w5564 w5554 w5544 w5534 w5524 w5514 w5504 w5494 w5484 w5474
      w5464 w5454
w5444 w5434 w5424 w5414 w5404 w5394 w5384 w5374 w5364 w5354 w5344
      w5334 w5324
w5314 w5304 w5294 w5284 w5274 w5264 w5254 w5244 w5234 w5224 w5214
      w5204 w5194
w5184 w5174 w5164 w5154 w5144 w5134 w5124 w5114 w5104 w5094 w5084
      w5074 w5064
w5054 w5044 w5034 w5024 w5014 w5004 w4994 w4984 w4974 w4964 w4954
      w4944 w4934
w4924 w4914 w4904 w4894 w4884 w4874 w4864 w4854 w4844 w4834 w4824
      w4814 w4804
w4794 w4784 w4774 w4764 w4754 w4744 w4734 w4724 w4714 w4704 w4694
      w4684 w4674
w4664 w4654 w4644 w4634 w4624 w4614 w4604 w4594 w4584 w4574 w4564
      w4554 w4544
w4534 w4524 w4514 w4504 w4494 w4484 w4474 w4464 w4454 w4444 w4434
      w4424 w4414
w4404 w4394 w4384 w4374 w4364 w4354 w4344 w4334 w4324 w4314 w4304
      w4294 w4284
w4274 w4264 w4254 w4244 w4234 w4224 w4214 w4204 w4194 w4184 w4174
      w4164 w4154
w4144 w4134 w4124 w4114 w4104 w4094 w4084 w4074 w4064 w4054 w4044
      w4034 w4024
w4014;
```

```
datalines;
;
run;

proc princomp data=work.jasnir out=prinvars std;
var w9994   w9984 w9974 w9964 w9954 w9944 w9934 w9924 w9914 w9904
      w9894 w9884 w9874
w9864 w9854 w9844 w9834 w9824 w9814 w9804 w9794 w9784 w9774 w9764
      w9754 w9744
w9734 w9724 w9714 w9704 w9694 w9684 w9674 w9664 w9654 w9644 w9634
      w9624 w9614
w9604 w9594 w9584 w9574 w9564 w9554 w9544 w9534 w9524 w9514 w9504
      w9494 w9484
w9474 w9464 w9454 w9444 w9434 w9424 w9414 w9404 w9394 w9384 w9374
      w9364 w9354
w9344 w9334 w9324 w9314 w9304 w9294 w9284 w9274 w9264 w9254 w9244
      w9234 w9224
w9214 w9204 w9194 w9184 w9174 w9164 w9154 w9144 w9134 w9124 w9114
      w9104 w9094
w9084 w9074 w9064 w9054 w9044 w9034 w9024 w9014 w9004 w8994 w8984
      w8974 w8964
w8954 w8944 w8934 w8924 w8914 w8904 w8894 w8884 w8874 w8864 w8854
      w8844 w8834
w8824 w8814 w8804 w8794 w8784 w8774 w8764 w8754 w8744 w8734 w8724
      w8714 w8704
w8694 w8684 w8674 w8664 w8654 w8644 w8634 w8624 w8614 w8604 w8594
      w8584 w8574
w8564 w8554 w8544 w8534 w8524 w8514 w8504 w8494 w8484 w8474 w8464
      w8454 w8444
w8434 w8424 w8414 w8404 w8394 w8384 w8374 w8364 w8354 w8344 w8334
      w8324 w8314
w8304 w8294 w8284 w8274 w8264 w8254 w8244 w8234 w8224 w8214 w8204
      w8194 w8184
w8174 w8164 w8154 w8144 w8134 w8124 w8114 w8104 w8094 w8084 w8074
      w8064 w8054
w8044 w8034 w8024 w8014 w8004 w7994 w7984 w7974 w7964 w7954 w7944
      w7934 w7924
w7914 w7904 w7894 w7884 w7874 w7864 w7854 w7844 w7834 w7824 w7814
      w7804 w7794
w7784 w7774 w7764 w7754 w7744 w7734 w7724 w7714 w7704 w7694 w7684
      w7674 w7664
w7654 w7644 w7634 w7624 w7614 w7604 w7594 w7584 w7574 w7564 w7554
      w7544 w7534
w7524 w7514 w7504 w7494 w7484 w7474 w7464 w7454 w7444 w7434 w7424
      w7414 w7404
w7394 w7384 w7374 w7364 w7354 w7344 w7334 w7324 w7314 w7304 w7294
      w7284 w7274
w7264 w7254 w7244 w7234 w7224 w7214 w7204 w7194 w7184 w7174 w7164
      w7154 w7144
w7134 w7124 w7114 w7104 w7094 w7084 w7074 w7064 w7054 w7044 w7034
      w7024 w7014
w7004 w6994 w6984 w6974 w6964 w6954 w6944 w6934 w6924 w6914 w6904
      w6894 w6884
w6874 w6864 w6854 w6844 w6834 w6824 w6814 w6804 w6794 w6784 w6774
      w6764 w6754
w6744 w6734 w6724 w6714 w6704 w6694 w6684 w6674 w6664 w6654 w6644
      w6634 w6624
```

```
w6614 w6604 w6594 w6584 w6574 w6564 w6554 w6544 w6534 w6524 w6514
      w6504 w6494
w6484 w6474 w6464 w6454 w6444 w6434 w6424 w6414 w6404 w6394 w6384
      w6374 w6364
w6354 w6344 w6334 w6324 w6314 w6304 w6294 w6284 w6274 w6264 w6254
      w6244 w6234
w6224 w6214 w6204 w6194 w6184 w6174 w6164 w6154 w6144 w6134 w6124
      w6114 w6104
w6094 w6084 w6074 w6064 w6054 w6044 w6034 w6024 w6014 w6004 w5994
      w5984 w5974
w5964 w5954 w5944 w5934 w5924 w5914 w5904 w5894 w5884 w5874 w5864
      w5854 w5844
w5834 w5824 w5814 w5804 w5794 w5784 w5774 w5764 w5754 w5744 w5734
      w5724 w5714
w5704 w5694 w5684 w5674 w5664 w5654 w5644 w5634 w5624 w5614 w5604
      w5594 w5584
w5574 w5564 w5554 w5544 w5534 w5524 w5514 w5504 w5494 w5484 w5474
      w5464 w5454
w5444 w5434 w5424 w5414 w5404 w5394 w5384 w5374 w5364 w5354 w5344
      w5334 w5324
w5314 w5304 w5294 w5284 w5274 w5264 w5254 w5244 w5234 w5224 w5214
      w5204 w5194
w5184 w5174 w5164 w5154 w5144 w5134 w5124 w5114 w5104 w5094 w5084
      w5074 w5064
w5054 w5044 w5034 w5024 w5014 w5004 w4994 w4984 w4974 w4964 w4954
      w4944 w4934
w4924 w4914 w4904 w4894 w4884 w4874 w4864 w4854 w4844 w4834 w4824
      w4814 w4804
w4794 w4784 w4774 w4764 w4754 w4744 w4734 w4724 w4714 w4704 w4694
      w4684 w4674
w4664 w4654 w4644 w4634 w4624 w4614 w4604 w4594 w4584 w4574 w4564
      w4554 w4544
w4534 w4524 w4514 w4504 w4494 w4484 w4474 w4464 w4454 w4444 w4434
      w4424 w4414
w4404 w4394 w4384 w4374 w4364 w4354 w4344 w4334 w4324 w4314 w4304
      w4294 w4284
w4274 w4264 w4254 w4244 w4234 w4224 w4214 w4204 w4194 w4184 w4174
      w4164 w4154
w4144 w4134 w4124 w4114 w4104 w4094 w4084 w4074 w4064 w4054 w4044
      w4034 w4024
w4014;
run;


proc reg data=prinvars outest=est press;
model MIT = prin1-prin10 / selection=stepwise vif p;
model TORV= prin1-prin10 / selection=stepwise vif p;
model TMML= prin1-prin10 / selection=stepwise vif p;
model TOXY= prin1-prin10 / selection=stepwise vif p;
model TRE= prin1-prin10 / selection=stepwise vif p;
model TME= prin1-prin10 / selection=stepwise vif p;
run;

proc print data=prinvars;
var prin1-prin10;
run;
ods html close;
```

Table D.16 ANOVA results and model parameter estimates for MIT (first derivative data model).

Analysis of Variance					
Source	**DF**	**Sum of Squares**	**Mean Square**	**F Value**	**Pr > F**
Model	8	6146.751	768.3439	105.29	<.0001
Error	21	153.249	7.29757		
Corrected Total	29	6300			
Root MSE	2.7014	**R-Square**	0.9757		
Dependent Mean	290	**Adj R-Sq**	0.9664		
Coeff Var	0.93152				

Parameter Estimates						
Variable	**DF**	**Parameter Estimate**	**Standard Error**	**t Value**	**Pr > |t|**	**Variance Inflation**
Intercept	**1**	290	0.49321	587.99	<.0001	0
Prin1	**1**	2.27234	0.50164	4.53	0.0002	1
Prin2	**1**	9.93925	0.50164	19.81	<.0001	1
Prin3	**1**	1.09205	0.50164	2.18	0.041	1
Prin4	**1**	6.38861	0.50164	12.74	<.0001	1
Prin5	**1**	2.32867	0.50164	4.64	0.0001	1
Prin6	**1**	-6.66013	0.50164	-13.28	<.0001	1
Prin7	**1**	-3.39066	0.50164	-6.76	<.0001	1
Prin9	**1**	2.17281	0.50164	4.33	0.0003	1

Table D.17 ANOVA results and model parameter estimates for TORV (first derivative data model).

Analysis of Variance					
Source	**DF**	**Sum of Squares**	**Mean Square**	**F Value**	**Pr > F**
Model	6	3348.447	558.0746	103.74	<.0001
Error	23	123.7242	5.37931		
Corrected Total	29	3472.172			

Root MSE	2.31933	**R-Square**	0.9644
Dependent Mean	283.8253	**Adj R-Sq**	0.9551
Coeff Var	0.81717		

Parameter Estimates						
Variable	**DF**	**Parameter Estimate**	**Standard Error**	**t Value**	**Pr > |t|**	**Variance Inflation**
Intercept	**1**	283.8253	0.42345	670.27	<.0001	0
Prin1	**1**	-3.85968	0.43069	-8.96	<.0001	1
Prin2	**1**	4.62802	0.43069	10.75	<.0001	1
Prin3	**1**	6.09119	0.43069	14.14	<.0001	1
Prin4	**1**	1.06455	0.43069	2.47	0.0213	1
Prin5	**1**	2.01164	0.43069	4.67	0.0001	1
Prin6	**1**	-6.0717	0.43069	-14.1	<.0001	1

Table D.18 ANOVA results and model parameter estimates for TMML (first derivative data model).

Analysis of Variance					
Source	**DF**	**Sum of Squares**	**Mean Square**	**F Value**	**Pr > F**
Model	8	6072.09	759.0113	43.64	<.0001
Error	21	365.279	17.39424		
Corrected Total	29	6437.369			
Root MSE	4.17064	**R-Square**	0.9433		
Dependent Mean	325.599	**Adj R-Sq**	0.9216		
Coeff Var	1.28091				

Parameter Estimates						
Variable	**DF**	**Parameter Estimate**	**Standard Error**	**t Value**	**Pr > |t|**	**Variance Inflation**
Intercept	**1**	325.599	0.76145	427.6	<.0001	0
Prin1	**1**	-1.70486	0.77447	-2.2	0.039	1
Prin2	**1**	4.58655	0.77447	5.92	<.0001	1
Prin3	**1**	8.90202	0.77447	11.49	<.0001	1
Prin4	**1**	3.79045	0.77447	4.89	<.0001	1
Prin5	**1**	3.87898	0.77447	5.01	<.0001	1
Prin6	**1**	-4.58461	0.77447	-5.92	<.0001	1
Prin7	**1**	-3.88601	0.77447	-5.02	<.0001	1
Prin9	**1**	6.3765	0.77447	8.23	<.0001	1

Table D.19 ANOVA results and model parameter estimates for TOXY (first derivative data model).

Analysis of Variance					
Source	**DF**	**Sum of Squares**	**Mean Square**	**F Value**	**Pr > F**
Model	8	6643.051	830.3814	10.37	<.0001
Error	21	1681.918	80.09131		
Corrected Total	29	8324.969			

Root MSE	8.94938	**R-Square**	0.798
Dependent Mean	292.497	**Adj R-Sq**	0.721
Coeff Var	3.05965		

Parameter Estimates						
Variable	**DF**	**Parameter Estimate**	**Standard Error**	**t Value**	**Pr > |t|**	**Variance Inflation**
Intercept	**1**	292.497	1.63392	179.01	<.0001	0
Prin2	**1**	6.20974	1.66186	3.74	0.0012	1
Prin3	**1**	6.56672	1.66186	3.95	0.0007	1
Prin4	**1**	4.34758	1.66186	2.62	0.0161	1
Prin5	**1**	4.32033	1.66186	2.6	0.0167	1
Prin6	**1**	-7.3818	1.66186	-4.44	0.0002	1
Prin7	**1**	-5.20823	1.66186	-3.13	0.005	1
Prin8	**1**	4.10755	1.66186	2.47	0.0221	1
Prin9	**1**	3.36644	1.66186	2.03	0.0557	1

Table D.20 ANOVA results and model parameter estimates for TRE (first derivative data model).

Analysis of Variance					
Source	**DF**	**Sum of Squares**	**Mean Square**	**F Value**	**Pr > F**
Model	8	4073.756	509.2195	31.48	<.0001
Error	21	339.682	16.17533		
Corrected Total	29	4413.438			

Root MSE	4.02186	**R-Square**	0.923
Dependent Mean	239.0813	**Adj R-Sq**	0.8937
Coeff Var	1.68221		

Parameter Estimates						
Variable	**DF**	**Parameter Estimate**	**Standard Error**	**t Value**	**Pr > |t|**	**Variance Inflation**
Intercept	**1**	239.0813	0.73429	325.6	<.0001	0
Prin1	**1**	4.96446	0.74684	6.65	<.0001	1
Prin2	**1**	8.69835	0.74684	11.65	<.0001	1
Prin3	**1**	-3.48872	0.74684	-4.67	0.0001	1
Prin4	**1**	3.29752	0.74684	4.42	0.0002	1
Prin5	**1**	-2.49227	0.74684	-3.34	0.0031	1
Prin6	**1**	-2.69359	0.74684	-3.61	0.0017	1
Prin7	**1**	-1.2945	0.74684	-1.73	0.0977	1
Prin8	**1**	1.40704	0.74684	1.88	0.0735	1

Table D.21 ANOVA results and model parameter estimates for TME (first derivative data model).

Analysis of Variance					
Source	**DF**	**Sum of Squares**	**Mean Square**	**F Value**	**Pr > F**
Model	7	5992.439	856.0627	26.8	<.0001
Error	22	702.8042	31.94565		
Corrected Total	29	6695.243			

Root MSE	5.65205	**R-Square**	0.895
Dependent Mean	387.7237	**Adj R-Sq**	0.8616
Coeff Var	1.45775		

Parameter Estimates						
Variable	**DF**	**Parameter Estimate**	**Standard Error**	**t Value**	**Pr > |t|**	**Variance Inflation**
Intercept	**1**	387.7237	1.03192	375.73	<.0001	0
Prin1	**1**	-3.41304	1.04956	-3.25	0.0037	1
Prin2	**1**	2.49212	1.04956	2.37	0.0267	1
Prin3	**1**	11.28486	1.04956	10.75	<.0001	1
Prin4	**1**	-1.96302	1.04956	-1.87	0.0748	1
Prin5	**1**	6.35524	1.04956	6.06	<.0001	1
Prin6	**1**	3.65403	1.04956	3.48	0.0021	1
Prin9	**1**	-1.95801	1.04956	-1.87	0.0755	1

Table D.22 Principal components (PC) obtained from first derivative NIR spectral data of biomass dusts used for internal validation of prediction models.

Biomass	Prin1	Prin2	Prin3	Prin4	Prin5	Prin6	Prin7	Prin8	Prin9	Prin10
Bermuda grass	0.23709	0.07055	-1.12748	-0.62248	0.09124	0.91432	1.00754	0.50764	1.83219	-0.47364
	0.35876	0.09027	-1.07557	-0.94639	0.29108	1.63573	1.32598	0.75982	1.63578	0.69481
	0.46058	0.07496	-1.05668	-0.92716	0.07252	1.30633	1.34043	0.88879	1.07812	-0.75664
Corn Cobs	-0.46104	0.50951	-0.53414	-1.44014	0.13721	1.32503	-1.33069	-1.14237	-1.02481	-0.45919
	-0.29453	0.54035	-0.45184	-1.29601	0.48665	1.1919	-1.4668	-0.80081	-0.30343	0.09419
	-0.1438	0.28218	-0.51219	-1.79695	-0.05935	0.98185	-1.47411	-1.45633	-1.08626	0.36754
Corn stover	1.7176	-0.28657	0.3703	1.06437	1.20328	0.84439	2.03573	-0.89898	-0.71359	0.86732
	1.56428	-0.1457	0.29698	1.03164	1.11174	0.25267	0.92201	-0.60479	-2.01108	-2.23954
	1.63173	-0.28744	0.3597	0.61067	0.67085	0.42377	0.10663	-1.08201	-1.1552	1.93848
Eucalyptus	-0.0868	0.65217	0.55395	-1.16482	-1.40663	-1.07495	0.80247	0.51087	-0.59534	-0.7846
	0.06562	0.56408	0.48619	-1.31249	-1.84716	-1.09302	1.58156	0.15209	-1.24806	-0.38367
	0.06182	0.51554	0.60961	-1.25461	-1.64023	-1.1052	1.12647	0.27398	-0.75767	1.76359
Pecan shell	-1.32757	-2.0528	1.43963	-0.12894	0.34686	0.28667	0.12002	0.54841	-0.17011	0.96005
	-1.41764	-2.02759	1.45493	-0.14133	0.4255	0.40266	-0.35117	0.37358	0.20311	0.68497
	-1.4677	-2.08026	1.4731	-0.42867	0.3477	0.16266	0.8882	-0.96569	0.49176	-1.80261
Pine	-1.01882	1.30733	0.02786	0.20903	1.92519	-1.29954	-0.32134	0.11285	-0.20049	0.45244
	-0.87613	1.27929	-0.02033	-0.15488	2.09127	-1.41046	0.51453	0.40955	0.57927	-0.1377
	-0.87852	1.34829	-0.0141	-0.27955	1.90361	-1.49945	0.1485	-0.12004	0.33369	-0.06095
Poultry Litter	-0.53391	-1.02772	-2.14891	0.82826	-0.54763	-1.04391	-0.00829	-0.30867	-0.27784	0.68977
	-0.55484	-1.21574	-2.28883	0.96941	-0.52798	-0.59823	-0.41169	0.09462	-0.42593	0.40119
	-0.50387	-1.16324	-2.2479	0.90542	-0.34998	-0.92892	-0.03646	0.20424	-0.77851	-0.74932
Sugarcane bagasse	1.31526	-0.2468	0.49145	0.0163	-0.52182	-0.92452	-1.36099	-0.97962	1.54468	-0.79424
	1.4844	-0.41211	0.44525	-0.04834	-0.51708	-1.05521	-0.9961	-0.61311	1.17353	-1.49569
	1.42437	-0.34069	0.51955	0.19154	-0.36686	-1.26628	-0.62471	-1.1747	2.11963	1.38741
Sweetgum	-0.9438	1.25193	0.50924	1.54208	-1.19795	0.92289	-0.17995	-0.63051	0.50852	-0.56547
	-1.08247	1.28196	0.50226	1.93162	-1.14347	1.03511	0.2352	-0.52212	0.32564	0.8635
	-1.03111	1.37259	0.52623	1.78056	-1.04982	0.82559	-0.09182	-0.24757	0.22561	-0.55512
Switchgrass	0.71656	0.07042	0.47897	0.13733	0.10404	0.28549	-1.09501	1.97331	-0.1741	1.09064
	0.80833	0.00722	0.44471	0.01652	-0.204	-0.08139	-1.1679	1.96439	-0.79398	-0.34423
	0.77616	0.06801	0.48808	0.70802	0.1712	0.58402	-1.23824	2.77319	-0.33514	-0.65329

Appendix E –Heating and Ignition Properties, NIR Spectra and SAS Code for Principal Component Analysis for Biomass Dusts Used for External Validation

Table E.1 Minimum hot surface ignition temperature (MIT) values for biomass dusts used for external validation of prediction models.

Sample	MIT (°C)	Mean MIT (°C)	Standard Deviation (°C)
Eucalyptus	280.00	280.00	0.00
	280.00		
	280.00		
Pine	320.00	320.00	0.00
	320.00		
	320.00		
Sweetgum	300.00	300.00	0.00
	300.00		
	300.00		
Switchgrass	290.00	290.00	0.00
	290.00		
	290.00		

Table E.2 Temperature of onset of rapid volatilization (TORV) values for biomass dusts used for external validation of prediction models.

Sample	TORV (°C)	Mean TORV (°C)	Standard Deviation (°C)
Eucalyptus	292.45 291.41 293.22	292.36	0.91
Pine	300.00 301.59 302.11	301.23	1.10
Sweetgum	301.16 291.11 288.46	293.58	6.70
Switchgrass	284.01 275.75 292.23	284.00	8.24

Table E.3 Temperature of maximum rate of mass loss (TMML) values for biomass dusts used for external validation of prediction models.

Sample	TMML (°C)	Mean TMML (°C)	Standard Deviation (°C)
Eucalyptus	328.09 327.93 323.96	326.66	2.34
Pine	353.12 347.87 354.50	351.83	3.50
Sweetgum	325.87 321.70 327.35	324.97	2.93
Switchgrass	324.31 310.26 322.55	319.04	7.65

Table E.4 Oxidation temperature (TOXY) values for biomass dusts used for external validation of prediction models.

Sample	TOXY (°C)	Mean TOXY (°C)	Standard Deviation (°C)
Eucalyptus	293.95	292.15	2.72
	289.03		
	293.48		
Pine	335.79	325.54	8.91
	319.65		
	321.17		
Sweetgum	299.48	300.43	2.19
	298.87		
	302.93		
Switchgrass	289.37	291.74	2.12
	293.47		
	292.38		

Table E.5 Temperature of rapid exothermic reaction (TRE) values for Biomass Dusts Used for External Validation of Prediction Models.

Sample	TRE (°C)	Mean TRE (°C)	Standard Deviation (°C)
Eucalyptus	237.84	238.76	0.81
	239.36		
	239.07		
Pine	239.32	244.32	4.45
	245.79		
	247.84		
Sweetgum	242.22	245.33	2.70
	247.00		
	246.77		
Switchgrass	231.90	237.20	5.18
	242.25		
	237.46		

Table E.6 Maximum temperature reached during exothermic reaction (TME) values for Biomass Dusts Used for External Validation of Prediction Models.

Sample	TME (°C)	Mean TME (°C)	Standard Deviation (°C)
Eucalyptus	399.86 397.88 398.35	398.70	1.03
Pine	403.66 390.86 400.10	398.21	6.61
Sweetgum	392.14 390.07 390.60	390.94	1.08
Switchgrass	397.87 381.74 396.63	392.08	8.98

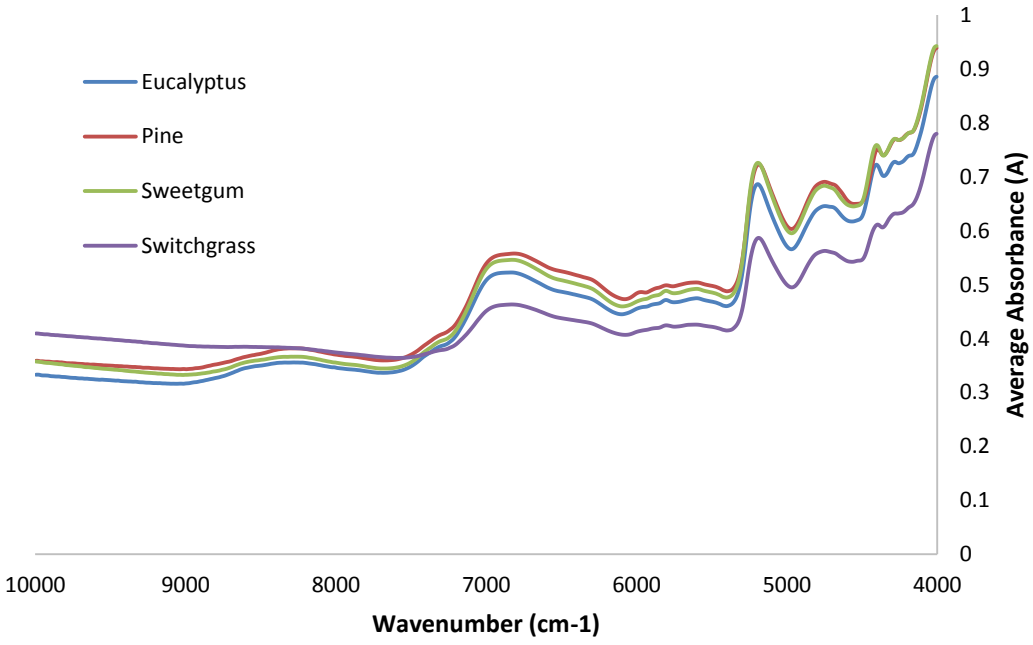

Figure E.1 NIR spectra showing average absorbance vs. wavenumber plot for biomass dusts used for external validation of prediction models.

SAS code: Obtaining principal components (PC) from raw NIR spectral data of biomass dusts used for external validation of prediction models.

```
/*******************************
 * Author: Jaskaran Dhiman      *
 * Research work                *
 * Date: 04/21/2014             *
 *******************************/

ods html file='C:\Users\jzd0028\Desktop\extvalraw.html';
options nodate pageno=1;
data work.jasnir;
infile 'C:\Users\jzd0028\Desktop\extvalraw.csv' delimiter = ','
MISSOVER DSD lrecl=32767 firstobs=1 n=1500;
input Biomass$
w9994 w9984 w9974 w9964 w9954 w9944 w9934 w9924 w9914 w9904 w9894
      w9884 w9874
w9864 w9854 w9844 w9834 w9824 w9814 w9804 w9794 w9784 w9774 w9764
      w9754 w9744
w9734 w9724 w9714 w9704 w9694 w9684 w9674 w9664 w9654 w9644 w9634
      w9624 w9614
w9604 w9594 w9584 w9574 w9564 w9554 w9544 w9534 w9524 w9514 w9504
      w9494 w9484
w9474 w9464 w9454 w9444 w9434 w9424 w9414 w9404 w9394 w9384 w9374
      w9364 w9354
w9344 w9334 w9324 w9314 w9304 w9294 w9284 w9274 w9264 w9254 w9244
      w9234 w9224
w9214 w9204 w9194 w9184 w9174 w9164 w9154 w9144 w9134 w9124 w9114
      w9104 w9094
w9084 w9074 w9064 w9054 w9044 w9034 w9024 w9014 w9004 w8994 w8984
      w8974 w8964
w8954 w8944 w8934 w8924 w8914 w8904 w8894 w8884 w8874 w8864 w8854
      w8844 w8834
w8824 w8814 w8804 w8794 w8784 w8774 w8764 w8754 w8744 w8734 w8724
      w8714 w8704
w8694 w8684 w8674 w8664 w8654 w8644 w8634 w8624 w8614 w8604 w8594
      w8584 w8574
w8564 w8554 w8544 w8534 w8524 w8514 w8504 w8494 w8484 w8474 w8464
      w8454 w8444
w8434 w8424 w8414 w8404 w8394 w8384 w8374 w8364 w8354 w8344 w8334
      w8324 w8314
w8304 w8294 w8284 w8274 w8264 w8254 w8244 w8234 w8224 w8214 w8204
      w8194 w8184
w8174 w8164 w8154 w8144 w8134 w8124 w8114 w8104 w8094 w8084 w8074
      w8064 w8054
w8044 w8034 w8024 w8014 w8004 w7994 w7984 w7974 w7964 w7954 w7944
      w7934 w7924
w7914 w7904 w7894 w7884 w7874 w7864 w7854 w7844 w7834 w7824 w7814
      w7804 w7794
w7784 w7774 w7764 w7754 w7744 w7734 w7724 w7714 w7704 w7694 w7684
      w7674 w7664
w7654 w7644 w7634 w7624 w7614 w7604 w7594 w7584 w7574 w7564 w7554
      w7544 w7534
w7524 w7514 w7504 w7494 w7484 w7474 w7464 w7454 w7444 w7434 w7424
      w7414 w7404
```

```
w7394 w7384 w7374 w7364 w7354 w7344 w7334 w7324 w7314 w7304 w7294
      w7284 w7274
w7264 w7254 w7244 w7234 w7224 w7214 w7204 w7194 w7184 w7174 w7164
      w7154 w7144
w7134 w7124 w7114 w7104 w7094 w7084 w7074 w7064 w7054 w7044 w7034
      w7024 w7014
w7004 w6994 w6984 w6974 w6964 w6954 w6944 w6934 w6924 w6914 w6904
      w6894 w6884
w6874 w6864 w6854 w6844 w6834 w6824 w6814 w6804 w6794 w6784 w6774
      w6764 w6754
w6744 w6734 w6724 w6714 w6704 w6694 w6684 w6674 w6664 w6654 w6644
      w6634 w6624
w6614 w6604 w6594 w6584 w6574 w6564 w6554 w6544 w6534 w6524 w6514
      w6504 w6494
w6484 w6474 w6464 w6454 w6444 w6434 w6424 w6414 w6404 w6394 w6384
      w6374 w6364
w6354 w6344 w6334 w6324 w6314 w6304 w6294 w6284 w6274 w6264 w6254
      w6244 w6234
w6224 w6214 w6204 w6194 w6184 w6174 w6164 w6154 w6144 w6134 w6124
      w6114 w6104
w6094 w6084 w6074 w6064 w6054 w6044 w6034 w6024 w6014 w6004 w5994
      w5984 w5974
w5964 w5954 w5944 w5934 w5924 w5914 w5904 w5894 w5884 w5874 w5864
      w5854 w5844
w5834 w5824 w5814 w5804 w5794 w5784 w5774 w5764 w5754 w5744 w5734
      w5724 w5714
w5704 w5694 w5684 w5674 w5664 w5654 w5644 w5634 w5624 w5614 w5604
      w5594 w5584
w5574 w5564 w5554 w5544 w5534 w5524 w5514 w5504 w5494 w5484 w5474
      w5464 w5454
w5444 w5434 w5424 w5414 w5404 w5394 w5384 w5374 w5364 w5354 w5344
      w5334 w5324
w5314 w5304 w5294 w5284 w5274 w5264 w5254 w5244 w5234 w5224 w5214
      w5204 w5194
w5184 w5174 w5164 w5154 w5144 w5134 w5124 w5114 w5104 w5094 w5084
      w5074 w5064
w5054 w5044 w5034 w5024 w5014 w5004 w4994 w4984 w4974 w4964 w4954
      w4944 w4934
w4924 w4914 w4904 w4894 w4884 w4874 w4864 w4854 w4844 w4834 w4824
      w4814 w4804
w4794 w4784 w4774 w4764 w4754 w4744 w4734 w4724 w4714 w4704 w4694
      w4684 w4674
w4664 w4654 w4644 w4634 w4624 w4614 w4604 w4594 w4584 w4574 w4564
      w4554 w4544
w4534 w4524 w4514 w4504 w4494 w4484 w4474 w4464 w4454 w4444 w4434
      w4424 w4414
w4404 w4394 w4384 w4374 w4364 w4354 w4344 w4334 w4324 w4314 w4304
      w4294 w4284
w4274 w4264 w4254 w4244 w4234 w4224 w4214 w4204 w4194 w4184 w4174
      w4164 w4154
w4144 w4134 w4124 w4114 w4104 w4094 w4084 w4074 w4064 w4054 w4044
      w4034 w4024
w4014 w4004;
datalines;
;
run;
```

```
proc princomp data=work.jasnir out=prinvars std;
var w9994   w9984 w9974 w9964 w9954 w9944 w9934 w9924 w9914 w9904
      w9894 w9884 w9874
w9864 w9854 w9844 w9834 w9824 w9814 w9804 w9794 w9784 w9774 w9764
      w9754 w9744
w9734 w9724 w9714 w9704 w9694 w9684 w9674 w9664 w9654 w9644 w9634
      w9624 w9614
w9604 w9594 w9584 w9574 w9564 w9554 w9544 w9534 w9524 w9514 w9504
      w9494 w9484
w9474 w9464 w9454 w9444 w9434 w9424 w9414 w9404 w9394 w9384 w9374
      w9364 w9354
w9344 w9334 w9324 w9314 w9304 w9294 w9284 w9274 w9264 w9254 w9244
      w9234 w9224
w9214 w9204 w9194 w9184 w9174 w9164 w9154 w9144 w9134 w9124 w9114
      w9104 w9094
w9084 w9074 w9064 w9054 w9044 w9034 w9024 w9014 w9004 w8994 w8984
      w8974 w8964
w8954 w8944 w8934 w8924 w8914 w8904 w8894 w8884 w8874 w8864 w8854
      w8844 w8834
w8824 w8814 w8804 w8794 w8784 w8774 w8764 w8754 w8744 w8734 w8724
      w8714 w8704
w8694 w8684 w8674 w8664 w8654 w8644 w8634 w8624 w8614 w8604 w8594
      w8584 w8574
w8564 w8554 w8544 w8534 w8524 w8514 w8504 w8494 w8484 w8474 w8464
      w8454 w8444
w8434 w8424 w8414 w8404 w8394 w8384 w8374 w8364 w8354 w8344 w8334
      w8324 w8314
w8304 w8294 w8284 w8274 w8264 w8254 w8244 w8234 w8224 w8214 w8204
      w8194 w8184
w8174 w8164 w8154 w8144 w8134 w8124 w8114 w8104 w8094 w8084 w8074
      w8064 w8054
w8044 w8034 w8024 w8014 w8004 w7994 w7984 w7974 w7964 w7954 w7944
      w7934 w7924
w7914 w7904 w7894 w7884 w7874 w7864 w7854 w7844 w7834 w7824 w7814
      w7804 w7794
w7784 w7774 w7764 w7754 w7744 w7734 w7724 w7714 w7704 w7694 w7684
      w7674 w7664
w7654 w7644 w7634 w7624 w7614 w7604 w7594 w7584 w7574 w7564 w7554
      w7544 w7534
w7524 w7514 w7504 w7494 w7484 w7474 w7464 w7454 w7444 w7434 w7424
      w7414 w7404
w7394 w7384 w7374 w7364 w7354 w7344 w7334 w7324 w7314 w7304 w7294
      w7284 w7274
w7264 w7254 w7244 w7234 w7224 w7214 w7204 w7194 w7184 w7174 w7164
      w7154 w7144
w7134 w7124 w7114 w7104 w7094 w7084 w7074 w7064 w7054 w7044 w7034
      w7024 w7014
w7004 w6994 w6984 w6974 w6964 w6954 w6944 w6934 w6924 w6914 w6904
      w6894 w6884
w6874 w6864 w6854 w6844 w6834 w6824 w6814 w6804 w6794 w6784 w6774
      w6764 w6754
w6744 w6734 w6724 w6714 w6704 w6694 w6684 w6674 w6664 w6654 w6644
      w6634 w6624
w6614 w6604 w6594 w6584 w6574 w6564 w6554 w6544 w6534 w6524 w6514
      w6504 w6494
w6484 w6474 w6464 w6454 w6444 w6434 w6424 w6414 w6404 w6394 w6384
      w6374 w6364
```

```
w6354 w6344 w6334 w6324 w6314 w6304 w6294 w6284 w6274 w6264 w6254
      w6244 w6234
w6224 w6214 w6204 w6194 w6184 w6174 w6164 w6154 w6144 w6134 w6124
      w6114 w6104
w6094 w6084 w6074 w6064 w6054 w6044 w6034 w6024 w6014 w6004 w5994
      w5984 w5974
w5964 w5954 w5944 w5934 w5924 w5914 w5904 w5894 w5884 w5874 w5864
      w5854 w5844
w5834 w5824 w5814 w5804 w5794 w5784 w5774 w5764 w5754 w5744 w5734
      w5724 w5714
w5704 w5694 w5684 w5674 w5664 w5654 w5644 w5634 w5624 w5614 w5604
      w5594 w5584
w5574 w5564 w5554 w5544 w5534 w5524 w5514 w5504 w5494 w5484 w5474
      w5464 w5454
w5444 w5434 w5424 w5414 w5404 w5394 w5384 w5374 w5364 w5354 w5344
      w5334 w5324
w5314 w5304 w5294 w5284 w5274 w5264 w5254 w5244 w5234 w5224 w5214
      w5204 w5194
w5184 w5174 w5164 w5154 w5144 w5134 w5124 w5114 w5104 w5094 w5084
      w5074 w5064
w5054 w5044 w5034 w5024 w5014 w5004 w4994 w4984 w4974 w4964 w4954
      w4944 w4934
w4924 w4914 w4904 w4894 w4884 w4874 w4864 w4854 w4844 w4834 w4824
      w4814 w4804
w4794 w4784 w4774 w4764 w4754 w4744 w4734 w4724 w4714 w4704 w4694
      w4684 w4674
w4664 w4654 w4644 w4634 w4624 w4614 w4604 w4594 w4584 w4574 w4564
      w4554 w4544
w4534 w4524 w4514 w4504 w4494 w4484 w4474 w4464 w4454 w4444 w4434
      w4424 w4414
w4404 w4394 w4384 w4374 w4364 w4354 w4344 w4334 w4324 w4314 w4304
      w4294 w4284
w4274 w4264 w4254 w4244 w4234 w4224 w4214 w4204 w4194 w4184 w4174
      w4164 w4154
w4144 w4134 w4124 w4114 w4104 w4094 w4084 w4074 w4064 w4054 w4044
      w4034 w4024
w4014 w4004;
run;


proc print data=prinvars;
var prin1-prin10;
run;
ods html close;
```

Table E.7 Principal components (PC) obtained from raw NIR spectral data of biomass dusts used for external validation of prediction models.

	Principal Components									
Sample	**Prin1**	**Prin2**	**Prin3**	**Prin4**	**Prin5**	**Prin6**	**Prin7**	**Prin8**	**Prin9**	**Prin10**
	0.435	-0.569	-1.087	-0.925	0.285	0.942	-1.293	-0.335	1.690	1.126
Eucalyptus	0.353	-0.978	-0.994	-0.743	1.976	0.457	1.078	-0.277	-1.100	-0.918
	0.382	-1.459	-1.092	-0.327	-1.932	-1.245	-0.160	0.736	-0.545	-0.245
	0.531	-0.250	-0.209	2.146	-0.458	0.754	0.652	-1.152	-0.800	1.373
Pine	0.617	0.358	-0.082	1.711	0.740	0.127	-0.682	1.413	1.107	-1.041
	0.777	2.471	-1.074	-0.322	-0.262	-0.852	0.132	-0.312	-0.360	-0.459
	0.638	0.592	1.259	-1.075	-0.815	1.903	-0.103	1.054	-0.985	0.165
Sweetgum	0.630	-0.280	1.503	-0.277	0.947	-1.668	0.654	0.874	0.235	1.411
	0.576	-0.414	1.543	-0.253	-0.450	-0.323	-0.241	-2.030	0.736	-1.443
	-1.696	-0.455	0.392	0.625	-0.058	0.226	-0.553	0.635	-0.480	-0.934
Switchgrass	-1.595	0.547	0.065	-0.241	0.600	-0.625	-1.517	-0.668	-0.915	0.808
	-1.649	0.437	-0.223	-0.319	-0.574	0.305	2.032	0.060	1.416	0.157